$^{40}Ar/^{39}Ar$ age variations among cogenetic feldspars from the Benson Mines, New York

by

James N. Gunn, III

A thesis submitted to the Graduate Faculty of
Auburn University
in partial fulfillment of the
requirements for the Degree of
Master of Science

Auburn, Alabama
August 6, 2016

Keywords: potassium feldspar, argon diffusion, volume diffusion

Approved by

Willis E. Hames, Chair, Professor of Geosciences
Mark G. Steltenpohl, Professor of Geosciences
Haibo Zou, Associate Professor of Geosciences
Dmitry V. Glotov, Associate Professor of Mathematics and Statistics

ABSTRACT

The alkali feldspar group constitutes one the most common mineral groups of Earth's crust. The $^{40}Ar/^{39}Ar$ method for dating potassium feldspars has proven to be a powerful analytical tool for evaluating low-temperature thermochronologic histories. Conventionally, for a vast number of studies, $^{40}Ar/^{39}Ar$ ages are determined for bulk concentrates of alkali feldspar of a particular grain size, separated and prepared following crushing of the host rock. In early studies of orthoclase from the Benson Mines in the northwestern Adirondack Highlands, Foland (1974) concluded that argon diffusion occurred over the physical scale of orthoclase crystals, a result reaffirmed by more recent studies of Foland & Xu (1990) and Cassata & Renne (2013). If the diffusion length scale is defined by physical grain size, the crushing and grain size reduction requisite for the analysis of bulk feldspar samples can sensibly be expected to alter and misrepresent the natural distribution of $^{40}Ar^{*}$.

The primary objective of the present study is to obtain $^{40}Ar/^{39}Ar$ ages of cogenetic orthoclase crystals for different lithologies of the Benson Mines. Argon analyses were accomplished via the incremental heating of mineral grains with either a CO_2 laser, or a diode laser in conjunction with a thermocouple to control temperature. To further assess the impact of grain size and other physical characteristics on resultant $^{40}Ar/^{39}Ar$ ages, this study utilizes the analysis of single crystals of potassium-bearing mineral phases from lithologies recollected at the Benson Mines. Lithologies sampled from the Benson Mines include magnetite-rich orthoclase-sillimanite gneiss, magnetite-rich orthoclase-garnet gneiss, biotite-

hornblende syenite, and pegmatite. In addition to orthoclase from various samples, single crystals of hornblende and biotite were also analyzed, and yield plateau ages of ca. 970 Ma and ca. 900 Ma, respectively. These results are consistent with a cooling history ($\leq 1^{o}$C/m.y.) through the retention temperatures of various phases following late stages of the Mesoproterozoic Grenville orogeny.

Argon release spectra produced from step-heating single crystals of orthoclase in the present study reveal significant discordance between cogenetic crystals of individual samples and also systematic differences in age between feldspar populations of different samples. Notable variation is also observed at the scale of individual grains between initial and final heating steps. Release spectra for single crystals of orthoclase from the sillimanite gneisses yield the oldest $^{40}Ar/^{39}Ar$ ages observed and generally are less discordant between crystals, considering all of the lithologies analyzed, with total gas ages ranging from 875 to 850 Ma. A highly perthitic feldspar from a hornblende syenite yields much younger ages ranging from ca. 750 to 670 Ma. In contrast, K-feldspars from post-metamorphic pegmatites yield the most discordant spectra for individual crystals, with ages ranging from ca. 800 to 500 Ma and total gas ages ranging from ca. 765 to 677 Ma. Differences in the age distributions observed for feldspars of a given rock (more or less discordance, or differences in absolute age) are consistent with analysis of fragments differing in size and shape that present variable representations of their natural grain-scale diffusion geometries. The younger and more discordant ages for the feldspars from the syenite and pegmatite are interpreted to result from a higher local water activity during cooling than was the case in the gneisses. Results of the present study expand the earlier work of Foland and others for the Benson Mines, and

emphasize the importance of analytical strategies to recover natural diffusion gradients in radiogenic $^{40}Ar^{*}$ concentrations at the scale of individual feldspar grains..

ACKNOWLEDGEMENTS

First and foremost, I would like to thank my God for my life, for saving me, and for his unconditional love. Without Him, I am nothing, but with Him, nothing is impossible.

I would like to express my sincere gratitude to my advisor Dr. Bill Hames for the continuous support of my M.S. study and research, his patience, his compassion, and his steady encouragement. Without his mentorship, this accomplishment would not have been achieved. It has been an honor to work with him, and I am privileged to call him not only a colleague, but also a dear friend.

In addition, I would like to thank my committee members Dr. Dmitry Glotov, Dr. Mark Steltenpohl, and Dr. Haibo Zou who provided extremely valuable input throughout the writing process.

I would also like to thank Dr. Robert Badger of State University of New York Potsdam for providing the samples used in this study.

This research was supported, in part, by funding from the National Science Foundation (Grant #0911687).

Last, but certainly not least, I would like to thank my parents Scott and Kathy Gunn for bringing me into this world and raising me to be the man that I am today. I could never thank them enough for all that they have done and continue to do for me.

TABLE OF CONTENTS

LIST OF FIGURES

LIST OF TABLES

INTRODUCTION

Isotopic evaluation of geochronologic systems provides an effective means for deciphering the mineral growth and cooling history of rocks within a region, resulting in a more comprehensive understanding of the geologic events that they have experienced. In the case of the K/Ar dating methods, a mineral phase will only begin to retain ^{40}Ar once it has cooled to a temperature sufficient to limit loss of radiogenic ^{40}Ar by diffusion. Dodson (1973) defines the closure temperature of a geochronologic system as the temperature it experienced at the time corresponding to its apparent age. Closure temperatures differ for various mineral phases, and are dependent upon a mineral's chemistry, structural state, physical grain size, and the cooling rate it experienced. Obtaining isotopic data for multiple mineral phases possessing varying closure temperatures that are collected from the same structural level permits the development of a pressure-temperature-time history (Hodges, 1991) and provides important information about the structural evolution of a terrane, because cooling ages serve as a proxy for the time-depth history of the terrane.

The minerals of the feldspar group are rich in potassium and constitute the most abundant phases in most crustal rocks and many extraterrestrial rocks, making them ideal candidates for thermochronologic studies. The $^{40}Ar/^{39}Ar$ dating technique provides powerful means for evaluating low-temperature thermochronologic histories of potassium feldspars. A comprehensive understanding of the mechanisms by which radiogenic argon diffuses from potassium feldspars is of the utmost importance for extracting meaningful cooling histories from $^{40}Ar/^{39}Ar$ data for feldspars.

The best type of feldspar sample for studying the diffusive behavior of $^{40}Ar^{*}$ would be from a locale possessing the simplest thermal history possible. Ideally, coarse, homogenous crystals of feldspar could be collected from multiple lithology types, representing a range in chemical composition and mineralogy, which have cooled, slowly and monotonically from temperatures that are initially so high that retention of $^{40}Ar^{*}$is limited. Analyzing potassium feldspars from old rocks would ensure the abundance of $^{40}Ar^{*}$ available for measurement. Additionally, the host-rock(s) should have experienced no thermal pulses after cooling from peak temperature began. This would provide confidence that there was no significant episodic loss of $^{40}Ar^{*}$ in feldspars analyzed, which would complicate the interpretation of the sample's original argon distribution when analyzing release spectra results. Lithologies from the Benson Mines meet the criteria for an ideal sample and were also the subject of the classic argon diffusion study on bulk samples of orthoclase by Foland (1974).

The physical alteration of orthoclase crystals that is common practice for bulk analyses also results in the alteration of crystals' natural $^{40}Ar^{*}$distribution, by reducing their original diffusion length-scale, producing homogenized degassing. This can be seen for Foland's (1974) data in Figure 1. Heating increments for his sample reveal very uniform release of radiogenic argon over the experiment, with very little discordance between high and low temperature steps. Incremental heating of individual feldspar crystals, in comparison to bulk analyses, provides much better insight into the spatial distribution of radiogenic argon in a crystal. In addition to Foland's work, Cassata & Renne (2013), have analyzed multiple size fractions of Benson Mines orthoclase providing a valuable comparison for the present study.

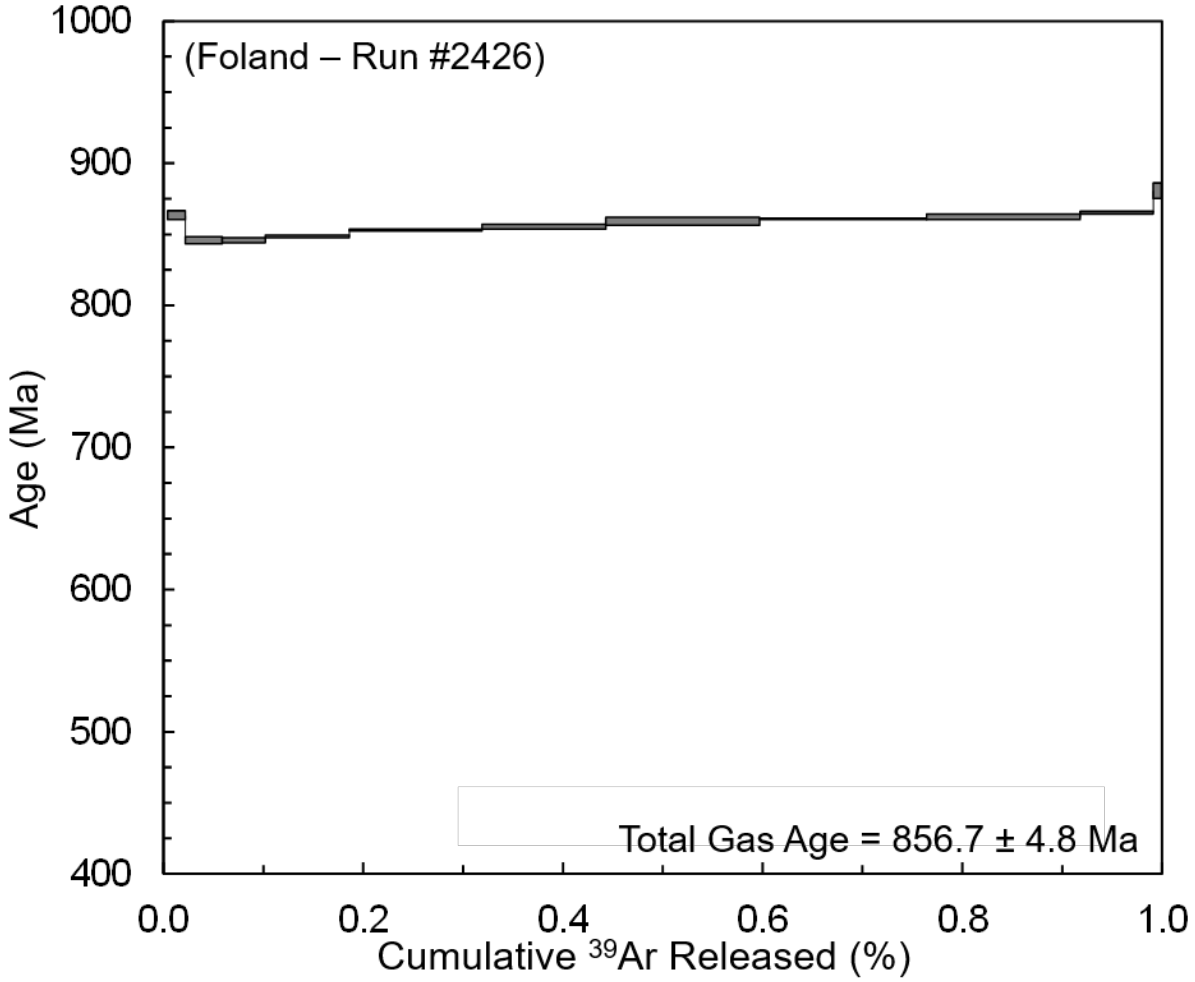

Figure 1. Age spectrum for run #2426 of 480 μm orthoclase from Foland (1974). (For all age spectra, box heights are 1σ.) Foland's bulk analysis of orthoclase from the Benson Mines yields a uniform age spectrum with minimal discordance among low and high temperature steps.

While there are aspects of Adirondack evolution that are still not yet well understood, a myriad of studies have been conducted by various researchers in attempt to decipher the orogen's tectonic and thermal evolution. These studies have resulted in the availability of a vast amount of structural, mineralogical, and isotopic analysis data for the region, allowing for a much more informed interpretation of feldspar age spectra. Findings from this study will contribute to a more precise understanding of the thermal evolution in the area at the local scale, complementing what is presently known about the area on a regional scale.

Previous Feldspar Research

The importance of understanding the diffusion behavior of $^{40}Ar^{*}$ in alkali feldspars has long been recognized, and numerous studies have been conducted for locations at a variety of tectonic settings. A few of the more notable studies include the Benson Mines of New York, U.S.A. (Foland, 1974; Foland & Xu, 1990, 1992; Cassata & Renne, 2013), which is the focus of the present study, the Chain of Ponds pluton in west central Maine and Quebec (Heizler et al., 1988; Lovera et al., 1989, 1991, 1993; Harrison et al., 1993), gem-quality alkali feldspars from Madagascar (Arnaud & Kelley, 1997; Wartho et al., 1999), the Shap Granite in northern England (Lee & Parsons, 1997; Parsons et al., 2010), and the Klokken syenite within the Gardar alkaline province in southern Greenland (Parsons et al., 1992, 2011, 2013).

GEOLOGIC SETTING OF THE BENSON MINES

The Benson Mines (Fig. 2a) represent a Precambrian gneiss-hosted iron-ore formation located in the central-northwest Adirondack Mountains, which comprises an area of more than 9,400 square miles. The Adirondack Mountains are a circular dome massif in northeastern New York State that expose an extension of the Grenville hinterland plateau of Quebec and Ontario, and are linked to the Central metasedimentary belt (CMB) of the Grenville province via the Frontenac arch. This terrane experienced multiple orogenies and other tectonic related events before and throughout the Grenville orogenic cycle (ca. 1.35 to 1.02 Ga) resulting from processes associated with the formation of the super-continent Rodinia. The Adirondacks are subdivided into two main provinces known as the Highlands and the Lowlands.

The Highlands, found in the southeast Adirondack Mountains, consist primarily of granulite facies rocks within which the Benson Mines are located. The Lowlands, found to the northwest, are composed primarily of upper-amphibolite facies rocks. These two provinces are separated by a northwest-dipping (45^{o}) kilometer scale zone of mylonite and ultramylonite known as the Carthage-Colton shear zone (CCSZ) (Fig. 2b) (McLelland et al., 2010; Tollo et al. 2004; Streepey et al., 2001). Previous studies by multiple researchers (Storm & Spear, 2005; Darling et al., 2004; Spear & Markussen, 1997; Kitchen & Valley, 1995; Bohlen et al., 1985) conclude crustal conditions of the Adirondack Highlands to have been 8 kbar and 800^{o}C, corresponding to a depth of ~20-25 km, as evidenced by metamorphic assemblages presently exposed at the surface of the Highlands. The high-grade sillimanite-orthoclase gneiss of the Benson Mines is considered to have been developed in a

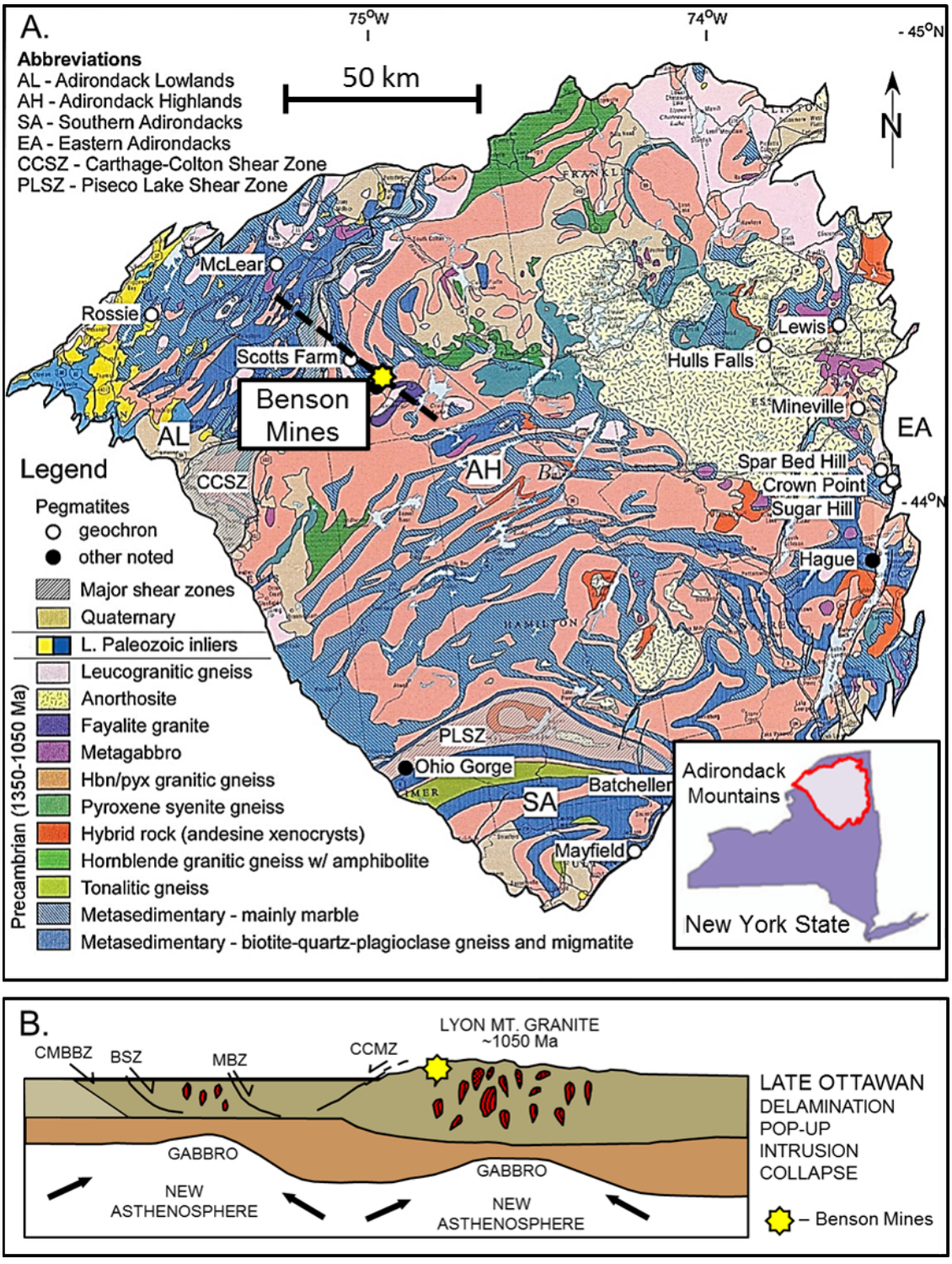

Figure 2. Geologic map of the Adirondack Mountains and the location of the Benson Mines (adapted from Lupuluscu et al., 2012). 1b) Northwest-southeast geologic cross section through the Adirondack Lowlands (southwest) and the Highlands (norththeast) during the Late Ottawan orogeny (ca. 1050 Ma) (adapted from McLelland et al., 2010).

footwall with respect to the CCSZ toward the end of the Grenville orogeny and was followed by the emplacement of pegmatite bodies in the Adirondack Highlands. According to Lupulescu et al. (2012) the main pegmatite bodies present in the Highlands occur in association with extensional A-type granites and were emplaced as a result of decompression melting during orogenic collapse.

McLelland et al. (2010) summarized the tectonic evolution of the Adirondack Mountains, which includes multiple phases of tectonic deformation and resulting metamorphism. This evolution began with the rifting and subsequent extension of the Grenville province Central metasedimentary belt (CMB), a Mesoproterozoic back-arc basin. Previously rifted Laurentian crustal material, termed 'Adirondis' by Gower (1996), was also affected by this rifting and extension from ca. 1300-1270 Ma. Material from the CMB and Adirondis provinces comprise the present-day Adirondack Mountains. Rifting was followed by contractional pulses and back-arc magmatism during the Elzevirian orogeny (1250-1220 Ma) that resulted in amphibolite-facies grade metamorphism of basin rocks and the emplacement of gabbroic, granodioritic, and granite plutons throughout the region. At ca. 1220 Ma, the back-arc basin began to close, and was followed by the northwest-directed thrusting of the CMB onto eastern Laurentia which ended by ca. 1190 Ma. This was followed by the Shawinigan orogeny (1190-1140 Ma) in which the Adirondacks collided with and were accreted onto the Central metasedimentary belt and Laurentia. The Adirondack Lowlands were affected by multiple episodes of plutonism ca. 1214-1172, the effects of which are not observed in the Highlands. Furthermore, only the Highlands exhibit effects of high-temperature metamorphism (granulite facies) produced by the collision of Amazonia with Laurentia to form Rodinia during the Ottawan phase (1090-1020 Ma) of the Grenville

orogeny. McLelland et al. (2010) interpreted that the Lowlands must have been thrust upon the Highlands during the Shawinigan collision based on mylonitic fabrics and kinematic indicators in the southern Carthage Colton zone (McLelland et al., 1996; Wasteneys et al., 1999; Baird et al., 2008). The tectonic evolution of the Adirondack Mountains and the rest of the Grenville province culminated with resumed contraction and continued collapse during the Rigolet phase of the Grenvillian orogeny from 1010-980 Ma (Rivers, 2008).

Models for Isotopic Data for the Benson Mines

Numerous isotopic studies have been previously conducted on various mineral phases collected in proximity to the Benson Mines (summarized in Table 1) enabling the deduction of a thermochronologic history for the area. These data have been combined with nominal closure temperature values, reported by the respective authors or with values estimated after Hodges (1991), to generate a general cooling history for the northwestern Adirondack Highlands and for the study area specifically (Fig. 3). The data imply a moderate cooling rate (2-3 ^{o}C/my) between 1150 and 990 Ma that decreased to a much slower, more gradual rate (< 1 ^{o}C/my) from 850 to 450 Ma.

TABLE 1. PREVIOUSLY PUBLISHED AGE DATA FOR THE ADIRONDACK HIGHLANDS

Dating Method	Mineral Phase	Age (Ma)	T_C (°C)	Source
U/Pb	Zircon	1147 ± 10	> 1000	McLelland et al., 1988
		1100 ± 12	> 1000	
	Garnet	1154 - 1013	> 800	Mezger et al., 1991
	Monazite	1033	700 - 650*	
	Sphene	1033 - 991	670 - 500*	
Ar/Ar	Hornblende	950	500	Streepey et al., 2000
		920 ± 20	500	Heizler & Harrison, 1986
		943.4 ± 1.7	451*	Onstott & Peacock, 1987
		935.4 ± 1.6	451*	
		910.5 ± 1.7	412*	
		904.6 ± 1.8	412*	
U/Pb	Rutile	911 - 885	430 – 380*	Mezger et al., 1991
Ar/Ar	Biotite	937	300	Streepey et al., 2000
		919	300	
		ca. 880	300	Heizler & Harrison, 1986
		837.2 ± 1.6	300	Onstott & Peacock, 1987
K/Ar	K-feldspar	ca. 850	275	Foland, 1974
		730 - 550	-	Heizler & Harrison, 1986

Closure temperature as reported by respective authors* or following values suggested by Hodges (1991).

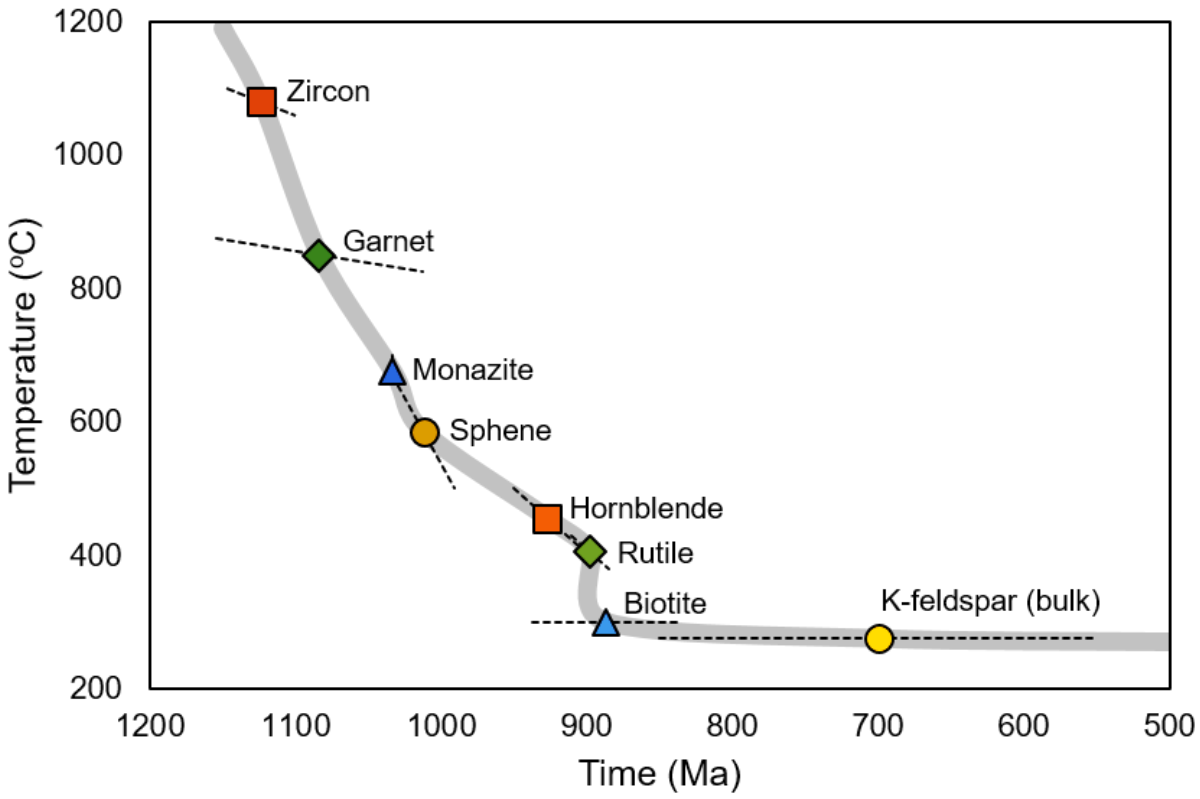

Figure 3. Temperature-time cooling history for the Adirondack Highlands based on previously published age data averages for zircon, garnet, monazite, sphene, hornblende, rutile, biotite, and K-feldspar. The dashed lines indicate the range in mineral ages and estimated closure temperatures (as reported by respective authors or as from Hodges, 1991), and are listed in Table 1. Note the wide range (300 m.y.) in K-feldspar age values reported by Heizler & Harrison (1986) and Foland (1974).

QUANTITATIVE FUNDAMENTALS OF DIFFUSION

Fick's Laws of Diffusion

This is a study of effects resulting from $^{40}Ar^{*}$ diffusion in natural feldspar. Diffusion can be defined as the transfer of a substance from a region of high conentration to a region of low concentration, in which the driving force is the random motion of the diffusant. Fick's First Law, discussed in Crank (1975), adapts Fourier's Law of Heat Conduction to mass flux, which provides a theoretical basis for molecular diffusion:

$$F = -D\,\frac{\partial C}{\partial x} \tag{1.1}$$

where F is the flux, D (D>0) is the diffusion coefficient, C is the concentration and x is the independent space variable. The minus sign indicates that mass flow is in the direction of decreasing concentration. In the case of unsteady-state diffusion, where concentration may vary in a solid region as a function of the space coordinates and time, Fick's Second Law can be used:

$$\frac{\partial C}{\partial t} = D\left(\frac{\partial^2 C}{\partial x^2} + \frac{\partial^2 C}{\partial y^2} + \frac{\partial^2 C}{\partial z^2}\right) \tag{1.2}$$

This equation can be adapted, using coordinate transformations, to describe radial flow in a symmetric sphere. The resulting concentration distribution for a sphere of radius r with an initially uniform concentration C_0 held in an infinite reservoir of zero concentration is given by:

$$C = C_0 \frac{2r}{\pi R} \sum_{n=1}^{\infty} \frac{(-1)^n}{n} sin \frac{n\pi R}{r} exp(-n^2\pi^2 Dt/r^2) \quad (1.3)$$

where R is the gas constant and t is time.

Fractional Loss

Fractional loss f can be found using the following equation from Foland (1974):

$$f = \frac{[Ar^{40}]^t - [Ar^{40}]^0}{[Ar^{40}]^e - [Ar^{40}]^0} \quad (1.4)$$

where $[Ar^{40}]^t$ is the concentration of ^{40}Ar in orthoclase after time t, $[Ar^{40}]^0$ is the initial concentration of ^{40}Ar in orthoclase, and $[Ar^{40}]^e$ is the concentration of ^{40}Ar in orthoclase at equilibrium. Assuming total loss at equilibrium, after infinite time, the quantity f is simply the fractional loss of ^{40}Ar. McDougall & Harrison (1999) note that, "In cases where we cannot directly image the distribution of the diffusant in the solid of interest, but can measure the amount of uptake or loss from the solid, solutions relating the degree to which the system has approached equilibrium to Dt/r^2 can be useful." McDougall & Harrison (1999) also show the fraction of loss can also be related to the diffusion coefficient by:

$$f = 1 - (6/\pi^2) \sum_{1}^{\infty} (1/n^2) exp(-n^2\pi^2 Dt/r^2) \quad (1.5)$$

Data obtained from a step-heating analysis can easily be substituted into Equation 1.4 to calculate the value of f, which can then be substituted into Equation 1.5 to solve for D, the diffusion coefficient at a given temperature.

The Arrhenius Equation

The diffusion of argon in a mineral lattice is a thermally controlled process with a net rate of transfer that increases with increasing temperature. This is due to the fact that intra-lattice migration is permitted mainly by the existence of lattice defects within a mineral's crystalline structure, which become more prominent with increasing temperature. The relationship between the diffusion coefficient and variation in temperature is expressed quantitatively by the Arrhenius equation:

$$D = D_0 exp(-E_a/R\mathrm{T}) \tag{1.6}$$

where D_0 is the maximum diffusion coefficient at infinite temperature, E is the activation energy, R is the gas constant, and T is temperature. By taking the logarithm of both sides of Equation 1.6 we obtain

$$log\ D = log\ D_0 - \frac{E_a}{2.303R}\ \frac{1}{T} \tag{1.7}$$

The activation energy E and frequency factor D_0 parameters can be acquired from a linear array of diffusion data on an Arrhenius-type plot (Fig. 4). For this type of plot, the logarithm of the diffusion coefficient D is plotted against the reciprocal of absolute temperature. Equation 1.7 is in the form of the equation for a straight line, $y = mx + b$, where y is the $log\ D$ coordinate, $E/(2.303R)$ is the slope of the line, $1/T$ is the x-axis, and $\log(D_0)$ is the y-axis intercept of the line. The diffusion coefficient D can be calculated using Equations 1.4 and 1.5, as discussed above. Arrhenius plots for specimens with a single scale of diffusion (i.e., a single, characteristic diffusion dimension) would be expected to yield a straight line.

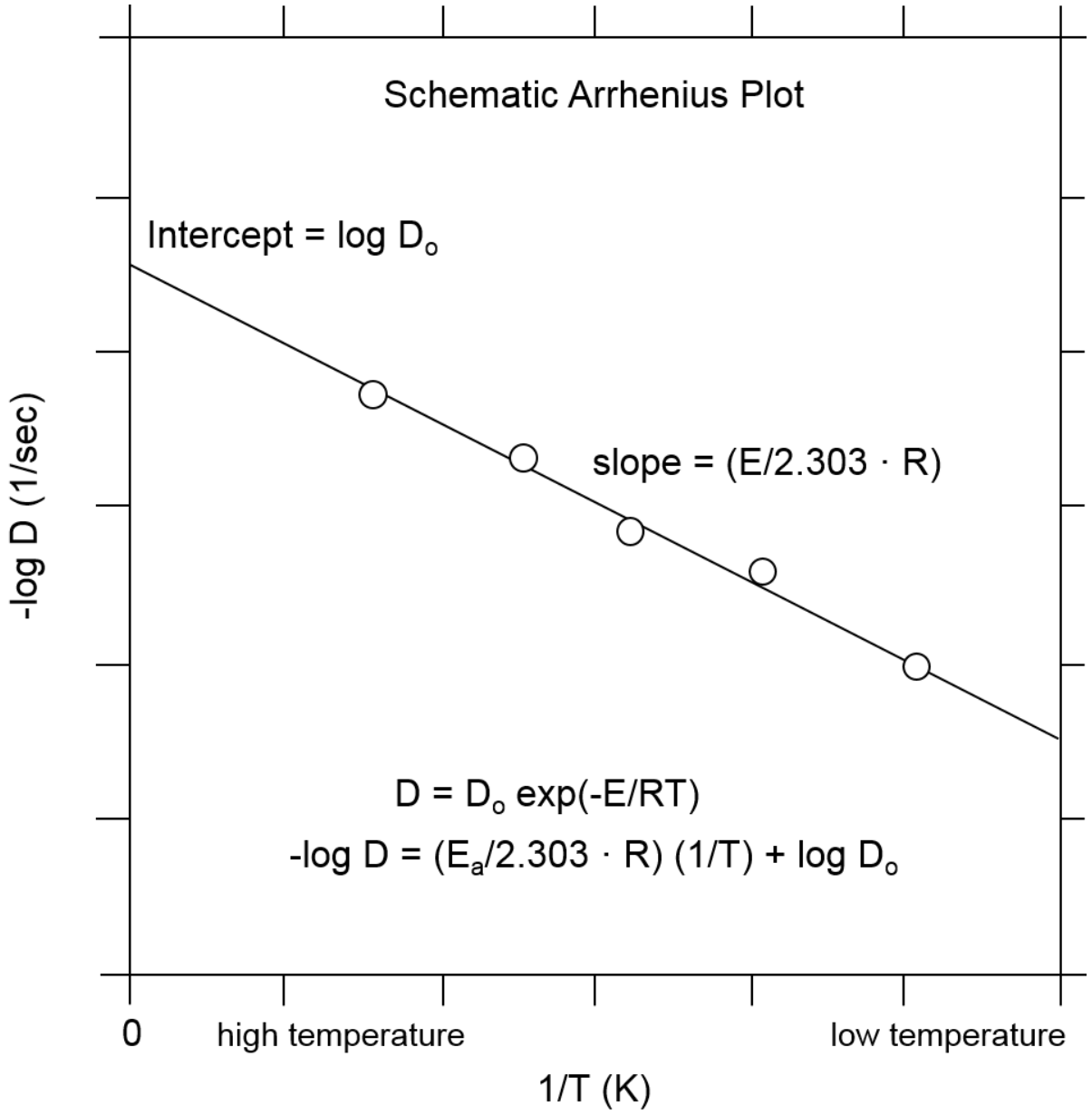

Figure 4. Schematic Arrhenius plot. D = diffusion coefficient; E = activation energy; D_o = frequency factor (adapted from Harrison and McDougall, 1999; Figure 5-6, p. 144). Activation energy and frequency factor can be determined graphically when the diffusion coefficient and temperature are known.

MODELS FOR RADIOGENIC ARGON DIFFUSION IN FELDSPARS

Grain-scale Diffusion

The first modern experiments on argon diffusion in feldspars to document stability during experimental runs and present results relevant to natural samples were the work of Foland (1974). Considering homogenous, unaltered grains, sampled from a pegmatite at the Benson Mines, he showed that the effective dimension for $^{40}Ar^{*}$ diffusion is the actual physical size of the crystal, except where broken by cleavage planes or fractures. The hypothesis that diffusion occurs at the grain scale, illustrated in Figures 5a and 5b, implies that feldspar crystals from a slowly cooled terrain will have a higher concentration of $^{40}Ar^{*}$ at their cores, with progressively lower concentrations toward their rim. Foland calculated diffusion coefficients for different size fractions using an isotropic model for spherical grains, and found them constant with time for a given size fraction at constant temperature and pressure. This result indicates that, for this sample, the primary mechanism of argon release was volume diffusion, and that radiogenic argon was contained within a single diffusion domain. Foland suggested that perthitization may reduce the effective grain size for diffusion and allow diffusional loss of $^{40}Ar^{*}$ at temperatures lower than characteristic of non-perthitic feldspars. The results were reaffirmed by Foland & Xu (1990) through similar experiments on orthoclase from the same samples, in which it was also demonstrated that sample irradiation required for $^{40}Ar/^{39}Ar$ age determinations does not induce any artificial diffusion of $^{40}Ar^{*}$.

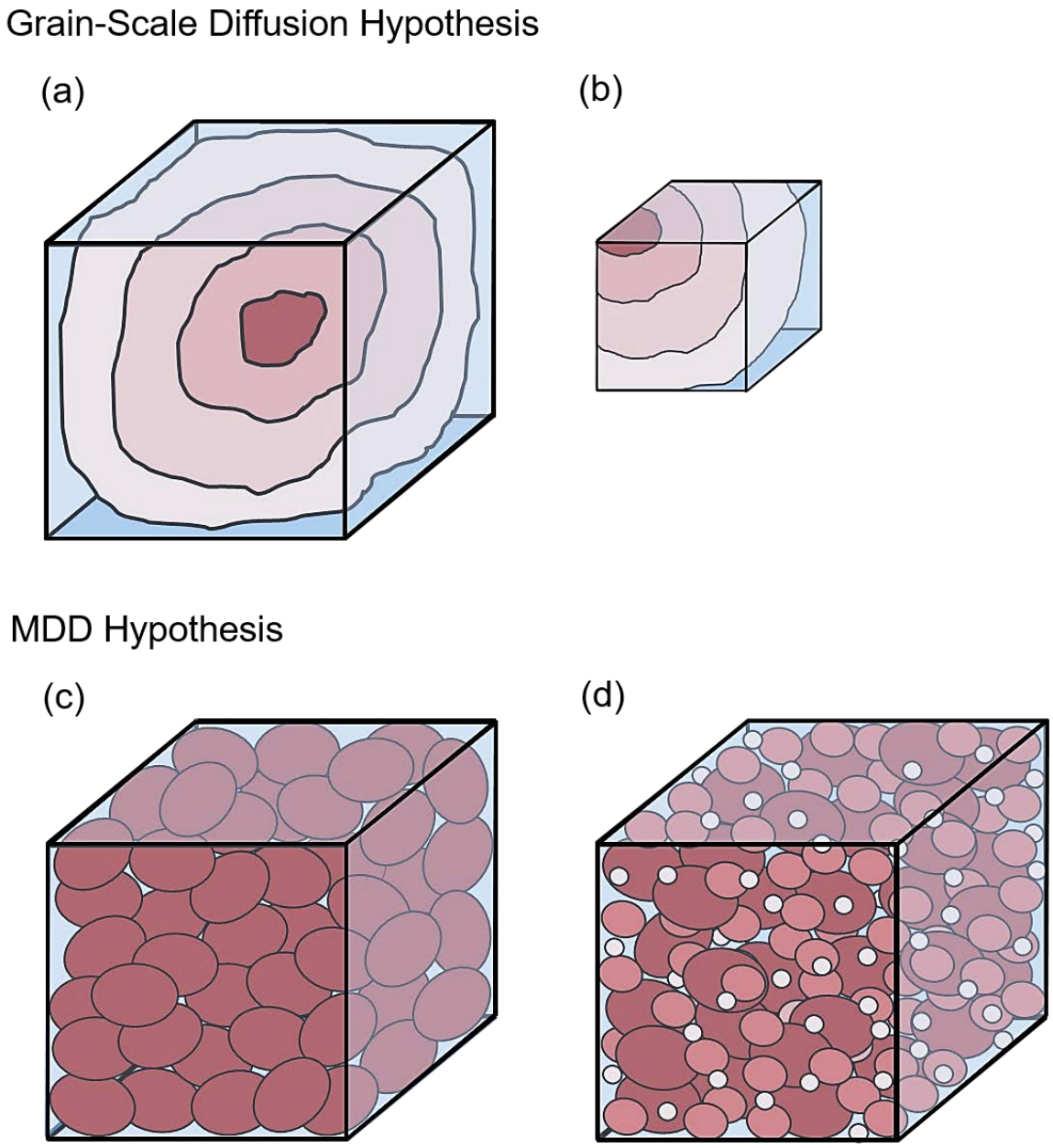

Figure 5. Illustrations of the grain-scale diffusion (top) and multi-diffusion domain (bottom) hypotheses. **(a)** Represents a whole grain with darker colors indicating higher concentrations of $^{40}Ar^{*}$. **(b)** Grain fragment with original core now exposed at the surface. **(c)** Represents a crystal possessing only one diffusion domain size that is independent of the physical grain size. **(d)** Represents a crystal possessing three domain sizes.

The Multi-Diffusion Domain Hypothesis

One of the more vigorously contested hypotheses to describe argon diffusion in feldspars is the Multi-Diffusion Domain (MDD) model (Lovera et al., 1989; Heizler & Harrison, 1988; Zeitler, 1987), and is thoroughly reviewed and described in McDougall & Harrison (1999) and in Harrison & Lovera (2014). The development of this model, represented in Figures 5c and 5d, was fostered by the observation of "saddle-shaped" $^{40}Ar/^{39}Ar$ age spectra (Zeitler, 1987) and non-linearity on Arrhenius diagrams for $^{40}Ar^{*}$ diffusion data from alkali feldspar, which appeared to be inconsistent with a single diffusion domain. The MDD model is based on the premise that within a given sample, radiogenic ^{40}Ar is distributed among multiple domains at the sub-grain scale that can differ in size, diffusion coefficient, and activation energies (as depicted in Figure 5c and 5d) (Lovera, 1989; Lovera et al., 1989). Figure 6 depicts hypothetical Arrhenius arrays for specimens possessing single and multiple diffusion domain sizes. According to the MDD model, during step-heating experiments, gas contributed by the smallest domain sizes will dominate the argon that is measured in the initial steps (low temperature). As the heating schedule progresses to higher temperatures, the smaller domains will become completely degassed, leaving only the larger domain sizes to contribute to the argon being measured. According to this model, the non-linearity common to feldspar data in Arrhenius diagrams (e.g., Fig. 6) represents the degassing of these different domain sizes. The utilization of the MDD hypothesis for modeling thermochronologic histories has gained widespread acceptance within the geochronlogy community and has been applied sucessfully to a range of geochronologic studies (Grove et al., 2003; Harrison et al., 2000, 1995; Quidelleur et al., 1997, etc.).

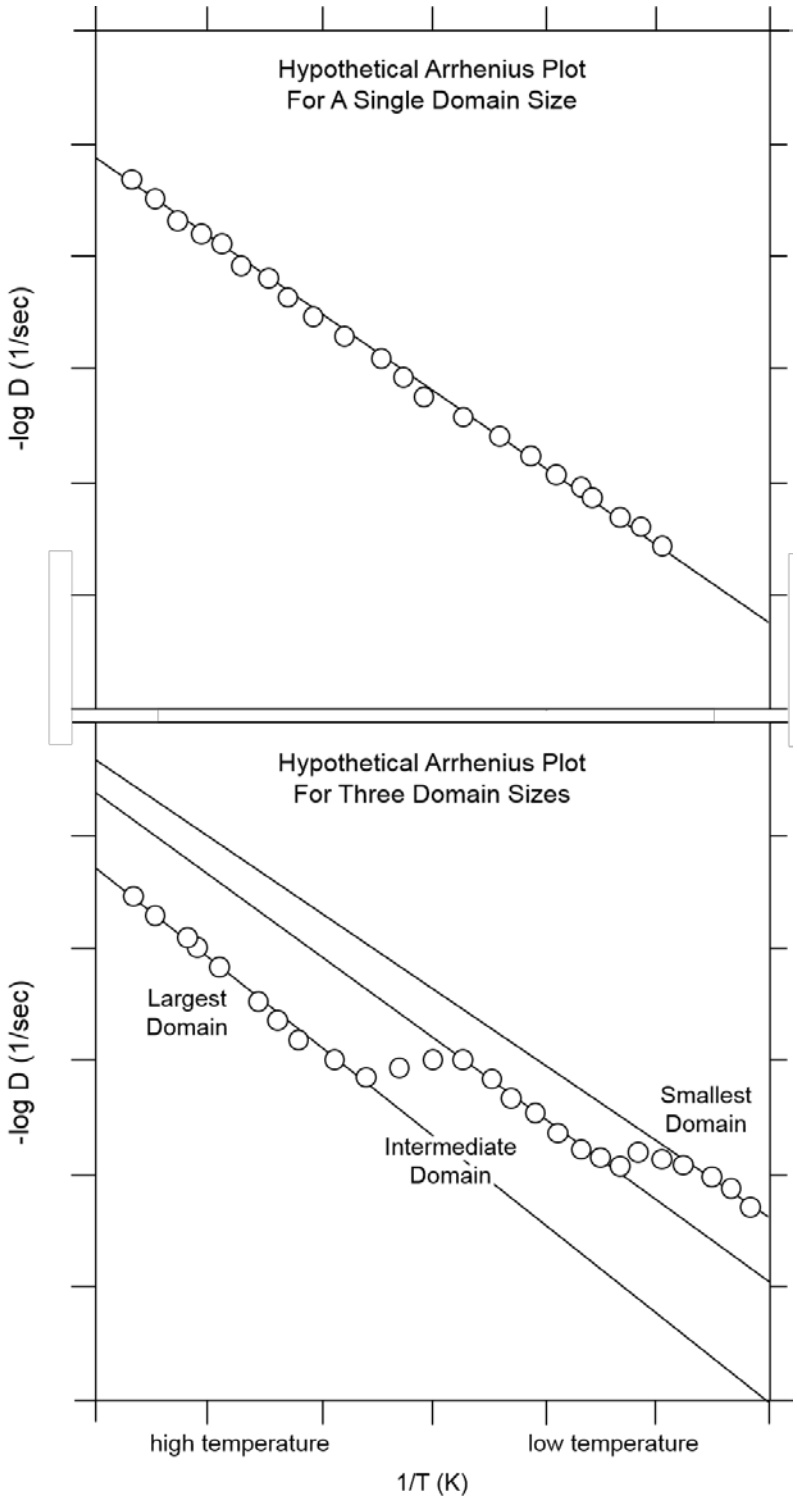

Figure 6. Illustrations of hypothetical Arrhenius plots for a specimen containing a single domain size (top) and three domain sizes (bottom) as interpreted through the multi-diffusion domain hypothesis.

Although the MDD hypothesis has been found suitable for modeling thermal histories from feldspars by a large group of researchers, there are still many that find the modelling method inappropriate for interpreting feldspar $^{40}Ar/^{39}Ar$ ages (Parsons et al. 1988, 1999, 2010; Burgess et al. 1992; Foland, 1994; Villa, 1994; Waldron et al. 1994; Lee, 1995; Reddy et al. 1999; Cassata & Renne, 2013). The observation of non-linearity on Arrhenius diagrams is one of the main factors that led to the development of MDD modelling. Multiple studies suggest, however, that non-linearity may arise through crystal chemical factors that are not consistent with the multi-diffusion domain hypothesis.

Xu & Foland (1991) and Foland et al. (1992) used the same 240 μm, homogenous, orthoclase crystals, already proven to diffuse at the grain-scale and yield linear Arrhenius arrays in Foland (1974), in a series of controlled experiments. Crystals were wrapped in Pt-foil and incrementally heated in a furnace to 700°C for a period of three weeks to induce the the loss of ^{40}Ar. These samples were then irradiated, and subsequently step-heated following the same heating schedule as the experiments in Foland (1974). The resultant data, however, were vastly different from those observed in the 1974 study. The age spectrum for the analysis yielded progressively older apparent ages for successive increments, from low-temperature to high, with an upwardly concave shape that steepens sharply following the first 80–85% of total $^{39}Ar_K$ released. Unlike the Arrhenius plot obtained for diffusion data in the 1974 study, diffusion rates begin to deviate from a straight line at ca. 800–850°C. Foland interprets this as resulting from extensive fracturing in the sample that was produced by heating prior to irradiation. This fracturing caused the orthoclase to behave as having multiple diffusion domains of different size. This evidence demonstrates the importance of practicing caution when selecting samples for $^{40}Ar/^{39}Ar$ incremental heating analyses.

Structural defects within a crystal can obscure natural radiogenic argon distribution and quite probably lead to an incorrect interpretation.

Arnaud & Kelley (1997) and Wartho et al. (1999) performed detailed Ar diffusion studies on gem-quality orthoclase from Madagascar in attempt to further investigate the mechanisms of argon diffusion in structurally simple feldspars. *In situ* UV-laserprobe analyses of these orthoclase grains from core to rim showed, for the crystal of their study, that Ar diffuses at the grain-scale. The Arrhenius arrays for this sample, however, were not linear, showing that non-linearity on Arrhenius diagrams can occur with crystals possessing a single diffusion domain, in contrast to the interpretations of Harrison and others (Lovera et al., 1989, 1991, 1993; Harrison et al., 1991).

Cassata & Renne (2013) expanded upon such work through step-heating Ar diffusion experiments for a range of feldspars of diverse compositions, structural states, and microstructural characteristics in order to better assess the accuracy of thermal models and to gain a more thorough understanding of the mechanisms and pathways by which argon diffuses in feldspars. The results of their experiments led Cassata & Renne (2013) to suggest that there is no single set of diffusion parameters that can be broadly applied in feldspar thermal modeling, and that data should be obtained individually for each sample. They found the conjecture presented by Foland (1974) to hold true – that unaltered feldspar crystals, with or without coherent exsolution lamellae, diffuse at the grain-scale – but feldspars affected by hydrothermal alteration and/or feldspars that display incoherent sub-grain intergrowths do not diffuse at the grain-scale. Cassata & Renne (2013) suggest that in cases of grain-scale diffusion, intrinsic diffusion kinetics and structural changes that occur within a crystal as it is heated in the laboratory account for non-linearity observed on Arrhenius-type plots.

In efforts to expand comprehension of how structural features, such as the boundaries of perthite lamellae, affect argon loss in alkali feldspars, Parsons et al. (1988) performed $^{40}Ar/^{39}Ar$ step-heating analyses on non-turbid, 'strain-controlled' cryptoperthites and turbid, coarse microperthites, fully characterized by transmission electron microscopy, from the Klokken syenite intrusion in South Greenland. The cryptoperthites yielded ages ranging from 1162-1125 Ma, whereas the coarse microperthites gave ages as low as 650 Ma. Parsons et al. (1988) concluded that only higher temperature release reflects volume diffusion, and that turbidity generated in feldspars by fluid-rock interactions results in argon loss that is amplified with increasing degree of turbidity. This is a process that laboratory degassing *in vacuo* does not duplicate (Burgess et al., 1992; Parsons et al., 1999, 2013, 2015).

Fluid-rock interactions play a very important role in the diffusion of an isotope from a mineral. Confirmed by modern petrology, the chemical and isotopic record of minerals can be greatly affected by aqueous recrystallization. Realizing the importance of microtextures generated in feldspars in the presence of a fluid, Villa & Hanchar (2013) studied microcline from the Aar metagranite, Central Alps, Switzerland, and combined data from stepwise leaching experiments for Rb-Sr and Pb-Pb, $^{40}Ar/^{39}Ar$ step-heating analyses, and microprobe analyses to evaluate the applicability of using hydrothermally altered feldspars for modeling its thermal history. Their findings show that the sample's Pb-Sr-Ar multi-isotope record was not a function of "thermally activated diffusion of U, Pb, Rb, Sr, Ba, Ar, Ca, Cl, K, and Na," but rather new growth of K-feldspar due to fluid interaction, indicating that the samples record a hygrochronologic history, not a thermochronologic one. $^{40}Ar/^{39}Ar$ age spectra for the samples exhibit a staircase-shaped age spectra having young ages for initial, low-temperature steps which 'step-up' in age for progressive, high-temperature steps. Villa & Hanchar (2013)

assert that the staircase-shaped age spectra is a result of polymineralic mixture within the sample. Estimation of diffusion parameters for the sample reveals a non-linear relationship between rate of diffusion and temperature, interpreted by the authors as reflecting "the rate of a sum of unrelated, non-linear *in vacuo* structural rearrangements," not proceeding from volume diffusion. Villa & Hanchar (2013) conclude that $^{40}Ar/^{39}Ar$ step-heating data for feldspars do not reflect that of Ar loss in nature, and, subsequently, should not be used for modeling thermal histories, but as hygrochronometers because they reflect the most recent fluid-induced recrystallization event. As a result of these findings, the authors emphasize the great importance of exercising caution when interpreting $^{40}Ar/^{39}Ar$ results in the absence of petrographic and petrologic characterization of the sample.

In efforts to further assess mechanisms of Ar release from K-feldspar samples degassed in the laboratory and in nature, Villa (2014) examines recent literature and modelling techniques. He concludes that, "the isotopic record of K-feldspar in geological samples is not a unique function of temperature, as recrystallization promoted by aqueous fluids is the predominant mechanism controlling isotope transport, and K-feldspar should, therefore, be considered a hygrochronometer, rather than a thermochronometer."

SAMPLE LOCATION & PETROGRAPHY

Samples

The Grenville-aged, gneiss-hosted, iron-ore deposits, that became the open pit mining operation at the Benson Mines, were discovered accidentally by engineers in 1810 while performing a survey for a military road, when the magnetite-rich rocks found in the area caused their compass needles to behave erratically. Production of iron-ore at the site did not commence until 1895. As detailed in Lupulescu et al. (2014), this marked the beginning of a long series of openings, closures, and transfers of ownership of the mines, until its final closure by its most recent owner, the New York Division of Jones & Laughlin Steel Corporation, in 1978. Over the life of the mine, the open-pit grew to be about 4 km long by 244 m wide. At peak of production in the 1960's, operations at the Benson Mines employed as many as 840 workers and had a capacity for processing just over 2 million tons of ore per year. Roughly 26 million tons of iron-ore are estimated to have been produced from the Benson Mines over its nearly 85 year life-span.

Since the closure of the Benson Mines in 1978, the open-pit has since been inundated and transformed into a small lake. The four samples used for this study were collected from waste piles on the Benson Mines site in 2013 by Dr. Robert Badger of State University of New York at Potsdam. The samples comprise magnetite-orthoclase-sillimanite gneiss, orthoclase-garnet-magnetite gneiss, clinopyroxene-hornblende syenite, and pegmatite. Each sample was labeled and described according to its mineralogical and petrographic characteristics. Petrographic thin-sections for the samples were prepared over the summer of

2013, and petrographic grain mounts were made for BEN-5, BEN-17, and BEN-24 in January 2014 by Spectrum Petrographic Inc. (Vancouver, WA).

Petrography

BEN-5: Magnetite-orthoclase-sillimanite Gneiss

In hand specimen, BEN-5 is a light to dark gray, medium- to coarse-grained, porphyritic rock having very coarse prisms of sillimanite (up to 6 cm long) that define a lineation (Fig. 7). The minerals magnetite, orthoclase, sillimanite, quartz, sericite, and chlorite were identified upon petrographic investigation (Fig. 8). Magnetite constitutes ca. 35% of the sample in thin-section and is found mostly as massive, subhedral grains that are 0.1–0.75 mm in size. Some crystals, however, are well formed and display an octahedral habit. Overall, magnetite is interstitial to orthoclase, which is the next most abundant mineral at ca. 30% by volume. Orthoclase crystals range in size from 1–4 mm and are generally subhedral, though some smaller grains are euhedral. A photomicrograph of a single orthoclase crystal in Figure 9 shows characteristic properties of K-feldspar in the sample. Fractures within orthoclase appear to be preferentially aligned perpendicular to a lineation defined by sillimanite, likely indicating that the rock experienced tectonic-related structural deformation. Minor amounts of sericitic alteration is common along internal fractures of orthoclase crystals. Coarse, prismatic sillimanite, ranging from 0.1–1.0 mm along its short axis, makes up ca. 25% of the total rock volume in thin-section. Sericitic alteration is evident in most sillimanite grains, and, in some instances, has completely altered sillimanite grains. Quartz is present in the sample as inclusions within feldspar grains, but is very minor, making up less than 5% of the sample.

Figure 7. Photograph of the magnetite-orthoclase-sillimanite gneiss, BEN-5, in hand specimen. A cm-thick layer rich in yellow to tan sillimanite is evident, and the upper half of the sample contains conspicuous anhedral magnetite crystals.

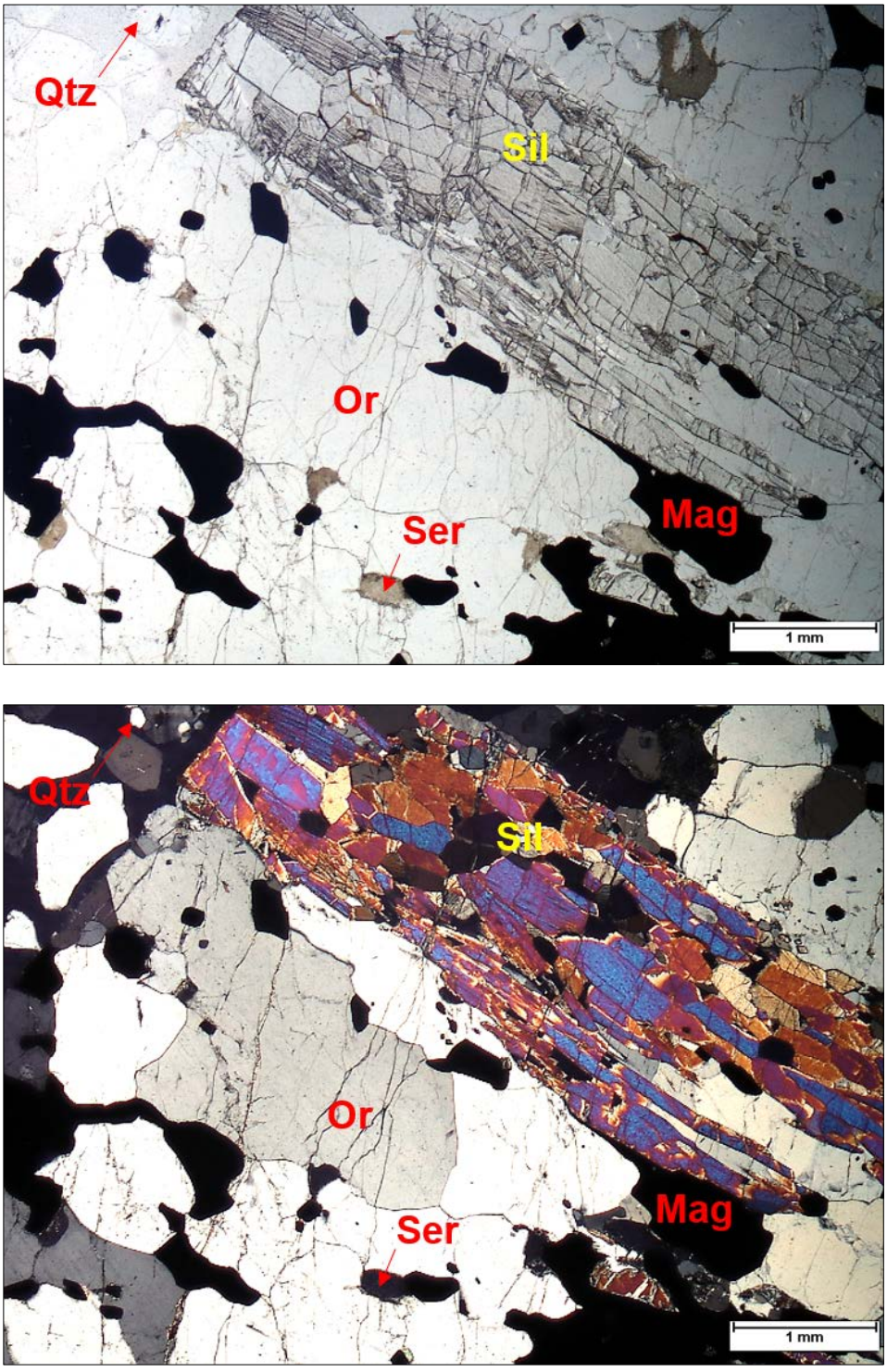

Figure 8. Photomicrographs of BEN-5 in plane-polarized light (top) and cross-polarized light (bottom) showing the petrography of the magnetite-orthoclase-sillimanite gneiss of the Benson Mines samples. Orthoclase crystals with minimal impurities were selected for $^{40}Ar/^{39}Ar$ analysis, although crystals within the sample commonly contain inclusions of magnetite.

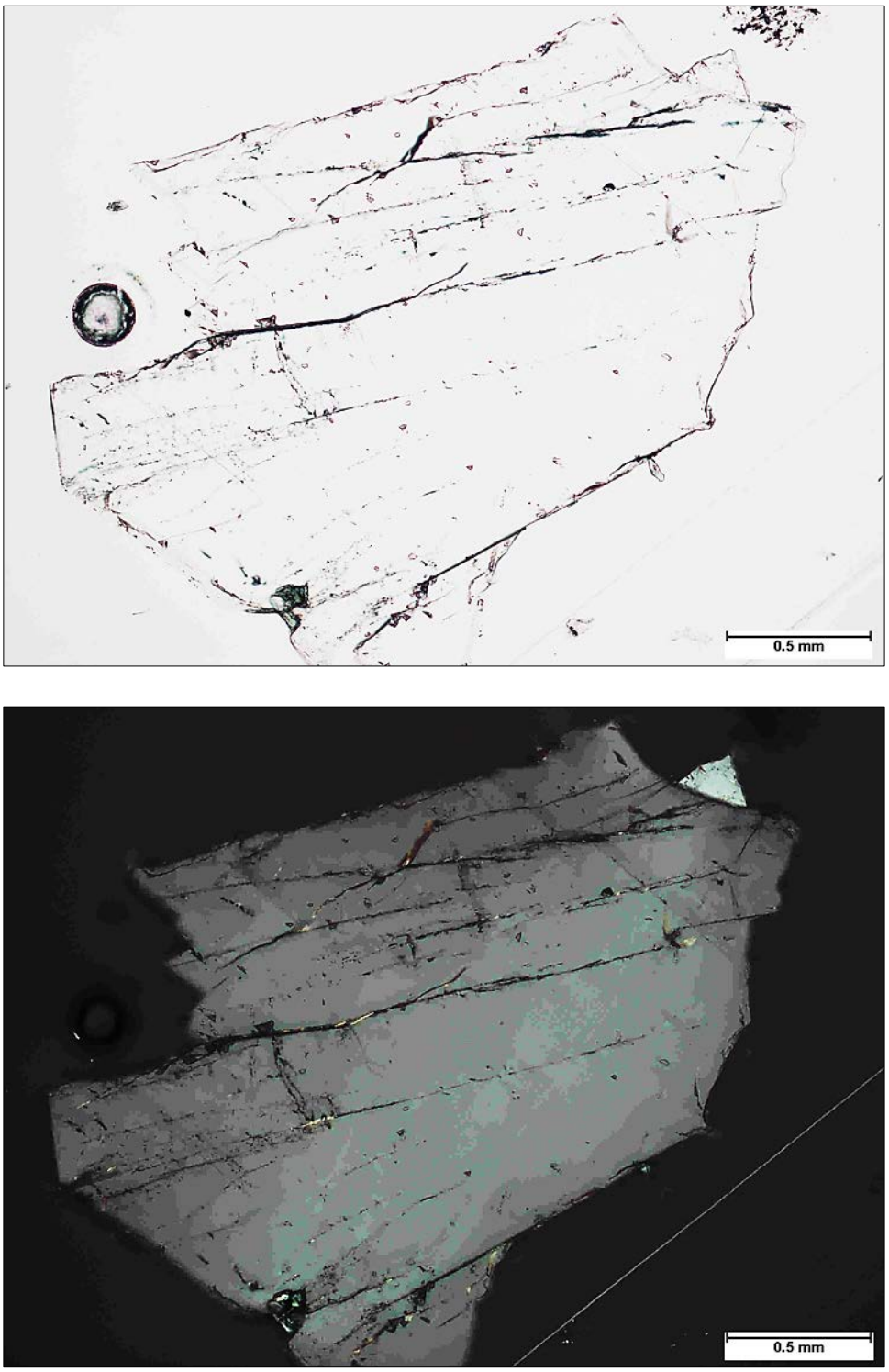

Figure 9. Photomicrographs of a single feldspar grain from BEN-5, mounted in epoxy, in plane-polarized light (top) and cross-polarized light (bottom).

BEN-6: Clinopyroxene-hornblende Syenite

Sample BEN-6 is a clinopyroxene-hornblende syenite that has the coloration of salt and pepper in hand specimen and is coarse-grained (Fig. 10). Lineation in the rock is weakly developed and defined by the alignment of pyroxene, amphibole, and biotite. In thin-section, clinopyroxene, hornblende, alkali feldspar, plagioclase, biotite, quartz, magnetite, and alteration minerals sericite and chlorite are observed (Fig. 11). Augite, at 30% by volume, is roughly equal in abundance with hornblende and occurs as 1.5–2.5 mm, subhedral, prismatic crystals that are light brown to dingy yellow in cross-polarized light. Augite grains are highly fractured and cleavage plane intersections of roughly 90^{o} are clearly apparent. Hornblende crystals are 1–2 mm, on average, in their longest dimension and commonly exhibit subhedral, prismatic habit. In cross-polarized light, hornblende crystals have a rusty brown to orange pleochroism, and are often in contact with pyroxene and orthoclase crystals. K-feldspars in this sample, having average grain size of 0.5–3.0 mm, constitute ca. 25% of total rock volume and are all extremely perthitic, with lamellae thickness ranging from 0.015–0.15 mm. K-feldspar crystals are anhedral to subhedral that exhibit a massive habit and formed interstitially to amphibole and pyroxene. Minor alteration of K-feldspar to sericite is observed along mineral fractures. Plagioclase feldspar is also found in the sample as 0.25 - 0.75 mm wide grains that are anhedral and exhibit prominent albite twinning (~5% total volume). Plagioclase crystallized interstitially to clinopyroxene and hornblende grains, and has experienced a small degree of sericitic alteration along crystal rims. Biotite crystals, comprising ca. 5–10% of the syenite, are distributed seemingly randomly in the sample and likely represent late-stage crystallization. Biotite crystals range from 1–3 mm in diameter, occurring as subhedral to euhedral grains possessing a lamellar to micaceous habit. Biotite has experienced minor chloritic and sericitic alteration near rims and fractures. Quartz is very

Figure 10. Photograph of the clinopyroxene-hornblende syenite, BEN-6, in hand specimen. The sample is porphyritic with grains of augite, hornblende, and biotite that are generally smaller than feldspar. A few large phenocrysts (~3 cm) of feldspar are also present (not pictured).

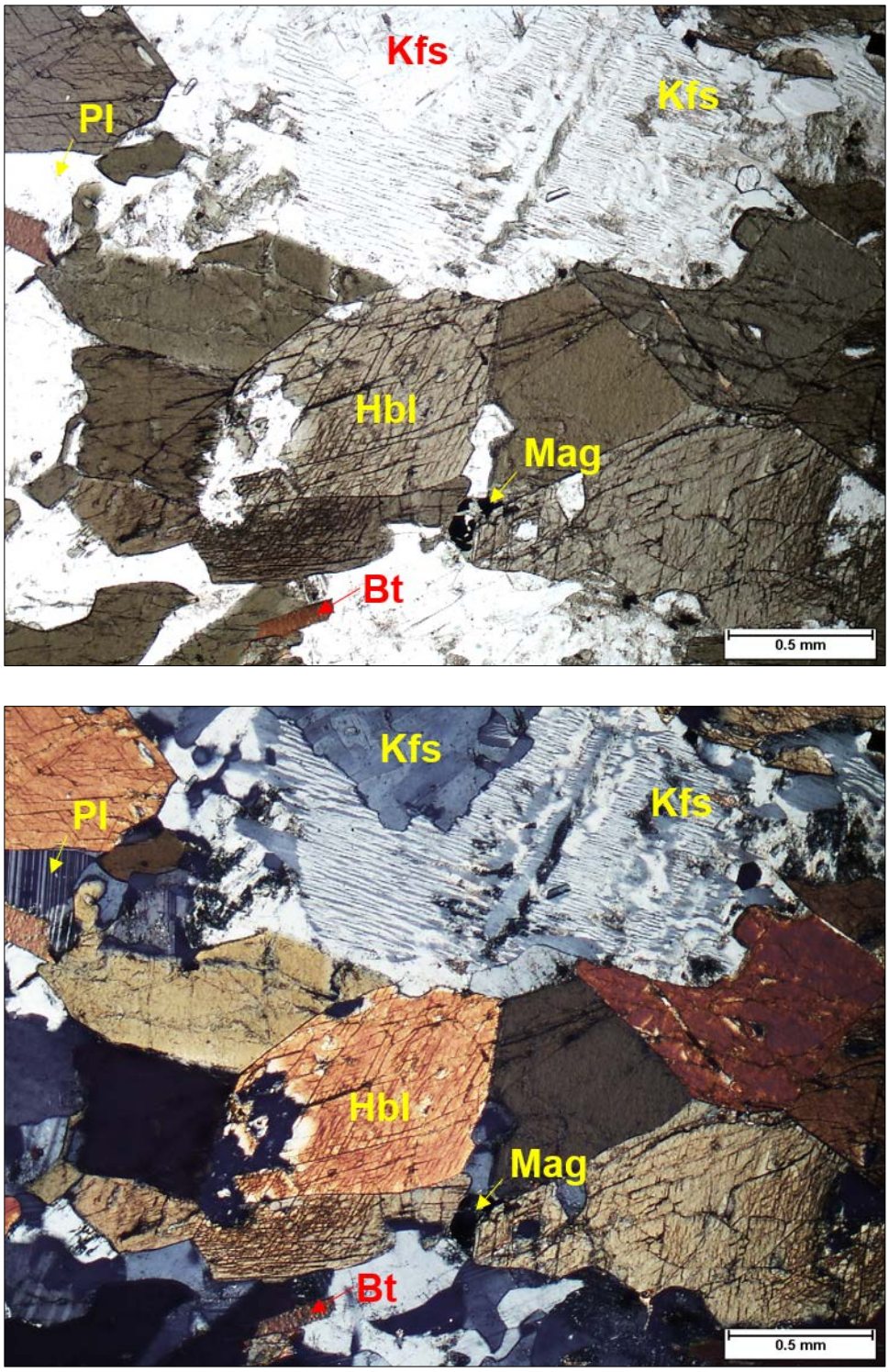

Figure 11. Photomicrographs of BEN-6 in plane-polarized light (top) and cross-polarized light (bottom) showing the petrography of the clinopyroxene-hornblende syenite of the Benson Mines samples. Note the microperthitic texture in feldspar grains. Lamellae range in thickness from 15 to 150 μm.

sparse (≤1%) and appears as 0.1–0.15 mm inclusions within feldspar and amphibole.

BEN-10: Orthoclase-garnet-magnetite Gneiss

Sample BEN-10 is an orthoclase-garnet-magnetite gneiss. In hand specimen, it is granoblastic and dark brown to black with compositional layers 0.5-2.0 cm thick (Fig. 12). Magnetite and biotite constitute darker layers, while lighter layers are richer in orthoclase. Upon petrographic investigation, orthoclase, garnet, magnetite, biotite, quartz, sericite, and chlorite were identified (Fig. 13). Orthoclase crystals, the most abundant phase (~50%), are generally ~0.75-1.5 mm in maximum dimension, though there are occasional grains up to 6 mm across. They are sub- to euhedral with a massive habit. Minor alteration to sericite is observed along fractures in some orthoclase crystal, and many crystals contain inclusions of quartz and/or magnetite. Twinning and perthitic textures are absent from this sample. Garnet comprises ~25% of the sample, and are found as 1-3 mm crystals that are sub- to euhedral. Most grains are isotropic in cross-polarized light, although some have a very weak birefringence. Garnets contain multiple quartz inclusions that tend to be round and lack preferred orientation. Magnetite makes up ~10% of the rock's volume, and crystals display an anhedral to subhedral, massive habit and are ~1.5 mm in size. Biotite crystals, ~1 mm in maximum dimension, constitute 5-10% of the sample and exhibit a brown to olive pleochroism. At less than 5%, quartz is found almost entirely as inclusions within orthoclase. Very minor alteration of orthoclase and biotite is observed.

Figure 12. Photograph of the gneiss, BEN-10, in hand specimen. The sample contains abundant 1-2 mm crystals of garnet, and displays prominent gneissic banding. The darker half of the sample at the top is more heavily concentrated in magnetite and biotite.

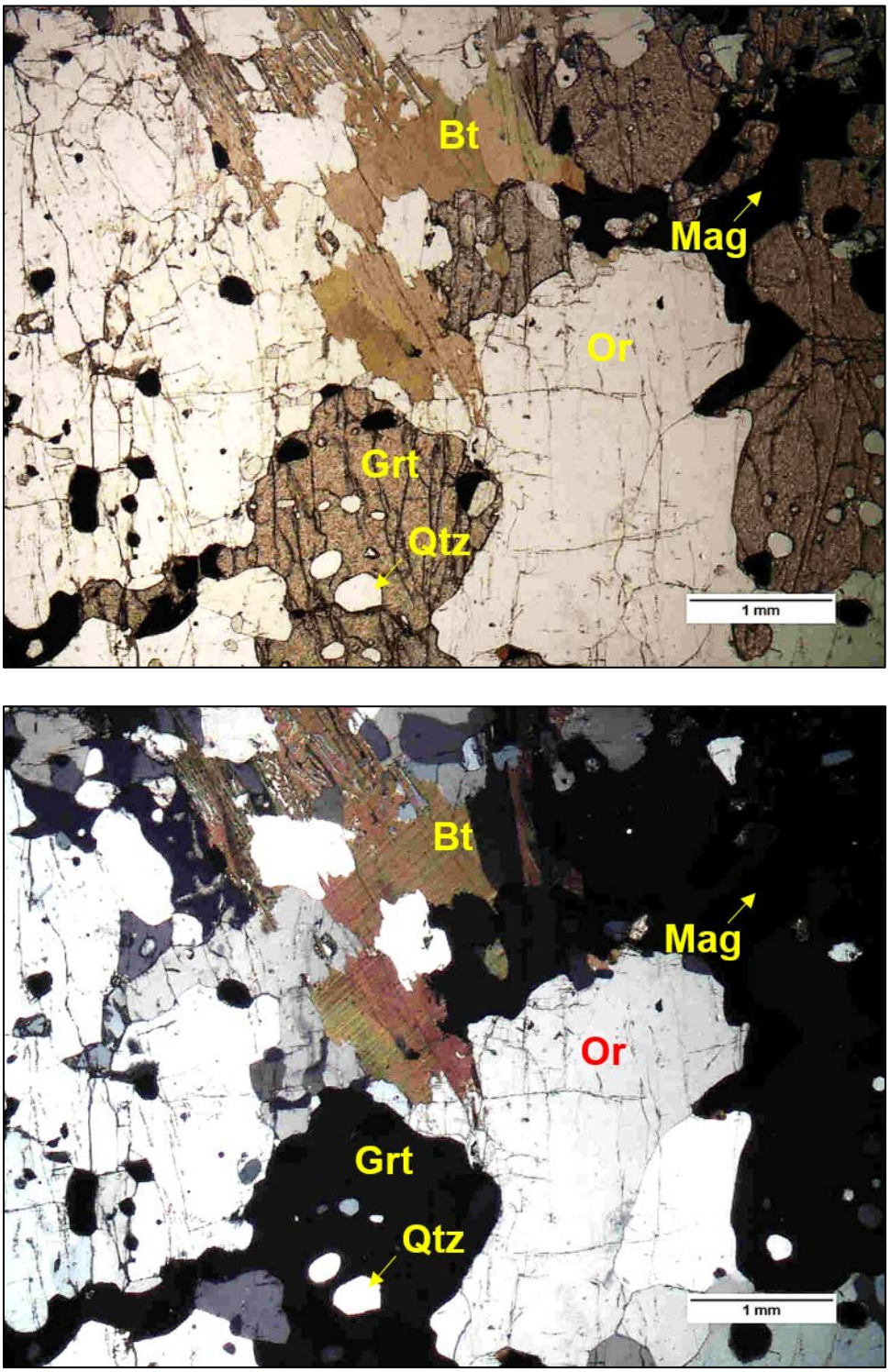

Figure 13. Photomicrographs in plane-polarized light (top) and cross-polarized light (bottom) showing the petrography of the gneiss sample, BEN-10. Feldspar are similar to that of BEN-5. Other more abundant phases such as garnet and biotite show a high degree of alteration.

BEN-17: Pegmatite

In hand sample, BEN-17 is translucent pink in color, and is composed almost entirely of blocky feldspar with cleavage planes well defined (Fig. 14). Very sparse inclusions of biotite and muscovite are also observed. Due to very large grain sizes, thin-sections were not prepared for pegmatite samples, however, a grain mount of orthoclase was made from the sample to examine K-feldspar characteristics as it pertains to $^{40}Ar/^{39}Ar$ analysis. Photomicrographs from BEN-17 (Fig. 15) illustrate the general character of orthoclase within the sample. Overall, grains are euhedral, exhibiting perfect cleavage on two planes, with no perthitization evident and only a weakly defined pattern of "gridiron" (albite and pericline law) twinning.

BEN-24: Pegmatite

BEN-24, which is also a pegmatite, is mainly composed of large books of biotite 1-3 cm in diameter on average (but up to 4.5 cm), blocky K-feldspar, and quartz (Fig. 16). Minor sulfide minerals are also found throughout. The rock has color that varies from a dull, translucent pink to white in areas where K-feldspar is most abundant, to dark-gray to black in areas where biotite is more prominent. A grain mount of orthoclase was also made from this sample for the examination of K-feldspar characteristics as it pertains to $^{40}Ar/^{39}Ar$ analysis. Photomicrographs of orthoclase from BEN-24 are in Figure 17. The grain pictured appears to be a crystal fragment and shows subtle polysynthetic twinning.

Figure 14. Photograph of the pegmatite, BEN-17, in hand specimen. The sample is composed, almost entirely, of blocky, translucent pink orthoclase.

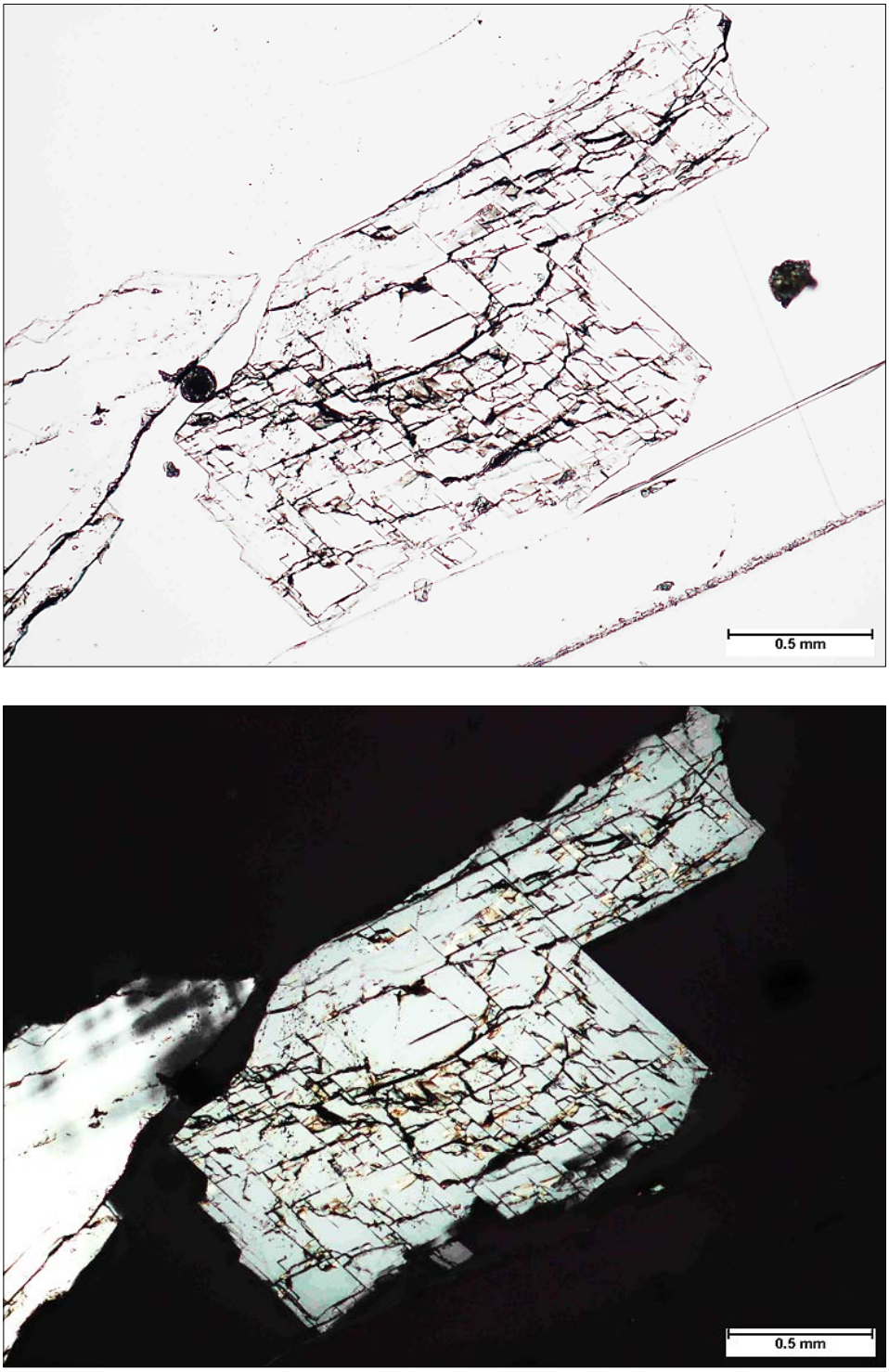

Figure 15. Photomicrographs of feldspar grains from BEN-17 in plane-polarized light (top) and cross-polarized light (bottom). The center grain displays prominent cleavage in two directions and lacks twinning, however, the grain pictured at the left of the photograph does exhibit minor "gridiron" twinning.

Figure 16. Photograph of the pegmatite, BEN-24, in hand specimen. Large "books" of biotite crystals (1-3 cm in diameter on average) are most prominent in this sample, along with cm-scale orthoclase (dull pink to white) and quartz crystals (grey).

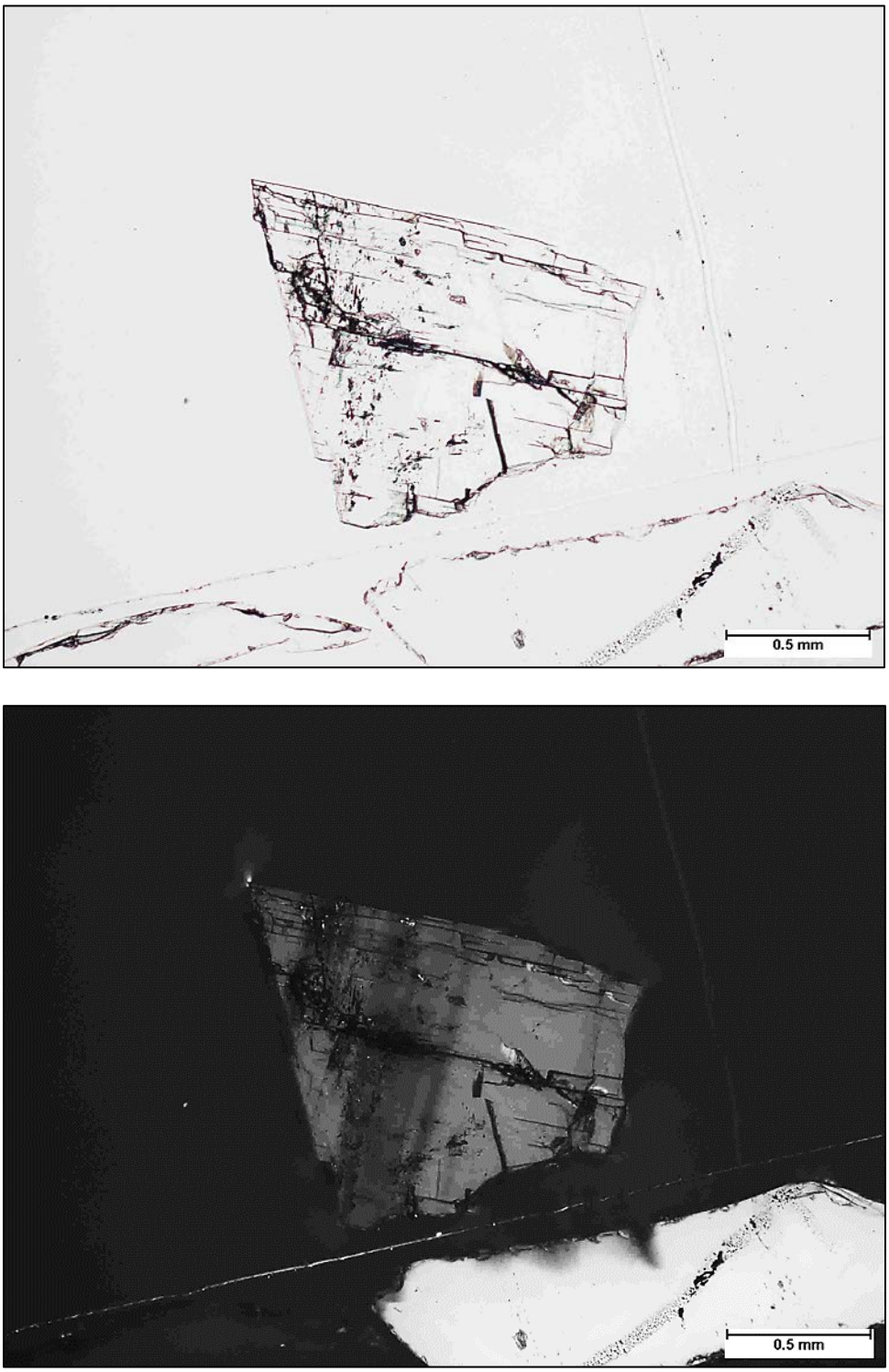

Figure 17. Photomicrographs of a single feldspar grain from BEN-24 in plane-polarized light (top) and cross-polarized light (bottom). The grain pictured is fractured and exhibits twinning.

ANALYTICAL METHODS

Sample Preparation

Bulk rock specimens were crushed with the use of a Braun 'Chipmunk' rock crusher and with a hammer and metal plate to disaggregate crystals, which were then repeatedly sieved to obtain size separates of grains between 420 and 1000 microns. For each sample, about 100 crystals of each potassium-bearing phase were manually separated by hand picking under a binocular microscope. All mineral separates were carefully labeled, and equipment was cleaned between the processing of each sample to prevent any cross-contamination of samples.

Powder X-ray Diffraction

Initial X-ray powder diffraction analyses of select feldspars were conducted using the Department of Geosciences' BRUKER D2 PHASER tool. Two to three analyses or "runs" were carried out for each of the following samples: BEN-5; BEN-17; and BEN-24 (BEN-5 is the gneiss represented in Figures 7-8, whereas BEN-17 and BEN-24 are the pegmatite samples represented in Figures 14-15 and 16-17, respectively). Each run was for 5-10 feldspar crystals that were powdered with an agate mortar and pestle. The resulting data (Fig. 18) document that the feldspars to be used in this study, for $^{40}Ar/^{39}Ar$ analyses, for BEN-5 are orthoclase crystals, and also structurally similar to the samples of Foland (1974). Results for the XRD analyses for BEN-17 and BEN-24 match most closely with microcline.

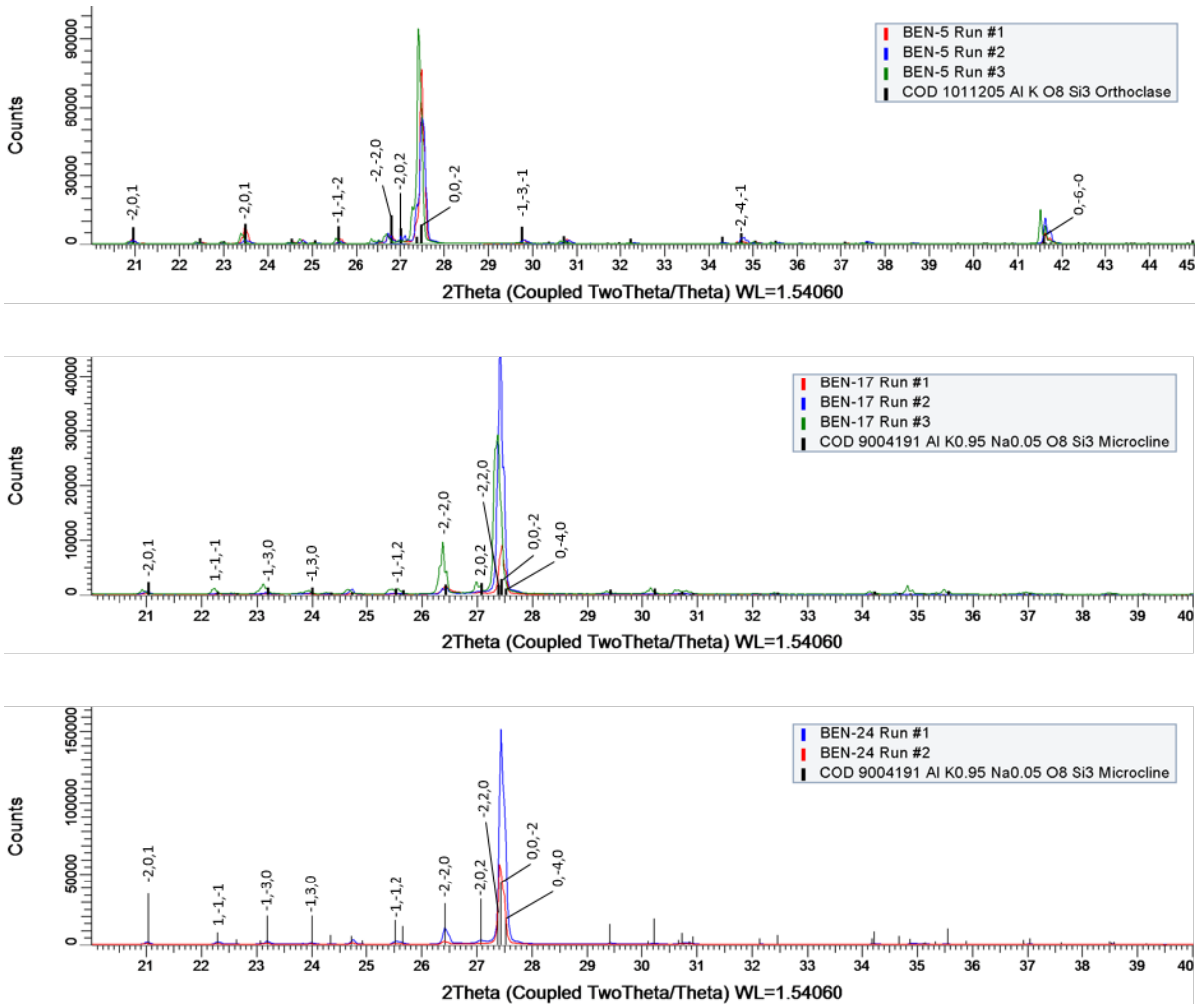

Figure 18. Graph displaying powder x-ray diffraction analyses results of the samples BEN-5, BEN-17 and BEN-24. Miller indices are indicated for the most prominent peaks.

$^{40}Ar/^{39}Ar$ Analytical Technique

Isotopic age determinations were conducted on single-crystals of orthoclase, hornblende and biotite from gneissic and pegmatitic samples obtained from the Benson Mines. Equidimensional crystals lacking obvious micro-fractures and inclusions were hand-picked under a binocular microscope.

Irradiation of Samples

Neutron irradiation for the production of ^{39}Ar followed standard procedures as described by Dalrymple et al. (1981), using the U.S. Geological Survey low-enriched uranium-fueled, pool-type TRIGA Reactor (GSTR) located at the Denver Federal Center in Denver, CO. Final sample separates were wrapped in aluminum foil and carefully loaded in custom aluminum disks that were then subjected to fast-neutron irradiation for 80 hours within the GSTR. In addition to unknowns, the standards GA-1550 biotite (age = 98.79 ± 0.96 Ma) and FC sanidine (age = 28.02 ± 0.28 Ma) (Renne et al., 1998) was also irradiated as a flux monitor. The mineral standard was irradiated in known geometric relation to the unknown samples to allow for the calculation of an appropriate J-value for each unknown. The J-value can be determined using the equation:

$$J = \frac{e^{\lambda t} - 1}{{}^{40}Ar^{*}/{}^{39}Ar_{K}} \tag{1.8}$$

where λ is the total decay constant of ^{40}K, t is the known age of the flux monitor, determined independently, $^{40}Ar^{*}$ is the total amount of radiogenic ^{40}Ar measured from the standard, and $^{39}Ar_{K}$ is the amount of nucleogenic ^{39}Ar generated by the reaction ^{39}K (n,p) ^{39}Ar in the standard (Dalrymple and Lanphere, 1969; Dalrymple et al., 1981). Standard corrections for

interfering isotopes created by the reactions ^{40}Ca (n,α) ^{36}Ar, ^{40}Ca (n,α) ^{37}Ar, ^{42}Ca (n, α) ^{39}Ar, and ^{40}K (n,p) ^{40}Ar were made following Brereton (1970).

Laser Systems

Following irradiation, age analyses were made in the Auburn Noble Isotope Mass Analysis Laboratory (ANIMAL) at Auburn University by single crystal incremental heating with either a CO_2 or diode laser.

The CO_2 laser system consists of a 50W Synrad CO_2 IR laser (λ = 10.6 μm) with variable laser power control. For each sample analyzed, individual crystals were incrementally heated with an incremental heating schedule containing ~25–60 steps. Typical step durations were 20–50 seconds. There were up to 4 replicate analyses of crystals per sample.

One sample was incrementally degassed using a 40W Jenoptik diode laser (λ = 980 nm) equipped with feedback-controlled heating over 31 heating increments for durations ranging from 300–3000 seconds. The sample was loaded into a small packet made from a high-purity Pt-Ir alloy tube to ensure homogenous heating of the sample. Temperature was manually regulated via a Eurotherm 2416 PID controller and monitored with the use of a C-type thermocouple mounted within the Pt-Ir packets. Temperature setpoints for each increment were programmed into the PID prior to heating. The amount of time taken to reach the desired temperature for each step was variable and tended to increase with higher temperature steps. Once the temperature setpoint was reached, temperature variations were within ± 5 ^{o}C for experimental temperatures below 800 ^{o}C and up to ± 10 ^{o}C for higher temperature steps.

Data Reduction

Data reduction and assessment of statistical ages were accomplished through the use of a custom Microsoft Excel application and Isoplot (Ludwig, 1991, 2003). Results were evaluated through use of standard isochron and age spectrum approaches for calculating single crystal ages.

Plateaus were defined such that the plateau increments constituted greater than 60% of the total $^{39}Ar_K$ released in three or more contiguous heating steps, there is no resolvable slope among steps of the plateau, there are no outliers at the beginning or the end of the plateau, and the probability of fit for the steps is greater than 5%. All ages discussed in the text and presented in figures are at the 95% confidence level (although incremental heating steps are graphed with 1σ errors). Complete data tables can be found in the Appendix.

Estimation of Closure Temperature Using Hydrothermal Experimental Data

When compiling temperature-time data from published studies, the closure temperatures used in the generation of figures were as provided by respective authors, or estimated from information provided by respective authors. For the present study, closure temperatures were estimated using experimentally determined diffusion parameters. Bulk closure temperatures were determined by using the following equation (after Dodson, 1973):

$$T_c = R/\mathrm{E} \ln\left(\frac{A\,\tau\,D_o}{a^2}\right) \tag{1.9}$$

where R is the gas constant, E is the activation energy, A is a numerical constant dependent on geometry of the sample, τ is the time constant with which the diffusion coefficient diminishes, D_0 is the frequency factor, and a is the effective diffusion radius of the sample. Nominal values for D_0 and E have been experimentally determined for hornblende (E = 66.1

kcal-mol^{-1}; D_o = 0.061 cm2-sec^{-1}; Harrison, 1981) and biotite (E = 47 kcal-mol^{-1}; D_o = 0.077 cm^2-sec^{-1}; Harrison et al., 1985). Geometric constant A was chosen for each sample based on its physical shape. A spherical geometry (A = 55; McDougall & Harrison, 1999) was assumed for hornblende samples, while an infinite cylinder geometry (A = 27; McDougall & Harrison, 1999) was assumed for biotite. An average of the size fraction from which a sample was picked and divided by two to estimate the diffusion dimension a (ex. a 20/40 mesh size fraction would provide a diffusion dimension of 315 microns). All closure temperatures were calculated based on a cooling rate of 1ºC/m.y.

Estimation of Closure Temperature Using In Vacuo Incremental Heating Data

As potassium feldspar is anhydrous, the incremental heating experiments can be used to estimate D_o and E, assuming release mechanisms *in vacuo* are the same as retention conditions in nature (e.g., Harrison et al., 1993). As discussed above, if the duration, temperature and fraction of ^{39}Ar released during each heating step are known, it is possible to calculate the diffusion coefficient (D) for the mineral of interest, using Equation 1.5, normalized to the characteristic length scale (D/a^2) using the equations of Crank (1975) following the algorithm of Fechtig and Kalbitzer (1966). Spherical geometry was used for all feldspar grains. To quantify the temperature dependence of the diffusion coefficients, $ln(D/a^2)$ was plotted against T^{-1}.

RESULTS

$^{40}Ar/^{39}Ar$ incremental heating analyses were performed on single crystals of potassium feldspar from the high-grade gneiss samples BEN-5 and BEN-10, pegmatite samples BEN-17 and BEN-24, along with K-feldspar, hornblende and biotite from syenite BEN-6 in the ANIMAL facility at Auburn University. These analyses were designed to provide insight of how radiogenic argon is distributed within the individual crystals, and to allow for the comparison of the resulting data with the data from Foland's (1974) bulk analyses on feldspars from the same location. Release spectra were obtained for hornblende and biotite to help to more precisely constrain the thermochronologic history of lithologies in the vicinity of the Benson Mines. $^{40}Ar/^{39}Ar$ release spectra produced from the incremental heating of single crystals of orthoclase in the present study reveal significant discordance between cogenetic crystals of individual samples, between the initial and final incremental heating steps of single crystals, and also among the different lithologies analyzed.

BEN-6: Hornblende from Syenite

Incremental heating analyses were performed on three individual hornblende crystals, possessing a prismatic habit and average diameter of 315 μm, from sample BEN-6 (Fig. 19). Low temperature increments for crystal 'a' (Fig. 19) yield apparent ages as young as 688 and old as 1054 Ma for the first ~ 9% of total $^{39}Ar_K$ released during the experiment. Subsequent increments, representing the next 88.2% of $^{39}Ar_K$ release, increase in age and define a plateau age of 962.7 ± 1.2 Ma. This pattern of younger ages followed by older ages in the first few percent of release, and the low apparent Ca/K ratios of these initial steps (Fig. 19), is suggestive of recoil redistribution of ^{39}Ar (perhaps into an exsolved phase in hornblende).

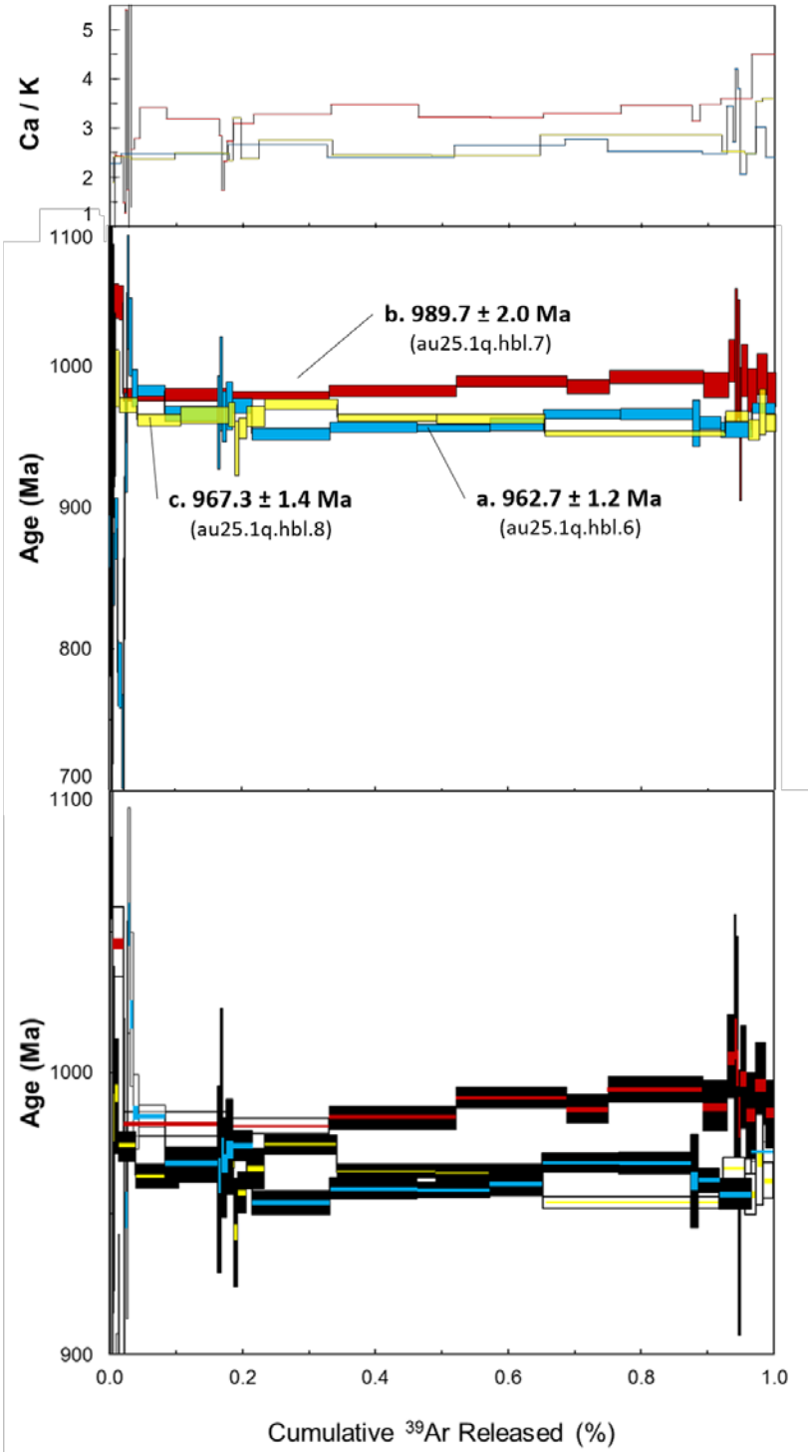

Figure 19. Plateau ages for three single crystals of hornblende from clinopyroxene-hornblende syenite BEN-6 (middle). The bottom figure displays the age spectra on a more precise scale. Plateau steps are indicated by filled black boxes.

The plateau age is interpreted to record $^{40}Ar^{*}$retention during cooling for this specific hornblende crystal.

The age spectrum for crystal ‘b’ (Fig. 19) has highly variable ages for the initial 2% of total $^{39}Ar_K$ measured. The subsequent 98% of $^{39}Ar_K$ release is defined by incremental heating ages beginning at 981.9 ± 4.3 that increase monotonically to ages of ca. 995 Ma at fusion. The spectrum has a resolvable slope, and thus no plateau age should be defined. The spectrum is interpreted to reflect ^{40}Ar closure in a hornblende crystal with a diameter of 315 µm that began at ca. 1.0 Ga, reaching final closure at ca. 980 Ma. The total gas age is 964.4 ± 7.2 Ma.

The release spectrum for the last hornblende sample analyzed from BEN-6, crystal ‘c’ (Fig. 19), is much like that of crystal ‘a’, but is slightly younger. A plateau of 967.3 ± 1.4 Ma is defined by 64.9% of $^{39}Ar_K$ release. The remainder represents fusion of the grain.

BEN-6: Biotite from Syenite

Two single cleavage flakes of biotite from BEN-6 (Fig. 20), with an average diameter of 315 µm, were incrementally heated and to obtain age spectra that are nearly identical. Low-temperature increments for crystal ‘a’ (Fig. 20) begin with a minimum age of 198.2 ± 18.4 Ma and then rise abruptly to ~ 915 Ma within the first ~ 5% of total $^{39}Ar_K$. The steps for release of the remaining ~ 95% of the $^{39}Ar_K$ released yield apparent ages that tend to monotonically decrease from 921.0 ± 2.3 to 901.6 ± 3.28 Ma. Crystal ‘a’ yields a total gas age of 910.8 ± 3.4 Ma. The initial heating increments for crystal ‘b’ (Fig. 20) also yield very young ages (~200 Ma) for the initial steps, which then increase to around 900 Ma during the release of the first 1–2% of total $^{39}Ar_K$ measured. Measurements for the final 65.5% of release define a plateau with an age of 903.3 ± 1.3 Ma. Results for these two crystals are

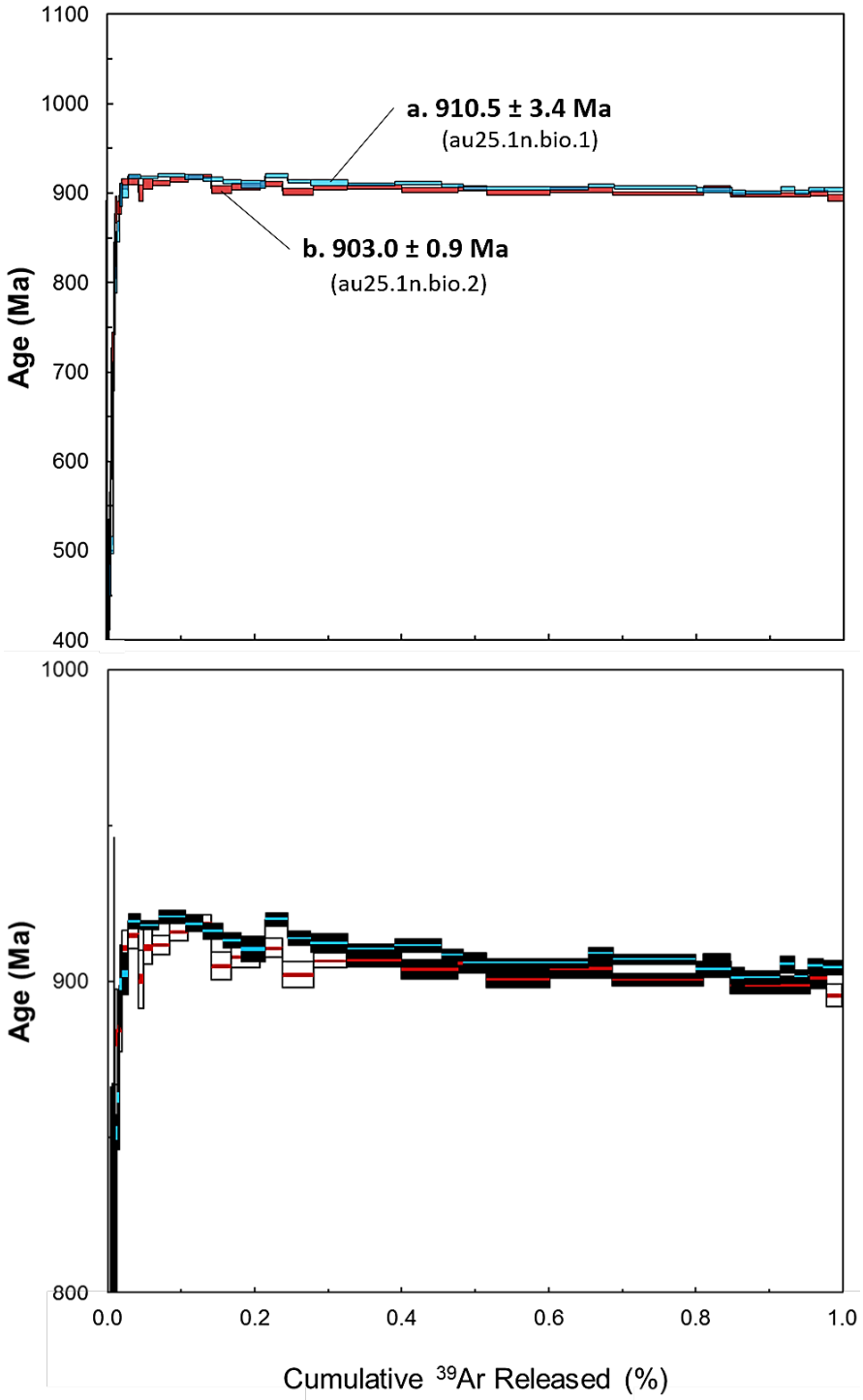

Figure 20. Age spectra for two single crystals of biotite from clinopyroxene-hornblende syenite BEN-6. The bottom figure displays the age spectra on a more precise scale. Plateau steps are indicated by filled black boxes.

comparable to the ca. 937 to 837 Ma age range for biotite in the Adirondack Highlands, as determined by previous researchers (see Table 1).

BEN-5: Potassium Feldspar from Gneiss

Separate analyses of four, cogenetic, potassium-feldspar crystals (Fig. 21) from the sillimanite-orthoclase-biotite-magnetite gneiss sample BEN-5 reveal significant discordance among crystals and between initial and final increments for each grain. These subhedral to euhedral crystals have an average width of 355 μm.

Analysis of crystal 'a' (Fig. 21a) produced a release spectra having relatively consistent ages for incremental heating steps. The release of extraneous argon is indicated by anomalously old ages in the initial steps, representing only the first ca. 1.5% of total $^{39}Ar_K$ measured. The remaining $^{39}Ar_K$ released yielded a mean age of 875.8 ± 7.1 Ma with a maximum difference of 53.5 ± 2.7 Ma among oldest and youngest increments. This is the least amount of discordance observed among all K-feldspar analyzed, and the result is very close in age to the bulk sample orthoclase age determined by Foland (1974). The fact that this total gas age is ca. 30-60 Ma younger than the total gas ages of other crystals from BEN-5 is interpreted to result from selection of grains with varying diffusion geometries. The fact that the incremental heating ages in the spectrum of sample 'd' are much more regular, and more consistent with an intracrystalline (core-to-rim) diffusion gradient is interpreted to result from a more homogenous distribution of heat by the foil. For the other three crystals, heating was concentrated at the top of the crystal, and the crystals 'rested' on a thick copper holder at room temperature. Essentially, crystals and crystal fragments comprising different diffusion domains released ^{40}Ar from different areas at different parts of the experiment.

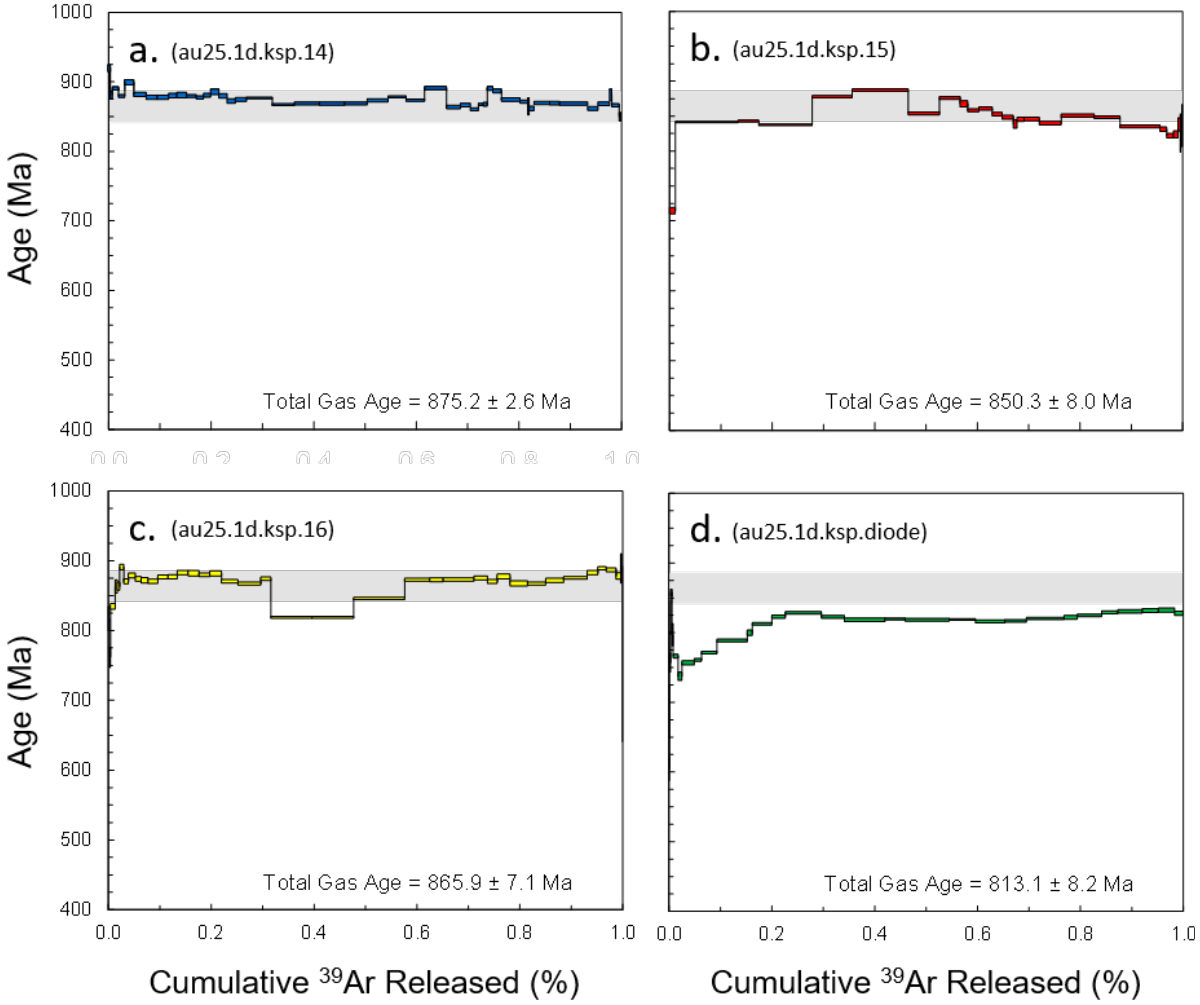

Figure 21. Four K-feldspar crystals from magnetite-orthoclase-sillimanite gneiss, BEN-5, yield the oldest $^{40}Ar/^{39}Ar$ ages observed, with ages as old as ~875 Ma and as young as ~840 Ma. Crystal 'd' was incrementally heated via a diode laser. Gray bands in spectra a-d represent the range in age for a bulk-sample of orthoclase as determined by Foland (1974).

Temperature data collected during the diode heating experiment, in combination with calculated values of fractional loss (see Equation 1.4), were used to estimate diffusion coefficients for each step, as in Equation 1.5. These values were then used to generate an Arrhenius plot (Fig. 22c) for the data in an attempt to estimate D_o, E and calculate closure temperature for BEN-5 'd' and compare with the results obtained by Foland (1974) and Cassata & Renne (2013) for similar samples of orthoclase from the Benson Mines.

Results of these calculations and the earlier studies are presented in Figure 22 along with the results from the present study. Results from the present study differ from those of Foland (1974) and Cassata & Renne (2013) in that the trendline projected for the data series yields a value for D_o that is much lower than the comparable values of the previous studies. The slope of the line, which correlates to activation energy, is similar to that of Foland (1974) and Cassata & Renne (2013). The most likely reason for discrepancy in estimating D_o is an error in thermocouple placement, resulting in temperature readings that were lower than actually experienced by the sample. It is believed that temperature was underestimated as a result of the C-type thermocouple being more in contact with the Pt-Ir packet the crystal was loaded in rather than the crystal itself. This underestimation and inaccuracy in temperature produced a shift to the right for the data series on the Arrhenius plot causing the y-intercept, or value for D_o, to be lower than those for Foland (1974) and Cassata & Renne (2013). The precision in achieving and holding temperature setpoints for each increment also needed improvement, but the systematic distribution in Arrhenius data for the present study indicates imprecision in measuring T is of little consequence. Data points depart from linearity for high temperature steps due to the structural alteration of orthoclase.

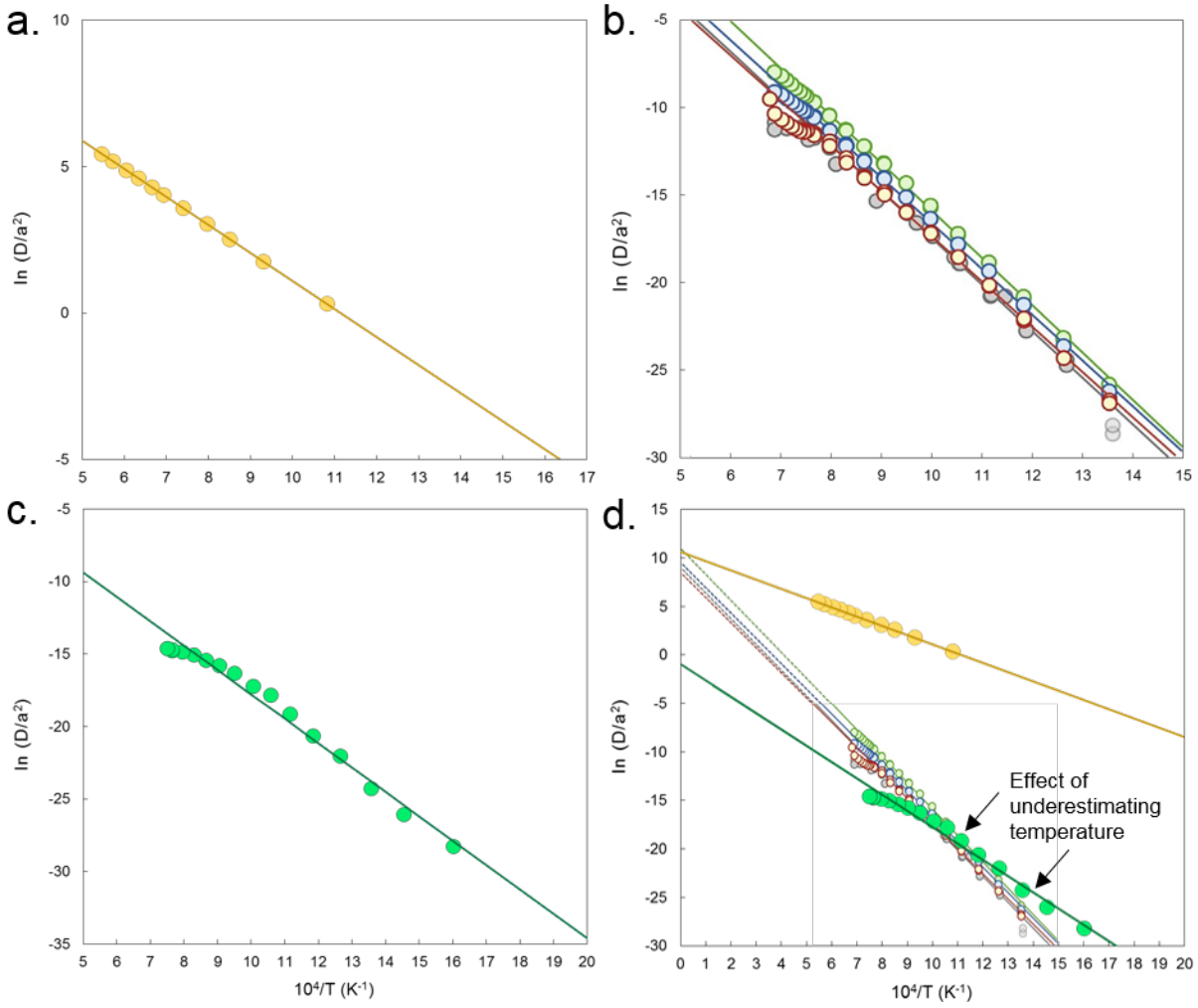

Figure 22. Arrhenius plots produced from analyses of Benson Mines orthoclase from **a.)** Foland (1974), **b.)** (adapted from) Cassata & Renne (2013) and **c.)** the present study. Values for E differ between Foland (1974) and Cassata & Renne (2013), however, they obtain similar values for D_o. **d.)** The analysis of the orthoclase from gneiss in the present study produced a lower value for D_o and is interpreted to result from the underestimation of temperature during the experiment.

BEN-6: Potassium Feldspar from Syenite

One analysis was performed on a single feldspar crystal from the syenite, and its resultant age spectrum is shown in Figure 23. Initial increments for this sample begin with apparent ages of ~700 Ma and steadily increase to a maximum of about ~710 Ma. The data yield a total gas age of 704.8 ± 7.4 Ma.

BEN-10: Potassium Feldspar from Gneiss

An individual crystal from the gneiss BEN-10 ~315 µm in diameter, was incrementally heated and yielded the age spectrum pictured in Figure 24. The spectrum for BEN-10 begins with heating increments having apparent ages of ~830 Ma that steadily increase to ~845 Ma over most of the remaining ^{39}Ar released. The data yield a plateau age of 833.8 ± 0.9 Ma defined by 62% of the $^{39}Ar_K$ released, and a total gas age (neglecting the first and last 2% of release) of 837.6 ± 3.2 Ma. This age is interpreted to record bulk $^{40}Ar^*$ retention in this feldspar crystal.

BEN-24: Potassium Feldspar from Pegmatite

Three grains of potassium feldspar the pegmatite sample BEN-24, with an average diameter of 315 µm in diameter on average, were incrementally heated. Initial increments for the age spectrum produced from crystal ‘a’ (Fig. 25a) possess a minimum age of 633.2 ± 2.7 Ma. Progressive steps exhibit a gradual increase in age to a peak of 718.7 ± 2.1 Ma over the first 87% of total $^{39}Ar_K$ release. The remaining 13% show a decrease in age values to ca. 690 Ma. The data for this sample yields a mean total gas age of 675.0 ± 11.0 Ma.

The age spectrum yielded from the analysis of orthoclase crystals ‘b’ and ‘c’ (Fig. 25b,c) are similar and have more discordance than observed for crystal ‘a’ of this sample. In

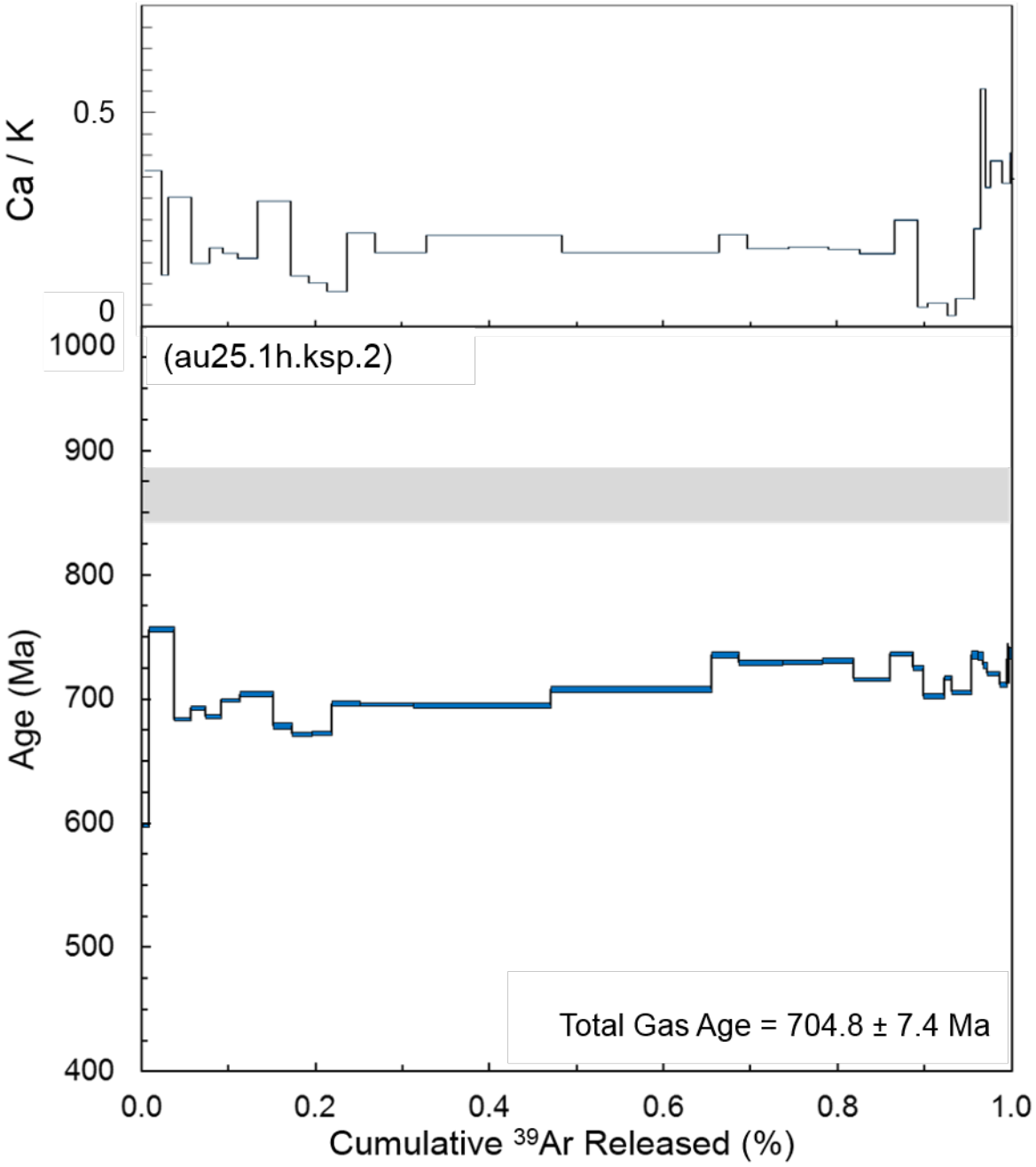

Figure 23. Ca/K ratio (top) and age spectrum (bottom) for the syenite sample BEN-6. BEN-6 is closest to ages for pegmatite and ~150 m.y. younger than results for gneiss. The apparent age for this highly perthitic feldspar likely reflects timing of recrystallization.

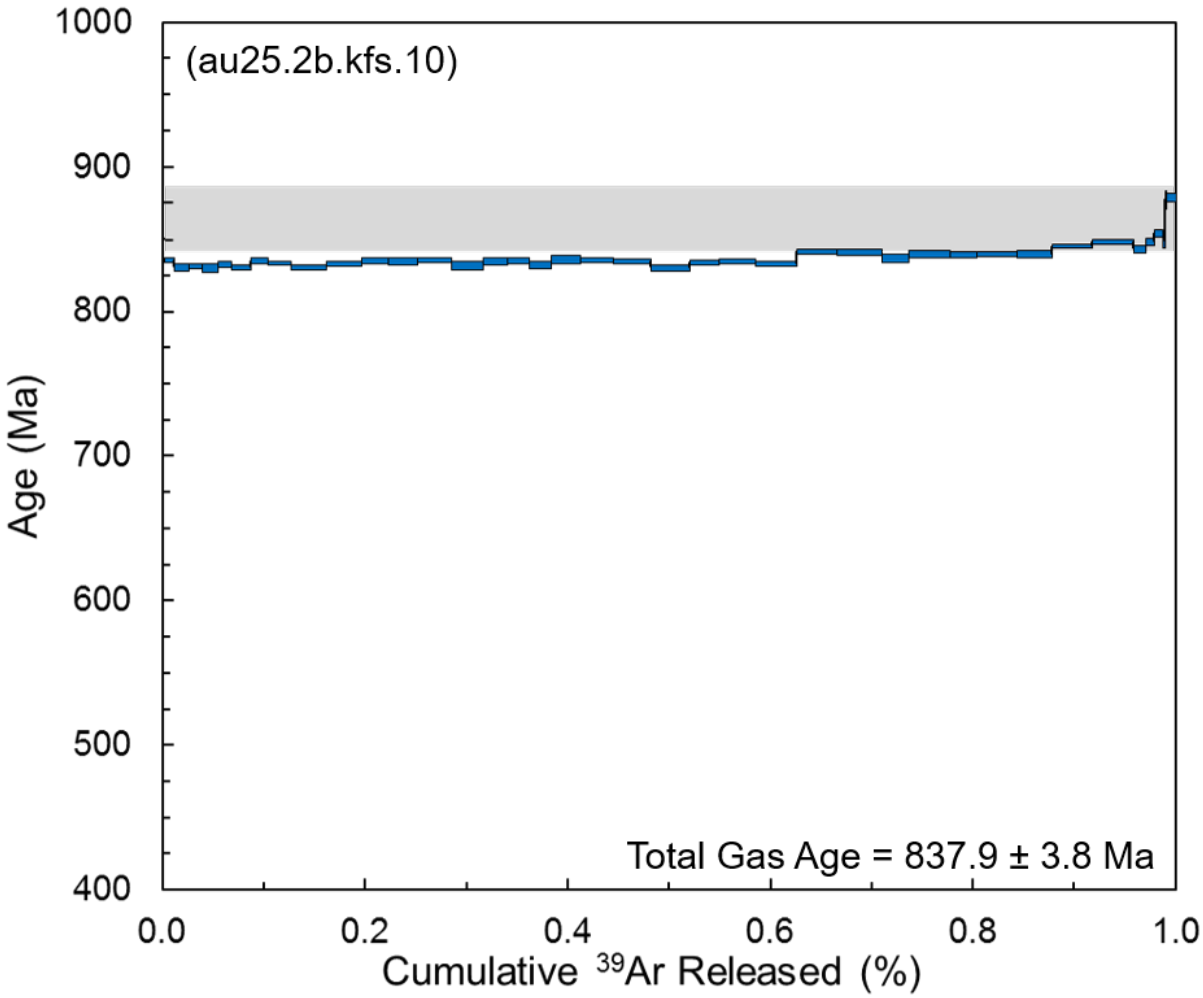

Figure 24. Analysis of orthoclase from the gneiss BEN-10 produces an age spectrum very similar to the results of Foland (1974), although yielding an age that is ~20 m.y. younger.

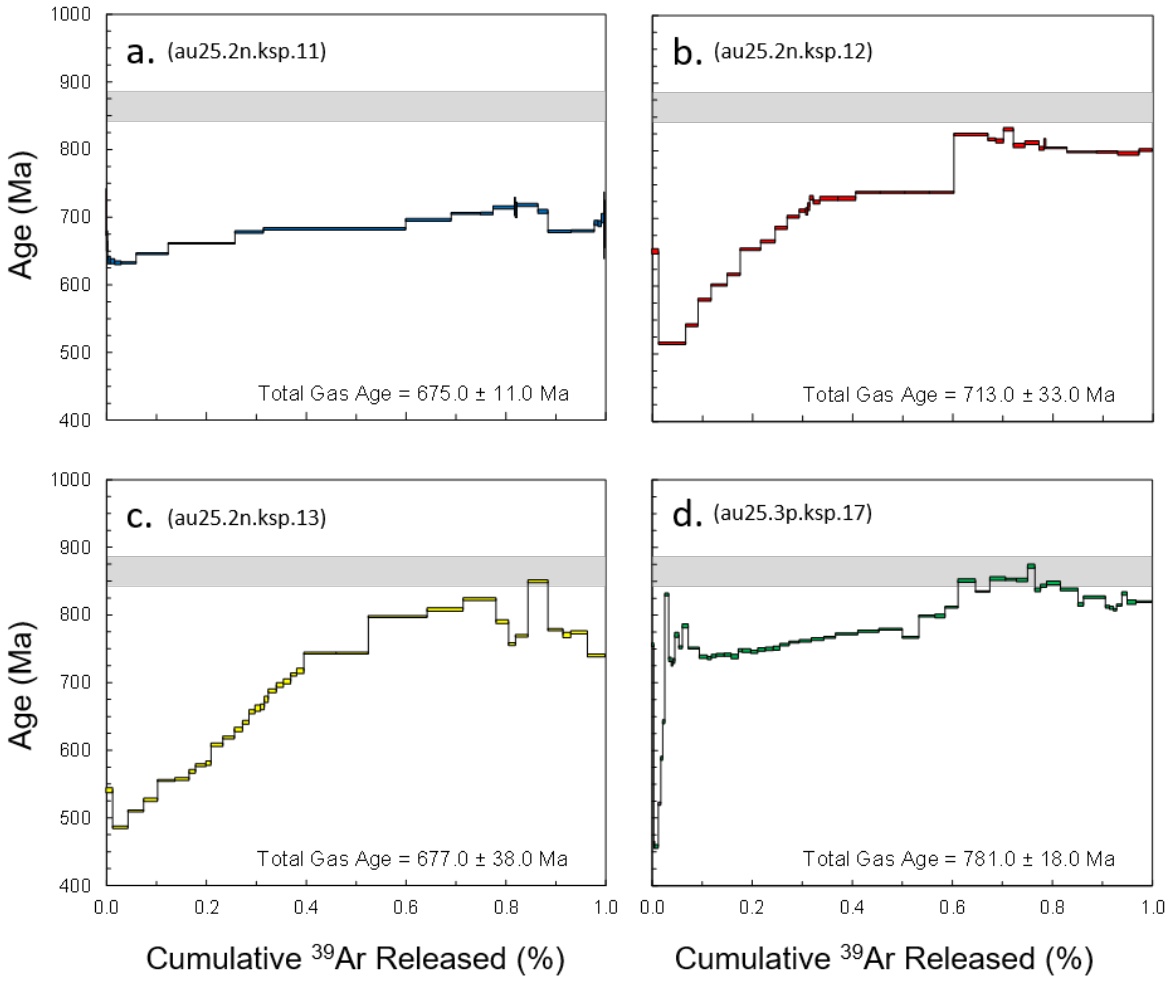

Figure 25. Age spectra for analyses of K-feldspar from pegmatite samples. Spectra **a.-c**. are from BEN-24, and **d.** from BEN-17. The pegmatite spectra possess the greatest degree of age discordance between low and high temperature steps and among the gneiss and syenite samples. Gray bands in spectra a-d represent range in age for feldspar from Foland (1974) (Figure 1).

‘b’ and ‘c’, the minimum initial ages of ca. 500 Ma, followed by a regular, essentially monotonic increase in ages to ca. 800 Ma at the highest temperature steps. As the pattern of discordance is greater for ‘b’ and ‘c’, these crystals are considered to represent more complete, natural diffusion gradients than was preserved and sampled by crystal ‘a’.

BEN-17: Potassium Feldspar from Pegmatite

A single grain of K-feldspar, roughly 460 μm in diameter (crystal ‘d’; Fig. 25d), from pegmatite BEN-17 begins with ages as low as 461.1 ± 5.1 Ma and as high as 831.1 ± 2.1 for the first ~3.6% of argon release. Age values for successive steps, representing the next ~47% of release, increase systematically from ca. 730 Ma to a maximum of ca. 870 Ma. The data yield a mean age of 781.0 ± 19.0 Ma. The total gas age for this feldspar from a pegmatite is thus about 65 Ma older than the oldest feldspar of pegmatite sample BEN-24.

DISCUSSION & INTERPRETATION

Summary of Results for Gneiss

Incremental heating analyses for the gneiss sample, BEN-5, yield the oldest age results (Fig. 21). These analyses also yield age spectra with the least overall age variation of K-feldspars for all lithologies analyzed in the present study. The age spectra generated for crystals a, b, and c appear a bit erratic in nature from step to step, but produce fairly non-discordant results, overall. This is interpreted as resulting from non-homogenous heating of grains, with varying diffusion geometries that allowed for the degassing of the crystals' rims simultaneously with their cores, the effect of which is a non-systematic sampling and homogenization of the crystals' natural $^{40}Ar^{*}$distribution.

In comparison with the first three crystals analyzed using the CO_2 laser, the data produced for crystal 'd' exhibits some quite significant differences. The Pt-Ir tube, along with relative temperature control with the diode laser, resulted in a much more homogenous heating of crystal 'd' from the outside in. This technique yielded results that closely correspond to what would be expected from incrementally heating a single crystal via a diode laser, having its original diffusion profile preserved, which exhibits a radiogenic argon concentration gradient. The youngest initial age spectrum increments represent the rim of the grain, the area of lowest expected concentration, and systematically increase in age as more interior regions of the crystal are degassed.

While these differences in results are readily attributed to changes in laboratory procedure, they prove the valuable point that different analysis techniques do, in fact, affect how radiogenic argon is released from a sample, and, consequently, how they can be

interpreted. It can be gathered from these results that, for some samples, the release of $^{40}Ar^{*}$ in the laboratory does not mimic that of nature, unless certain experimental precautions are taken.

The analysis of a single orthoclase grain from the gneiss BEN-10 (Fig. 24) produced results very similar to crystals a-c of BEN-5 but have much less discordance among low and high temperature heating increments. These results also match very closely with that of Foland (1974) (Fig. 1), though the apparent age for this grain is ~20 m.y. younger. Similar to those of BEN-5, this result is interpreted to reflect the degassing of a grain fragment having its rim and core contributing to $^{40}Ar^{*}$measured, simultaneously.

Summary of Results for Syenite

This single feldspar from syenite (Fig. 23) exhibits release behavior very similar to that of the gneiss samples, in that their age spectra are flat with minimal differences between initial and final heating increments. BEN-6 is different from the gneiss, in that it is ca. 150 m.y. younger than the gneiss samples. This is interpreted to result from the perthitization of the samples, and the apparent age may reflect the timing of recrystallization in the sample. Perthitization of a sample will also decrease the effective diffusion dimension of the crystal (Burgess et al., 1992). The effective diffusion dimension becomes the half-width of the lamellae, rather than the radius of the whole grain, and will result in younger apparent ages.

Summary of Results for Pegmatite

Analyses of single K-feldspar grains from pegmatite samples reveal the highest degree of variation observed between initial and final incremental heating steps for single grains and also for different grain populations. Such is observed best in crystals ‘b’ and ‘c’ from BEN-24 (Fig. 25), which are interpreted as representing whole, unaltered grains having

their original core to rim diffusion profiles intact. For these grains, the first steps of each of their respective spectra represent the degassing of the outermost parts of the crystal, or the original crystal surfaces. As more interior parts of the crystals are degassed, apparent ages increase. This behavior indicates a concentration gradient within the crystals, with the highest concentration of $^{40}Ar^{*}$ at the center of crystals. In contrast, crystal 'd' (Fig. 25), from BEN-17 and crystal 'a' of BEN-24, produced age spectra having less variation between initial and final heating steps. These results are consistent with the analysis of crystal fragments that have areas, which were once most interior to the crystals, now exposed at their surfaces. As a result, during step-heating analyses, the portions of the crystals with the highest concentrations of $^{40}Ar^{*}$, originally the crystal cores, are degassed simultaneously with portions of the crystals having low concentrations of $^{40}Ar^{*}$, which represent crystal rims or surfaces. The degassing of grains possessing this type of profile results in the homogenization of their original $^{40}Ar^{*}$ distributions, resulting in the misinterpretation of their true total gas ages.

The effects of analyzing crystal fragments is apparent when comparing the present data, produced from the analyses of single-crystals, along with the data from Foland's (1974) bulk loss experiments. His analysis of orthoclase obtained from Benson Mines pegmatite yielded a total gas age of 856.5 ± 3.3 Ma (Fig. 1), a result 75 m.y. older than analyses of comparable lithologies in the present study. The release spectrum from Foland's work displays very little discordance among heating steps, and exhibits only a ca. 35 m.y. difference between the youngest and oldest step. This, inevitably, is the result Foland's crushing of grains prescribed for analyzing bulk samples, and reaffirms the great importance

of making every effort to preserve the original grain geometry for extracting information about the true distribution of radiogenic argon in feldspars.

Significant age discordance is also noted between the different lithologies with an almost 200 m.y. maximum age difference between the oldest and youngest total gas ages for gneiss and pegmatite. The younger and more discordant results for the feldspars for pegmatites may reflect the fact they are post-metamorphic intrusions with a higher activity of fluids than that which characterizes the high-grade gneiss, as suggested by Villa & Hanchar (2014).

Thermochronology for the Benson Mines

A summary of all $^{40}Ar/^{39}Ar$ age data, along with average grain sizes and estimated closure temperatures for all lithologies analyzed in the present study, are presented in Table 2. These data are combined in Figure 26 to illustrate the thermochronologic history of the vicinity of the Benson Mines. In comparison with the high temperature portion of thermochronologic history of the Adirondack Highlands, indicated by the dashed line in Figure 26a, the results from the present study coincide well with age data presented by previous researchers (summarized in Table 1).

Assuming a path with cooling rates of ca. 0.5 ^{o}C to 0.1 ^{o}C per m.y., bulk closure temperatures for feldspar occur over a range of only 22 ^{o}C, from 268-290 ^{o}C, and a period of 200 m.y. Differences in apparent ages and closure temperatures between cogenetic crystals and between the different lithologies, are interpreted to reflect the differing $^{40}Ar^{*}$ retention characteristics and the varying preservation of natural diffusion gradients in crystals.

TABLE 2. $^{40}Ar/^{39}Ar$ AGE RESULTS FOR THE PRESENT STUDY

Mineral Phase	Size Range (mm)	T_c Range (°C)	Total Gas Age (Ma)	Plateau Age (Ma)	Youngest Step (Ma)	Oldest Step (Ma)
BEN-5 – sillimanite-biotite-magnetite gneiss						
K-feldspar	0.420 - 1.00	268 - 290	875.2 ± 2.6	-	867.0 ± 2.7	920.5 ± 4.7
			850.3 ± 8.0	-	715.1 ± 4.7	887.9 ± 1.7
			865.9 ± 7.1	-	763.4 ± 14.8	892.6 ± 4.0
			*813.1 ± 8.2	-	*604.9 ± 16.7	*833.4 ± 2.9
BEN-6 – Clinopyroxene-hornblende syenite						
K-feldspar	0.420 - 0.841	268 - 286	704.8 ± 7.4	-	672.0 ± 1.6	737.3 ± 4.4
Hornblende	0.420 - 0.841	502 - 527	964.4 ± 7.2	962.7 ± 1.2	688.4 ± 1%	974.4 ± 5.3
			987.0 ± 1.0	989.7 ± 2.0	981.1 ± 2.7	1009.8 ± 1%
			963.5 ± 3.4	967.3 ± 1.4	943.8 ± 19.3	969.5 ± 16.1
Biotite	0.420 - 0.841	288 - 307	910.8 ± 3.4	-	804.4 ± 15.2	921.0 ± 2.3
			906.4 ± 3.3	903.3 ± 1.3	885.0 ± 7.2	919.1 ± 2.4
BEN-10 – Orthoclase-garnet-magnetite gneiss						
K-feldspar	0.420 - 0.841	268 - 286	837.9 ± 3.8	833.8 ± 0.9	830.2 ± 3.1	1006.9 ± 7.2
BEN-17 – pegmatite						
K-feldspar	0.841 - 1.00	286 - 290	781.0 ± 18.0	-	458.9 ± 2.6	872.9 ± 3.1
BEN-24 – pegmatite						
K-feldspar	0.420 - 0.841	268 - 286	675.0 ± 11.0	-	633.2 ± 2.7	718.7 ± 2.1
			713.0 ± 33.0	-	517.5 ± 1.4	825.7 ± 1.8
			677.0 ± 38.0	-	486.9 ± 1.6	850.3 ± 2.1

*Analyzed with diode laser system.

1% assigned by experience.

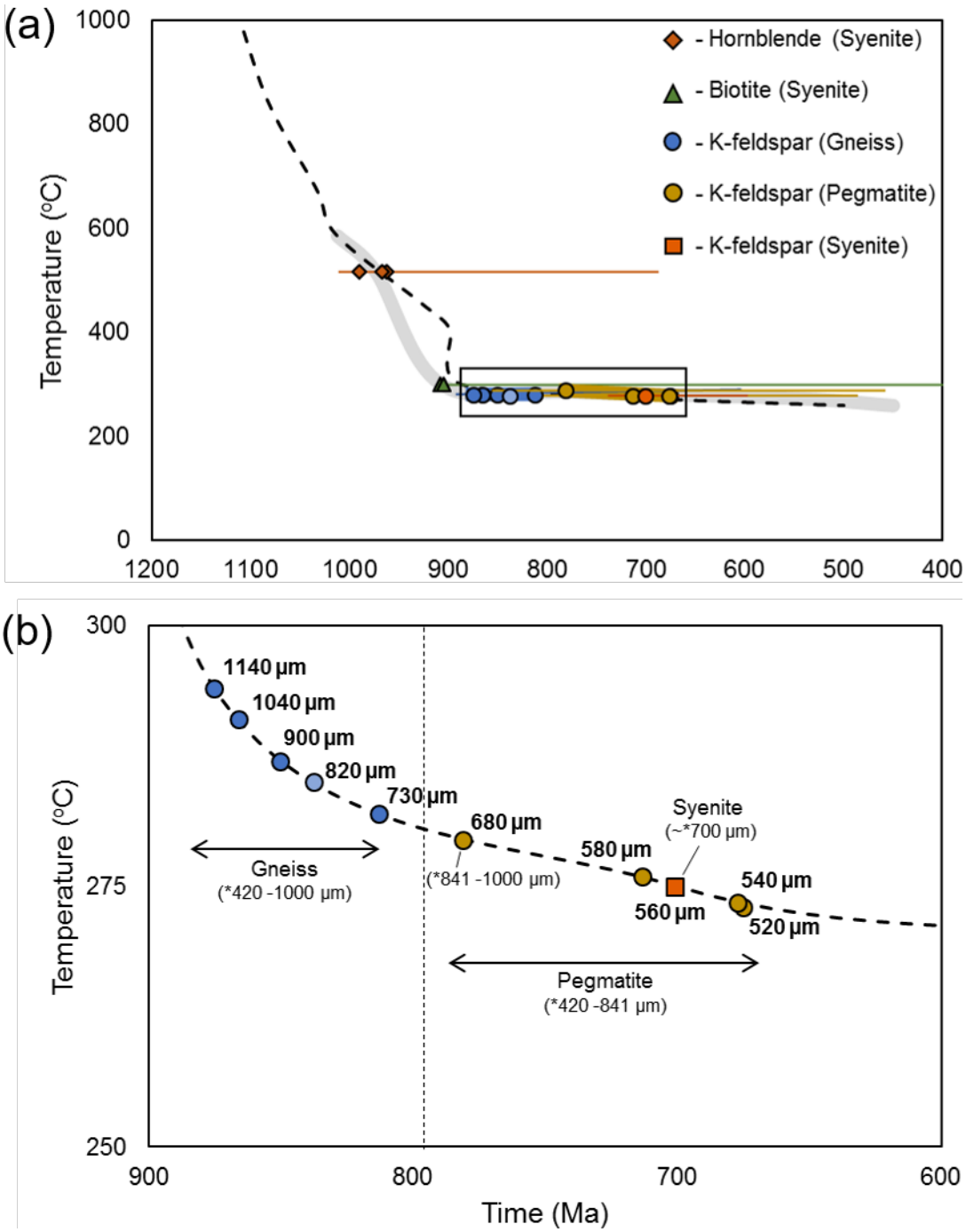

Figure 26. **(a)** Temperature-time cooling history based on $^{40}Ar/^{39}Ar$ analyses of hornblende, biotite, and K-feldspar from the present study with the regional cooling history of Figure 3 (dashed). Total gas ages are represented by diamonds, triangles, circles, and squares, and solid lines indicate the maximum range of variation observed between early and late incremental heating steps for a given analysis. **(b)** Shows hypothetical diameters (in bold) of grains would be required for analyses from the present study to perfectly agree with the cooling history for the Adirondack Highlands (Fig. 3).

All K-feldspar ages for crystals separated from the pegmatites and the syenite in this study are younger than ca. 800 Ma, whereas all K-feldspars from the orthoclase-sillimanite gneiss and the orthoclase-garnet gneiss are older than 800 Ma (Fig. 26). This results from the fact that the pegmatites are post-metamorphic intrusions that have undergone fluid-induced recrystallization. Apparent age variations among feldspars from the pegmatites and syenite most likely represent ages of the most recent aqueous recrystallization event experienced by the samples, a result that agrees with Villa & Hanchar (2013). This is especially true for the analysis of the highly perthitic K-feldspar from the syenite sample BEN-6, which does not likely reflect volume diffusion. The gneisses are interpreted to have been very dry for all times following peak metamorphism, and thus the K-feldspar ages for the gneisses are interpreted to more closely approximate a temperature-dependent time as in the model of Dodson (1973).

The oldest K-feldspar ages, of the gneisses, are similar to the crystallization ages of post-Shawinigan pegmatites reported in the region (McLelland et al., 2010). Any thermal gradients associated with advective heat transfer during pegmatite intrusion would be expected to decay to the regional geotherm within a few to tens of millions of years. The fact that K-feldspar ages of the syenite and pegmatite are tens to hundreds of millions of years younger than the gneisses means that hypothetical thermal gradients cannot be used to account for the observed age variation in K-feldspar.

CONCLUSIONS

It is apparent from the varying levels of age variation within and among cogenetic crystals of the present study that radiogenic argon is not retained under exactly the same conditions in any two crystals, even though they experienced the exact same thermochronologic history. This observation also holds true for different lithology types as seen from age discordance between gneiss and pegmatite samples, an effect which seems to be amplified for feldspars that have experienced recrystallization due to a high activity of fluids. The results of this study provide strong evidence that the diffusion of radiogenic argon in potassium feldspars from the Benson Mines, and likely feldspars from many other geologic settings, occurs at the grain-scale, rather than from multiple diffusion domains. However, careful control of experimental parameters are essential for this mechanism to be observed in the laboratory and to ensure that the degassing of a sample mimics that of nature. If true, the crushing and grain-size reduction prescribed for the performance of bulk analyses will homogenize the natural $^{40}Ar^{*}$ distribution of the crystals leading to the misinterpretation of their age histories. The same can be said for single crystals of feldspar whose geometries are unintentionally altered prior to incremental heating analyses.

The Benson Mines, due to its cooling history, provides an excellent case study of the diffusion behavior of radiogenic argon in potassium feldspars, and much can still be learned from further study. Electron microprobe analyses would enable a more thorough understanding of how diffusion behavior in the Benson Mines orthoclase relates to chemical composition and microstructural features. Additional analyses of these orthoclase grains by experiments providing temperature control with improved use of the diode laser would

provide further insight into the diffusion kinetics of these samples. Furthermore, additional bulk heating analyses of these samples could help further solidify the hypothesis that physical alteration of grains will, in fact, homogenize the natural distribution of radiogenic argon in those grains.

The continued development and utilization of analytical techniques to recover natural diffusion gradients in radiogenic ^{40}Ar concentrations at the scale of individual feldspar crystals is imperative for accurately interpreting $^{40}Ar/^{39}Ar$ data and related release spectra. Future research utilizing techniques that allow homogenous incremental heating of single crystals will provide an opportunity to elucidate poorly understood aspects of argon diffusion in minerals of the feldspar group. This type of work will allow for more accurate and precise interpretation of $^{40}Ar/^{39}Ar$ analysis results and, subsequently, a more thorough understanding of the geological settings from which they are obtained.

REFERENCES

Arnaud, N.O., and Kelley, S.P., 1997, Argon behavior in gem-quality orthoclase from Madagascar: Experiments and some consequences for $^{40}Ar/^{39}Ar$ geochronology: Geochimica et Cosmochimica Acta, v. 61, p. 3227-3255.

Baird, G.B., Shrady, C., and Jones, H., 2008, Preliminary constraints on the timing deformation in the northwest Adirondack lowlands and along the Black Creek shear zone, New York [abs]: Geological Association of Canada-Mineralogical Association of Canada Programs with Abstracts, v. 33, p.58.

Bohlen, S.R., Valley, J.W., and Essene, E.J., 1985, Metamorphism in the Adirondacks, I. Petrology, pressure and temperature: Journal of Petrology, v. 26, p. 971-992.

Brereton, N.R., 1970, Corrections for interfering isotopes in the $^{40}Ar/^{39}Ar$ dating method: Earth and Planetary Science Letters, v. 8, p. 427-433.

Burgess, R., Kelley, S.P., Parsons, I., Walker, F.D.L., and Worden, R.H., 1992, $^{40}Ar/^{39}Ar$ analysis of perthite microtextures and fluid inclusions in alkali feldspars from the Klokken syenite, South Greenland: Earth and Planetary Science Letters, v. 109, p. 147-167.

Cassata, W.S., and Renne, P.R., 2013, Systematic variations of argon diffusion in feldspars and implications for thermochronometry: Geochimica et Cosmochimica Acta, v. 112, p. 251-287.

Crank, J., 1975, The mathematics of diffusion: Oxford, Clarendon Press, p. 414.

Dalrymple, G.B., Alexander, E.C., Lanphere, M.A., and Kraker, G.P., 1981, Irradiation of samples for $^{40}Ar/^{39}Ar$ dating using the Geological Survey TRIGA Reactor: Geological Survey Professional Paper 1176, p. 1-55.

Dalrymple, G.B., and Lanphere, M.A., 1969, Potassium-argon dating: Principles, techniques, and applications to geochronology: San Francisco, W.H. Freeman and Co., p. 258.

Darling, R.S., Florence, F.P., Lester, G.W., and Whitney, P.R., 2004, Petrogenesis of prismatine-bearing, metapelitic gneisses along the Moose River, west-central Adirondacks, New York: in Tollo, R.P., Corriveau, L., McLelland, J., and Bartholomew, M.J., [eds.], Proterozoic tectonic evolution of the Grenville orogen in North America: Geological Society of America Memoir 197, p. 325-336

Dodson, M.H., 1973, Closure temperature in cooling geochronological and petrological systems: Contributions to Mineralogy and Petrology, v. 40, p. 259-274.

Fechtig, H., and Kalbitzer, S., 1966, The diffusion of argon in potassium-bearing solids, in Schaeffer, O.A., and Zähringer, J., eds, Potassium argon dating: Berlin-Heidelberg, Springer, p. 68-107.

Foland, K.A., 1974, ^{40}Ar diffusion in homogenous orthoclase and an interpretation of Ar diffusion in K-feldspars: Geochimica et Cosmochimica Acta, v. 38, p. 151-166.

Foland, K.A., 1994, Argon diffusion in feldspars, in Parsons, I., ed, Feldspars and Their Reactions: Kluwer Academic, Dordrecht, The Netherlands, p. 415-447.

Foland, K.A., and Xu, Y., 1990, Diffusion of ^{40}Ar and ^{39}Ar in irradiated orthoclase: Geochimica et Cosmochimica Acta, v. 54, p. 3147-3158.

Foland, K.A., and Xu, Y., 1992, Reality of the "Ar Loss" ^{40}Ar/^{39}Ar step-heating spectrum: Confirmation and complications for K-feldspars [abs]: Eos (Transactions, American Geophysical Union), v. 73, p. 363.

Gower, C., 1996, The evolution of the Grenville Province in eastern Labrador, Canada, in Brewer, T.S., ed., Precambrian Crustal Evolution in the North Atlantic Region: Geological Society of London Special Publication 112, p. 197-218.

Grove, M., Lovera, O.M., and Harrison, T.M., 2003, Late Cretaceous cooling of the east-central Peninsular Ranges Batholith (33^{o}N): relationships to La Posta pluton emplacement, Laramide shallow subduction, and forearc sedimentation: Geological Society of America Special Paper, v. 374, p. 355-380.

Harrison, T.M., 1981, Diffusion of ^{40}Ar in Hornblende: Contributions to Mineralogy and Petrology, v. 78, p.324-331.

Harrison, T.M., and Lovera, O.M., 2014, The multi-diffusion domain model: past, present and future: Special Publication – Geological Society of London, v. 378, p. 91-106.

Harrison, T.M., Copeland, P., Kidd, W.S.F., and Lovera, O.M., 1995, Activation of the Nyainqentanghla shear zone: implications for uplift of the southern Tibetan Plateau: Tectoncis, v. 14, p. 658-676.

Harrison, T.M., Duncan, I., and McDougall, I., 1985, Diffusion of ^{40}Ar in biotite: Temperature, pressure and compositional effects: Geochemica et Cosmochimica Acta, v. 49, p. 2461-2468.

Harrison, T.M., Heizler, M.T, and Lovera, O.M., 1993, In vacuo crushing experiments and K-feldspar thermochronometry: Earth and Planetary Science Letters, v. 117, p.169-180.

Harrison, T.M., Lovera, O.M., and Matthew, T.H., 1991, $^{40}Ar/^{39}Ar$ results for alkali feldspar containing diffusion domains with differing activation energy: Geochimica et Cosmochimica Acta, v. 55, p. 1435-1448.

Harrison, T.M., Yin, A., Grove, M., Lovera, O.M. and Ryerson, F.J., 2000, The Zedong Window: a record of superposed Tertiary convergence in southeastern Tibet: Journal of Geophysical Research, v. 105, p. 19211-19230.

Heizler, M.T., and Harrison, T.M., 1988, Multiple trapped argon isotope components revealed by $^{40}Ar/^{39}Ar$ isochron analysis: Geochimica et Cosmochimica Acta, v. 52, p. 1295-1303.

Heizler, M.T., and Harrison, T.M.., 1986, The chronology of Adirondack epeirogeny: EOS, Transactions, American Geophysical Union, v. 67.16, p. 400.

Heizler, M.T., Lux, D.R., and Decker, E.R., 1988, The age and cooling history of the Chain of Ponds and Big Island Pond plutons and the Spider Lake granite, west-central Maine and Quebec: American Journal of Science, v. 288, p. 925-952.

Hodges, K.V., 1991, Pressure-temperature-time paths: Annual Review of Earth and Planetary Sciences, v. 19, p. 207-236.

Kitchen, N.E., and Valley, J.W., 1995, Carbon isotope thermometry in marbles of the Adirondack Mountains, New York: Journal of Metamorphic Geology, v. 13, p. 577-594.

Lee, J.K.W., 1995, Multipath diffusion in geochronology: Contributions to Mineralogy and Petrology, v. 120, p. 60-82.

Lee, M.R., and Parsons, I., 1997, Dislocation formation and albitization in alkali feldspars from the Shap granite: American Mineralogist, v. 82, p. 557-570.

Lovera, O.M., 1989, $^{40}Ar/^{39}Ar$ thermochronometry: Implications of having samples with a distribution of domain sizes [Ph.D. thesis]: Chicago, University of Chicago, 119 pp.

Lovera, O.M., Heizler, M.T., and Harrison, T.M., 1993, Argon diffusion domains in K-feldspar II: kinetic properties of MH-10: Contributions to Mineralogy and Petrology, v.113, p. 381-393.

Lovera, O.M., Richter, F.M., and Harrison, T.M., 1989, The $^{40}Ar/^{39}Ar$ thermochronometry for slowly cooled samples having a distribution of domain sizes: Journal of Geophysical Research, v. 94, p. 17917-17935.

Lovera, O.M., Richter, F.M., and Harrison, T.M., 1991, Diffusion domains determined by ^{39}Ar released during step heating: Journal of Geophysical Research, v. 96, p. 2057-2069.

Ludwig, K.R., 1991, ISOPLOT, A plotting and regression program for radiogenic-isotope data: U.S. Geological Survey Open-File Report 91-445.

Ludwig, K.R., 2003, User's manual for Isoplot, v. 3.0, a geochronological toolkit for Microsoft Excel: Berkeley Geochronological Center, Special Publication no. 4.

Lupulescu, M.V., Bailey, D.G., Hawkins, M., Carl, J.D., and Chiarenzelli, J.R., 2014, The Benson Mines, St. Lawrence County, New York: History of the discovery, mining, and mineralogy of the deposit: Rocks & Minerals, v. 89, p. 118-131.

Lupulescu, M.V., Chiarenzelli, J.R., and Bailey, D.G., 2012, Mineralogy, classification, and tectonic setting of the granitic pegmatites of New York State, USA: The Canadian Mineralogist, v. 50, p.1713-1728.

McDougall, I., and Harrison, T.M., 1999, Geochronology and Thermochronology by the $^{40}Ar/^{39}Ar$ method: New York, Oxford University Press, 269 p.

McLelland, J.M., Chiarenzelli, J., Whitney, P., and Isachsen, Y., 1988, U-Pb zircon geochronology of the Adirondack Mountains and implications for their geologic evolution: Geology, v. 16, p. 920-924.

McLelland, J.M., Daly, J.S., and McLelland, 1996, The Grenville orogenic cycle (ca. 1350-1000 Ma): an Adirondack perspective: Tectonophysics, v. 265, p. 1-28.

McLelland, J.M., Selleck, B.W., Hamilton, M.A., and Bickford, M.E., 2010, Late- to post-tectonic setting of some major Proterozoic anorthosites-mangerite-charnockite-granite (AMCG) suites: The Canadian Mineralogist, v. 48, p. 729-750.

Mezger, K., Rawnsley, C.M., Bohlen, S.R., and Hanson, G.N., 1991, U-Pb garnet, sphene, monazite, and rutile ages: Implications for the duration of high-grade metamorphism and cooling histories, Adirondack Mts., New York: Journal of Geology, v. 99, p. 415-428.

Onstott, T.C., and Peacock, M.W., 1987, Argon retentivity of hornblendes: A field experiment in a slowly cooled metamorphic terrane: Geochimica et Cosmochimica Acta, v. 51, p. 2891-2903.

Parsons, I., and Fitz Gerald, J.D., 2011, Coarsening kinetics of coexisting peristerite and film microperthite over 10^4 to 10^5 years: American Mineralogist, v. 96, p. 1575-1584.

Parsons, I., Brown, W.L., Smith, J.V., 1999, $^{40}Ar/^{39}Ar$ thermochronology using alkali feldspars: real thermal history or mathematical mirage of microtexture?: Contributions to Mineralogy and Petrology, v. 136, p. 92-110.

Parsons, I., Fitz Gerald, G.D., Lee, J.K.W., Ivanic, T., and Golla-Schindler, U., 2010, Time-temperature evolution of microtextures and contained fluids in a plutonic alkali feldspar during heating: Contributions to Mineralogy and Petrology, v. 160, p. 155-180.

Parsons, I., Fitz Gerald, J.D., and Lee, M.R., 2015, Routine characterization and interpretation of complex alkali feldspar intergrowths: American Mineralogist, v. 100, p. 1277-1303.

Parsons, I., Fitz Gerald, J.D., Heizler, M.T., Heizler, L.L., Ivanic, T., and Lee, M.R., 2013, Eight-phase alkali feldspars: Low-temperature cryptoperthite, peristerite and multiple replacement reactions in the Klokken intrusion: Contributions to Mineralogy and Petrology, v. 165, p. 931-961.

Parsons, I., Rex, D.C., Guise, P., and Halliday, A.N., 1988, Argon-loss by alkali feldspars: Geochimica et Cosmochimica Acta, v. 52, p. 1097-1112.

Quidelleur, X., Grove, M., Lovera, O.M., Harrison, T.M., Yin, A., and Ryerson, F.J., 1997, The thermal evolution and slip history of the Renbu Zedong Thrust, Southeastern Tibet: Journal of Geophysical Research, v. 102, p. 2659-2679.

Reddy, S.M., Potts, G.J., Kelley, S.P., and Arnaud, N.O., 1999, The effects of deformation-induced microstructures on intragrain $^{40}Ar/^{39}Ar$ ages in potassium feldspar: Geology, v. 27, p. 363-366.

Renne, P.R., Swisher, C.C., Deino, A.L., Karner, D.B., Owens, T.L., and DePaolo, D.J., 1998, Intercalibration of standards, absolute ages and uncertainties in $^{40}Ar/^{39}Ar$ dating: Chemical Geology, v. 145, p. 117-152.

Rivers, T., 2008, Assembly and preservation of upper, middle, and lower orogenic crust in the Grenville Province – Implications for the evolution of large, hot, long-duration orogens: Precambrian Research, v. 167, p. 237-259.

Spear, F.S., and Markussen, J.C., 1997, Mineral zoning, P-T-X-M phase relations, and metamorphic evolution of some Adirondack Granulites, New York*: Journal of Petrology, v. 38, p. 757-783.

Storm, L.C., and Spear, F.S., 2005, Pressure, temperature and cooling rates of granulite facies migmatitic pelites from the southern Adirondack highlands, New York: Journal of Metamorphic Geology, v. 23, p. 107-130.

Streepey, M.M., Johnson, E.L., Mezger, K., and van der Pluijm, B.A., 2001, Early History of the Carthage-Colton Shear Zone, Grenville Province, Northwest Adirondacks, New York (U.S.A.): The Journal of Geology, v. 109, p. 479-492.

Streepey, M.M., van der Pluijm, B.A., Essene, E.J., Hall, C.M., and Magloughlin, J.F., 2000, Late Proterozoic (ca. 930 Ma) extension in eastern Laurentia: Geological Society of America Bulletin, p. 1522-1530.

Tollo, R.P., Corriveau, L., McLelland, J.M., and Bartholomew, M.J., 2004, Proterozoic tectonic evolution of the Grenville orogen in North America: An introduction: Geological Society of America Memoir 197, p. 1-18.

Villa, I., 1994, Multipath Ar transport in K-feldspar deduced from isothermal heating experiments: Earth and Planetary Science Letters, v. 122, p. 393-401.

Villa, I., 2014, Diffusion of Ar in K-feldspar: Present and absent: Special Publication – Geological Society of London, v. 378, p. 107-116.

Villa, I., and Hanchar, J.M., 2013, K-feldspar hygrochronology: Geochimica et Cosmochimica Acta, v. 101, p. 24-33.

Waldron, K., Lee, M.R., and Parsons, I., 1994, The microstructures of perthitic alkali feldspars revealed by hydrofluoric-acid etching: Contributions to Mineralogy and Petrology, v. 116, p. 360-364.

Wartho, J., Kelley, S.P., Brooker, R.A., Carroll, M.R., Villa, I.M., and Lee, M.R., 1999, Direct measurement of Ar diffusion profiles in gem-quality Madagascar K-feldspar using the ultra-violet laser ablation microprobe (UVLAMP): Earth and Planetary Science Letters, v. 170, p.141-153.

Wasteneys, H., McLelland, J., and Lumbers, S., 1999, Precise zircon geochronology in the Adirondack Lowlands and implications for plate tectonic models of the Central metasedimentary belt, Grenville Province, Ontario, and Adirondack mountains, New York: Canadian Journal of Earth Sciences, v. 36, p. 967-984.

Xu, Y, and Foland, K.A., 1991, Diffusion of Ar isotopes in irradiated minerals during $^{40}Ar/^{39}Ar$ incremental heating [abs]: Eos (Transactions, American Geophysical Union), v. 72, p. 291.

Zeitler, P.K., 1987, Argon diffusion in partially outgassed alkali feldspars: Insights from $^{40}Ar/^{39}Ar$ analysis: Chemical Geology, v. 65, p.167-181.

APPENDIX: ARGON DATA

ID	P	t	^{40}Ar (*+ atm)	± 1σ	$^{39}Ar_K$	± 1σ	^{38}Ar (atm)	± 1σ	$^{37}Ar_{Ca}$	± 1σ	^{36}Ar	± 1σ	$^{40}Ar^*$	%Rad	R	Age	± 1σ	%-sd
#		(sec)	(V)		(V)		(V)		(V)		(V)		(mol)			(Ma)		

Date Ran:	06/23/2014	Sensitivity (Moles/volt):	1.62E-14	2E-16	Incremental heating and fusion analyses were accomplished with a CO2 and diode laser.
Volts ^{40}Ar from air:	7.238709677	J-Value:	98790000	395160	Data are corrected for interfering nuclear reactions, blank, and mass discrimination.
Irradiation Package:	AU-25	Measured 40/36 of Air:	291.0	1.5	
Elapsed Days:	284	Mass Discrimination (% per amu);	-0.003807	0.00101523	Data are in volts and errors are the standard deviation unless indicated otherwise.
GA1550 Biotite Monitor Age:	9.879E+07	(36/37)Ca:	0.0003005	0.0000044	Plateau ages include errors arising from precision of measurement and in estimating the J-value.
FC Sanidine Monitor Age:	2.802E+07	(39/37)Ca:	0.0008200	0.0000820	
		(40/39)K:	0	4E-04	All samples were analyzed within 250 days of irradiation
		(38/39)Cl	0.01	0.01	
		Date of Irradiation	9/9/2013		

BEN-6: Hornblende

au25.1q.hbl.6

1	0.6	30	0.24751	0.00051	0.00641	0.00012	0.00015	0.00002	-0.00255	0.00293	0.00001	0.00001	4.02E-15	99.0%	38.164	877.56	18.58	2.12%
2	0.7	30	0.13692	0.00041	0.00369	0.00009	0.00017	0.00002	0.00601	0.00294	0.00000	0.00001	2.22E-15	99.4%	37.080	857.71	25.44	2.97%
3	0.8	30	0.21646	0.00056	0.00545	0.00011	0.00030	0.00003	0.00868	0.00248	0.00002	0.00001	3.51E-15	96.9%	38.655	886.47	21.47	2.42%
4	0.9	30	0.17665	0.00064	0.00522	0.00013	0.00023	0.00002	0.00833	0.00307	0.00002	0.00001	2.87E-15	97.5%	33.181	784.46	23.11	2.95%
5	1	30	0.07974	0.00042	0.00260	0.00009	0.00007	0.00003	0.00140	0.00269	0.00000	0.00001	1.29E-15	100.2%	30.777	737.77	33.13	4.49%
6	1.05	30	0.04628	0.00029	0.00164	0.00009	0.00010	0.00002	0.00050	0.00288	0.00000	0.00001	7.51E-16	100.5%	28.301	688.39	57.51	8.35%
7	1.1	30	0.06204	0.00040	0.00168	0.00010	0.00020	0.00003	0.00820	0.00174	0.00000	0.00001	1.01E-15	100.4%	37.596	867.18	57.74	6.66%
8	1.15	30	0.14469	0.00164	0.00319	0.00008	0.00066	0.00003	0.00267	0.00442	0.00004	0.00001	2.35E-15	92.6%	42.117	948.13	34.93	3.68%

APPENDIX: ARGON DATA

ID	P	t	^{40}Ar (*+ atm)	± 1σ	$^{39}Ar_K$	± 1σ	^{38}Ar (atm)	± 1σ	$^{37}Ar_{Ca}$	± 1σ	^{36}Ar	± 1σ	$^{40}Ar^*$	%Rad	R	Age	± 1σ	%-sd
#		(sec)	(V)		(V)		(V)		(V)		(V)		(mol)			(Ma)		
9	1.18	30	0.13544	0.00052	0.00286	0.00010	0.00065	0.00003	0.02029	0.00260	0.00000	0.00001	2.20E-15	100.9%	48.363	1054.31	39.96	3.79%
10	1.21	30	0.23733	0.00045	0.00513	0.00011	0.00119	0.00003	0.00900	0.00248	0.00000	0.00001	3.85E-15	100.1%	46.479	1022.94	27.31	2.67%
11	1.24	30	0.39572	0.00090	0.00896	0.00010	0.00209	0.00003	0.01785	0.00336	0.00000	0.00001	6.42E-15	99.8%	44.328	986.45	13.19	1.34%
12	1.27	30	1.91757	0.00155	0.04326	0.00013	0.01099	0.00011	0.11621	0.00336	0.00006	0.00001	3.11E-14	99.0%	44.244	985.00	3.82	0.39%
13	1.3	30	3.63281	0.00308	0.08386	0.00044	0.02031	0.00027	0.20425	0.00410	0.00009	0.00001	5.90E-14	99.2%	43.295	968.65	5.29	0.55%
14	1.33	30	0.19157	0.00054	0.00449	0.00011	0.00098	0.00004	0.00923	0.00274	-0.00001	0.00002	3.11E-15	100.9%	42.944	962.56	32.98	3.43%
15	1.36	30	0.14512	0.00039	0.00327	0.00009	0.00078	0.00003	0.00267	0.00366	0.00000	0.00001	2.36E-15	100.1%	44.522	989.76	33.25	3.36%
16	1.39	30	0.24729	0.00042	0.00575	0.00009	0.00139	0.00003	0.00850	0.00394	-0.00001	0.00001	4.01E-15	101.1%	43.173	966.53	17.61	1.82%
17	1.42	30	0.44555	0.00069	0.01028	0.00017	0.00251	0.00005	0.01986	0.00298	-0.00001	0.00001	7.23E-15	100.4%	43.604	973.98	16.79	1.72%
18	1.45	30	1.38035	0.00162	0.03174	0.00014	0.00741	0.00008	0.07399	0.00313	0.00002	0.00001	2.24E-14	99.6%	43.625	974.36	5.31	0.54%
19	1.5	30	5.25723	0.00439	0.12365	0.00052	0.02978	0.00017	0.31415	0.00482	0.00015	0.00002	8.54E-14	99.1%	42.468	954.27	4.19	0.44%
20	1.55	30	5.98281	0.00618	0.14002	0.00051	0.03389	0.00022	0.38616	0.01244	0.00015	0.00002	9.71E-14	99.2%	42.756	959.29	3.77	0.39%
21	1.6	30	4.94064	0.00371	0.11561	0.00030	0.02832	0.00019	0.28602	0.00690	0.00013	0.00001	8.02E-14	99.2%	42.725	958.75	2.66	0.28%
22	1.65	30	3.63615	0.00303	0.08488	0.00036	0.02056	0.00016	0.20897	0.00299	0.00009	0.00001	5.90E-14	99.3%	42.854	960.99	4.33	0.45%
23	1.7	30	5.33252	0.00626	0.12325	0.00039	0.03027	0.00024	0.31517	0.00569	0.00013	0.00001	8.66E-14	99.3%	43.284	968.45	3.36	0.35%
24	1.8	30	4.98174	0.00679	0.11521	0.00041	0.02795	0.00023	0.31508	0.00769	0.00012	0.00001	8.09E-14	99.3%	43.271	968.23	3.77	0.39%
25	1.9	20	0.47752	0.00100	0.01120	0.00015	0.00262	0.00003	0.02673	0.00390	0.00000	0.00002	7.75E-15	99.9%	42.907	961.92	16.52	1.72%
26	2	20	1.48013	0.00129	0.03441	0.00014	0.00857	0.00012	0.09515	0.00440	0.00005	0.00001	2.40E-14	99.0%	42.921	962.17	4.31	0.45%
27	2.1	20	2.14580	0.00135	0.05033	0.00026	0.01321	0.00015	0.14581	0.00455	0.00006	0.00001	3.48E-14	99.2%	42.643	957.33	5.35	0.56%
28	2.2	20	1.54224	0.00230	0.03535	0.00010	0.01045	0.00009	0.13751	0.00436	0.00007	0.00001	2.50E-14	98.6%	43.513	972.42	3.49	0.36%

APPENDIX: ARGON DATA

ID	P	t	^{40}Ar (*+ atm)	± 1σ	$^{39}Ar_K$	± 1σ	^{38}Ar (atm)	± 1σ	$^{37}Ar_{Ca}$	± 1σ	^{36}Ar	± 1σ	$^{40}Ar^*$	%Rad	R	Age	± 1σ	%-sd
#		(sec)	(V)		(V)		(V)		(V)		(V)		(mol)			(Ma)		

Plateau Age = 962.7±1.2 Ma
(1σ, including J-error of .000011%)
MSWD = 1.4, probability = 0.13
88.2% of the 39Ar, steps 13 through 27

BEN-6: Hornblende

au25.1q.hbl.7

1	0.5	30	0.00000	0.00019	0.00000	0.00005	-0.00001	0.00002	-0.00444	0.00335	-0.000013	0.00002	1.55E-17	495.6%	124.757	2010.63	86.4E5	43.0E4%
2	0.6	30	0.01292	0.00034	0.00030	0.00006	0.00002	0.00002	0.00108	0.00364	0.000006	0.00001	2.10E-16	85.5%	36.666	850.08	357.93	42.11%
3	0.7	30	0.01903	0.00028	0.00042	0.00005	0.00002	0.00002	-0.00305	0.00344	-0.000007	0.00002	3.09E-16	110.8%	44.786	994.28	306.88	30.86%
4	0.75	30	0.01952	0.00026	0.00037	0.00005	0.00004	0.00002	-0.00281	0.00212	0.000013	0.00001	3.17E-16	80.4%	41.489	937.12	295.93	31.58%
5	0.78	30	0.00451	0.00019	0.00011	0.00006	0.00000	0.00002	-0.00033	0.00271	-0.000001	0.00001	7.32E-17	106.8%	40.681	922.82	909.32	98.54%
6	0.81	30	0.00842	0.00019	0.00024	0.00009	0.00001	0.00002	0.00204	0.00370	-0.000004	0.00002	1.37E-16	115.7%	35.488	828.17	560.67	67.70%
7	0.84	30	0.00535	0.00020	0.00024	0.00009	0.00003	0.00002	0.00288	0.00217	0.000017	0.00001	8.69E-17	5.1%	2.236	65.04	549.94	845.53%
8	0.87	30	0.01019	0.00029	0.00030	0.00008	0.00005	0.00002	-0.00210	0.00259	-0.000002	0.00001	1.65E-16	105.8%	33.051	781.98	409.14	52.32%
9	0.9	30	0.01462	0.00023	0.00033	0.00008	0.00008	0.00002	-0.00146	0.00206	0.000028	0.00001	2.37E-16	43.7%	18.899	487.49	455.95	93.53%
10	0.98	30	0.00225	0.00016	0.00010	0.00006	0.00003	0.00002	0.00144	0.00223	-0.000028	0.00002	3.65E-17	472.4%	23.921	597.58	1686.9	282.30%
11	1.03	30	0.00853	0.00017	0.00018	0.00005	0.00003	0.00002	0.00211	0.00262	0.000028	0.00001	1.38E-16	2.1%	2.091	60.89	846.12	1389.51%
12	1.18	30	0.56455	0.00127	0.01165	0.00008	0.00294	0.00007	0.02668	0.00211	0.000034	0.00002	9.17E-15	98.2%	47.898	1046.63	12.38	1.18%
13	1.23	30	4.92248	0.00335	0.11155	0.00047	0.02702	0.00024	0.27737	0.00609	0.000144	0.00002	7.99E-14	99.1%	44.062	981.88	4.34	0.44%
14	1.28	30	4.62830	0.00494	0.10482	0.00025	0.02541	0.00020	0.27952	0.00758	0.000169	0.00001	7.51E-14	98.9%	44.019	981.13	2.73	0.28%
15	1.33	30	5.93966	0.00551	0.13413	0.00054	0.03275	0.00013	0.32322	0.00367	0.000178	0.00002	9.64E-14	99.1%	44.199	984.23	4.15	0.42%

APPENDIX: ARGON DATA

ID	P	t	^{40}Ar (*+ atm)	± 1σ	$^{39}Ar_K$	± 1σ	^{38}Ar (atm)	± 1σ	$^{37}Ar_{Ca}$	± 1σ	^{36}Ar	± 1σ	$^{40}Ar^*$	%Rad	R	Age	± 1σ	%-sd
#		(sec)	(V)		(V)		(V)		(V)		(V)		(mol)			(Ma)		
16	1.48	30	5.21257	0.00395	0.11653	0.00042	0.02815	0.00014	0.30979	0.00671	0.000181	0.00001	8.46E-14	99.0%	44.614	991.33	3.76	0.38%
17	1.53	30	1.96494	0.00175	0.04421	0.00019	0.01039	0.00009	0.12281	0.00692	0.000063	0.00002	3.19E-14	99.1%	44.382	987.36	5.05	0.51%
18	1.58	30	4.47788	0.00354	0.09979	0.00044	0.02405	0.00010	0.25266	0.00760	0.000135	0.00002	7.27E-14	99.1%	44.794	994.42	4.62	0.46%
19	1.63	30	1.15942	0.00093	0.02605	0.00023	0.00610	0.00006	0.06479	0.00299	0.000033	0.00001	1.88E-14	99.2%	44.447	988.48	8.96	0.91%
20	1.68	30	0.31688	0.00038	0.00700	0.00009	0.00163	0.00004	0.02415	0.00337	0.000006	0.00001	5.14E-15	99.4%	45.467	1005.86	14.88	1.48%
21	1.7	30	0.09003	0.00046	0.00198	0.00007	0.00046	0.00002	0.00540	0.00117	-0.000003	0.00001	1.46E-15	100.9%	45.702	1009.85	46.72	4.63%
22	1.8	30	0.12684	0.00053	0.00274	0.00009	0.00067	0.00002	0.01152	0.00327	0.000012	0.00001	2.06E-15	97.2%	45.530	1006.94	41.75	4.15%
23	1.9	30	0.07383	0.00034	0.00176	0.00006	0.00040	0.00002	0.00671	0.00315	-0.000003	0.00001	1.20E-15	101.4%	42.453	954.01	47.19	4.95%
24	2	30	0.29478	0.00029	0.00658	0.00009	0.00163	0.00005	0.01366	0.00358	-0.000013	0.00001	4.79E-15	101.3%	45.047	998.72	18.38	1.84%
25	2.1	30	0.42115	0.00033	0.00945	0.00011	0.00229	0.00006	0.02350	0.00247	0.000021	0.00002	6.84E-15	98.5%	44.233	984.82	15.43	1.57%
26	2.2	30	0.50178	0.00088	0.01117	0.00014	0.00261	0.00003	0.03380	0.00293	0.000015	0.00001	8.15E-15	99.1%	44.902	996.26	14.54	1.46%
27	2.3	30	0.39929	0.00091	0.00905	0.00009	0.00201	0.00002	0.02185	0.00326	0.000005	0.00001	6.48E-15	99.6%	44.267	985.39	12.15	1.23%

Plateau Age = 989.7±2.0 Ma
(1σ, including J-error of .000011%)
MSWD = 0.50, probability = 0.92
67.4% of the 39Ar, steps 4 through 16

BEN-6: Hornblende

au25.1q.hbl.8

1	0.5	30	0.00462	0.00036	0.00007	0.00007	-0.00002	0.00002	-0.00325	0.00286	-0.000010	0.00001	7.50E-17	164.5%	55.677	1171.19	16.3E2	139.54%
2	0.6	30	0.04484	0.00039	0.00024	0.00008	0.00000	0.00002	-0.00192	0.00275	-0.000024	0.00001	7.28E-16	115.5%	185.122	2518.47	929.69	36.91%
3	0.7	30	0.11998	0.00040	0.00060	0.00011	0.00006	0.00002	-0.00404	0.00301	-0.000010	0.00001	1.95E-15	102.5%	199.171	2618.65	479.29	18.30%

APPENDIX: ARGON DATA

ID	P	t	^{40}Ar (*+ atm)	± 1σ	$^{39}Ar_K$	± 1σ	^{38}Ar (atm)	± 1σ	$^{37}Ar_{Ca}$	± 1σ	^{36}Ar	± 1σ	$^{40}Ar^*$	%Rad	R	Age	± 1σ	%-sd
#		(sec)	(V)		(V)		(V)		(V)		(V)		(mol)			(Ma)		
4	0.8	30	0.27012	0.00044	0.00140	0.00010	0.00018	0.00002	0.00030	0.00243	-0.000006	0.00001	4.39E-15	100.6%	192.328	2570.55	183.02	7.12%
5	0.9	30	0.20134	0.00051	0.00137	0.00010	0.00013	0.00002	-0.00577	0.00423	0.000002	0.00001	3.27E-15	99.7%	145.663	2203.11	164.65	7.47%
6	1	30	0.07460	0.00040	0.00097	0.00009	0.00008	0.00002	-0.00280	0.00141	-0.000008	0.00001	1.21E-15	103.1%	76.119	1462.64	146.68	10.03%
7	1.03	30	0.03198	0.00035	0.00076	0.00008	0.00006	0.00002	-0.00917	0.00446	-0.000005	0.00001	5.19E-16	104.4%	40.654	922.33	126.29	13.69%
8	1.06	30	0.02144	0.00025	0.00045	0.00005	0.00007	0.00002	-0.00579	0.00243	0.000003	0.00001	3.48E-16	96.0%	44.230	984.76	193.57	19.66%
9	1.09	30	0.02831	0.00022	0.00074	0.00008	0.00006	0.00002	-0.00225	0.00276	0.000003	0.00001	4.60E-16	96.8%	36.767	851.94	132.12	15.51%
10	1.12	30	0.04257	0.00026	0.00092	0.00006	0.00015	0.00002	0.00240	0.00301	0.000006	0.00001	6.91E-16	95.7%	44.562	990.45	96.80	9.77%
11	1.15	30	0.08892	0.00038	0.00195	0.00008	0.00043	0.00002	0.00203	0.00261	0.000015	0.00001	1.44E-15	95.0%	43.420	970.81	55.59	5.73%
12	1.18	30	0.08731	0.00054	0.00198	0.00007	0.00041	0.00003	-0.00154	0.00312	-0.000004	0.00001	1.42E-15	101.5%	43.990	980.63	57.59	5.87%
13	1.21	30	0.32195	0.00090	0.00723	0.00014	0.00193	0.00005	0.01373	0.00350	0.000003	0.00001	5.23E-15	99.8%	44.659	992.11	20.43	2.06%
14	1.24	30	1.40860	0.00181	0.03227	0.00016	0.00827	0.00010	0.07816	0.00433	0.000037	0.00001	2.29E-14	99.2%	43.616	974.20	5.21	0.54%
15	1.27	30	3.41547	0.00234	0.07932	0.00034	0.01979	0.00007	0.18874	0.00440	0.000093	0.00001	5.55E-14	99.2%	43.016	963.81	4.32	0.45%
16	1.3	30	3.83459	0.00203	0.08863	0.00052	0.02205	0.00026	0.22180	0.00600	0.000115	0.00001	6.23E-14	99.1%	43.202	967.04	5.70	0.59%
17	1.33	30	0.44708	0.00078	0.01038	0.00008	0.00238	0.00003	0.02588	0.00167	0.000005	0.00001	7.26E-15	99.7%	43.249	967.86	8.64	0.89%
18	1.36	30	0.29454	0.00052	0.00708	0.00012	0.00158	0.00004	0.01660	0.00409	0.000000	0.00001	4.78E-15	100.0%	41.869	943.80	19.26	2.04%
19	1.39	30	0.66086	0.00120	0.01554	0.00010	0.00367	0.00003	0.04990	0.00622	0.000014	0.00001	1.07E-14	99.4%	42.678	957.93	7.27	0.76%
20	1.42	30	1.40658	0.00100	0.03280	0.00022	0.00771	0.00009	0.07824	0.00299	0.000003	0.00001	2.28E-14	99.9%	43.167	966.43	7.13	0.74%
21	1.46	30	5.84419	0.00334	0.13364	0.00045	0.03327	0.00034	0.36898	0.01173	0.000192	0.00001	9.49E-14	99.0%	43.657	974.90	3.39	0.35%
22	1.5	30	7.84293	0.00636	0.18169	0.00045	0.04466	0.00026	0.44686	0.00545	0.000223	0.00001	1.27E-13	99.2%	43.114	965.51	2.57	0.27%
23	1.54	30	8.52297	0.00951	0.19748	0.00062	0.04852	0.00027	0.48416	0.00607	0.000268	0.00001	1.38E-13	99.1%	43.067	964.70	3.25	0.34%

APPENDIX: ARGON DATA

ID	P	t	^{40}Ar (*+ atm)	± 1σ	$^{39}Ar_K$	± 1σ	^{38}Ar (atm)	± 1σ	$^{37}Ar_{Ca}$	± 1σ	^{36}Ar	± 1σ	$^{40}Ar^*$	%Rad	R	Age	± 1σ	%-sd
#		(sec)	(V)		(V)		(V)		(V)		(V)		(mol)			(Ma)		
24	1.58	30	14.12366	0.00944	0.33199	0.00068	0.08152	0.00022	0.95384	0.01520	0.000483	0.00001	2.29E-13	99.0%	42.473	954.36	2.09	0.22%
25	1.62	30	1.75092	0.00201	0.04073	0.00011	0.01011	0.00013	0.10303	0.00369	0.000019	0.00001	2.84E-14	99.7%	43.174	966.55	3.65	0.38%
26	1.68	30	0.86815	0.00114	0.02048	0.00013	0.00510	0.00004	0.05105	0.00335	0.000005	0.00001	1.41E-14	99.8%	42.632	957.13	7.21	0.75%
27	1.74	30	0.50469	0.00060	0.01176	0.00017	0.00323	0.00007	0.04170	0.00446	0.000001	0.00001	8.19E-15	99.9%	43.346	969.53	16.06	1.66%
28	1.85	30	0.81708	0.00060	0.01905	0.00011	0.00498	0.00008	0.06880	0.00387	0.000028	0.00001	1.33E-14	99.0%	42.915	962.06	6.17	0.64%

Plateau Age = 967.3±1.4 Ma
(1σ, including J-error of .000011%)
MSWD = 0.89, probability = 0.58
64.9% of the 39Ar, steps 7 through 23 of 28

BEN-6: Biotite

au25.1n.bio.1

1	0.4	30	0.00056	0.00034	0.00002	0.00007	0.00000	0.00005	-5.67210	6.74224	-0.000022	0.00001	9.05E-18	1242.15%	36.357	844.36	44.4E3	5264.1%
2	0.45	30	0.00392	0.00034	0.00012	0.00006	0.00004	0.00003	2.36157	9.19340	0.000023	0.00001	6.37E-17	-70.95%	-22.738	-842.91	-1446.6	171.62%
3	0.5	30	0.00172	0.00039	0.00015	0.00007	0.00006	0.00003	2.08607	8.18240	-0.000029	0.00001	2.79E-17	601.37%	11.266	306.14	10.2E2	334.27%
4	0.55	30	0.00952	0.00036	0.00029	0.00007	0.00011	0.00003	4.06773	5.67061	-0.000030	0.00001	1.55E-16	193.73%	32.489	771.15	420.58	54.54%
5	0.6	30	0.01794	0.00035	0.00128	0.00008	0.00017	0.00003	13.63142	11.38415	0.000023	0.00001	2.91E-16	61.76%	8.674	240.16	65.08	27.10%
6	0.63	30	0.03050	0.00028	0.00397	0.00009	0.00020	0.00002	9.69801	6.01764	0.000008	0.00001	4.95E-16	92.00%	7.075	198.23	18.39	9.28%
7	0.66	30	0.03251	0.00081	0.00238	0.00008	0.00009	0.00002	-3.44014	9.62251	-0.000002	0.00001	5.28E-16	101.71%	13.680	365.49	31.90	8.73%
8	0.69	30	0.06674	0.00040	0.00397	0.00010	0.00016	0.00002	-22.27560	9.04988	0.000011	0.00001	1.08E-15	95.19%	15.986	420.42	19.79	4.71%
9	0.72	30	0.08675	0.00043	0.00440	0.00010	0.00017	0.00002	-2.74320	7.13852	0.000025	0.00001	1.41E-15	91.61%	18.070	468.65	17.53	3.74%
10	0.75	30	0.04472	0.00034	0.00223	0.00009	0.00003	0.00002	-0.96223	7.74466	-0.000004	0.00001	7.26E-16	102.97%	20.016	512.56	35.36	6.90%

APPENDIX: ARGON DATA

ID	P	t	^{40}Ar (*+ atm)	± 1σ	$^{39}Ar_K$	± 1σ	^{38}Ar (atm)	± 1σ	$^{37}Ar_{Ca}$	± 1σ	^{36}Ar	± 1σ	$^{40}Ar^*$	%Rad	R	Age	± 1σ	%-sd
#		(sec)	(V)		(V)		(V)		(V)		(V)		(mol)			(Ma)		
11	0.78	30	0.22565	0.00080	0.01056	0.00013	0.00046	0.00002	1.06855	8.83733	0.000056	0.00001	3.66E-15	92.65%	19.790	507.52	9.66	1.90%
12	0.81	30	0.09504	0.00043	0.00322	0.00008	0.00014	0.00002	1.10351	6.24590	-0.000036	0.00001	1.54E-15	111.32%	29.534	713.15	32.89	4.61%
13	0.84	30	0.11568	0.00039	0.00359	0.00009	0.00010	0.00003	-9.46807	9.31310	-0.000005	0.00001	1.88E-15	101.39%	32.251	766.55	24.10	3.14%
14	0.87	30	0.21555	0.00064	0.00624	0.00009	0.00028	0.00002	-5.86934	11.62009	0.000006	0.00001	3.50E-15	99.12%	34.227	804.42	15.19	1.89%
15	0.91	30	0.38429	0.00080	0.01031	0.00012	0.00049	0.00002	-19.64350	12.78615	0.000007	0.00001	6.24E-15	99.47%	37.085	857.80	11.48	1.34%
16	0.95	30	0.50129	0.00090	0.01263	0.00017	0.00061	0.00002	-3.84443	8.66291	0.000015	0.00001	8.14E-15	99.13%	39.350	899.02	13.31	1.48%
17	1	30	0.94970	0.00108	0.02400	0.00016	0.00115	0.00003	-1.09887	6.61074	-0.000016	0.00001	1.54E-14	100.50%	39.569	902.96	6.82	0.76%
18	1.05	30	2.06105	0.00197	0.05089	0.00010	0.00262	0.00007	-6.02969	7.66159	-0.000008	0.00001	3.35E-14	100.11%	40.501	919.62	2.55	0.28%
19	1.1	30	2.99797	0.00208	0.07389	0.00010	0.00355	0.00003	-6.09559	13.75986	0.000034	0.00001	4.87E-14	99.67%	40.438	918.49	1.56	0.17%
20	1.15	30	4.59279	0.00418	0.11283	0.00025	0.00548	0.00003	4.07612	4.13037	0.000048	0.00001	7.46E-14	99.69%	40.580	921.03	2.28	0.25%
21	1.17	30	3.01885	0.00176	0.07460	0.00018	0.00358	0.00004	12.01050	8.00460	0.000000	0.00002	4.90E-14	100.00%	40.468	919.03	2.78	0.30%
22	1.2	30	3.32309	0.00117	0.08203	0.00022	0.00395	0.00003	-1.02501	9.27017	0.000050	0.00001	5.40E-14	99.55%	40.330	916.57	2.65	0.29%
23	1.25	30	3.07645	0.00252	0.07624	0.00017	0.00362	0.00005	-1.48770	6.97530	0.000048	0.00001	4.99E-14	99.53%	40.164	913.61	2.46	0.27%
24	1.3	30	4.02612	0.00252	0.10017	0.00044	0.00470	0.00006	-2.54527	9.88428	0.000065	0.00001	6.54E-14	99.52%	40.000	910.69	4.16	0.46%
25	1.35	30	3.80490	0.00336	0.09355	0.00018	0.00445	0.00004	8.27213	6.08211	0.000042	0.00002	6.18E-14	99.68%	40.541	920.32	2.24	0.24%
26	1.4	30	3.86564	0.00259	0.09592	0.00023	0.00458	0.00005	22.58231	9.03851	0.000033	0.00001	6.28E-14	99.75%	40.197	914.20	2.32	0.25%
27	1.5	30	6.26484	0.00528	0.15611	0.00052	0.00744	0.00003	37.41067	8.95597	0.000008	0.00001	1.02E-13	99.96%	40.115	912.74	3.18	0.35%
28	1.6	30	7.80422	0.00726	0.19501	0.00028	0.00944	0.00007	21.38966	4.96471	0.000007	0.00002	1.27E-13	99.97%	40.008	910.83	1.67	0.18%
29	1.7	30	7.75817	0.00819	0.19338	0.00041	0.00908	0.00006	41.27072	12.55401	0.000030	0.00001	1.26E-13	99.89%	40.073	911.98	2.21	0.24%
30	1.8	30	3.63803	0.00313	0.09104	0.00016	0.00443	0.00006	41.83105	12.08447	0.000019	0.00001	5.91E-14	99.85%	39.900	908.89	1.87	0.21%

APPENDIX: ARGON DATA

ID	P	t	^{40}Ar (*+ atm)	± 1σ	$^{39}Ar_K$	± 1σ	^{38}Ar (atm)	± 1σ	$^{37}Ar_{Ca}$	± 1σ	^{36}Ar	± 1σ	$^{40}Ar^*$	%Rad	R	Age	± 1σ	%-sd
#		(sec)	(V)		(V)		(V)		(V)		(V)		(mol)			(Ma)		
31	1.9	30	20.69123	0.00887	0.52027	0.00084	0.02544	0.00024	151.12783	13.27099	0.000024	0.00002	3.36E-13	99.97%	39.756	906.32	1.54	0.17%
32	2	30	4.25819	0.00229	0.10665	0.00022	0.00507	0.00006	4.79050	7.56566	-0.000023	0.00001	6.91E-14	100.16%	39.928	909.39	2.05	0.23%
33	2.1	30	13.67816	0.00633	0.34294	0.00057	0.01627	0.00012	136.19948	7.61536	0.000077	0.00001	2.22E-13	99.83%	39.819	907.44	1.58	0.17%
34	2.2	20	5.87341	0.00626	0.14815	0.00038	0.00720	0.00009	-13.00917	7.10601	-0.000008	0.00001	9.54E-14	100.04%	39.645	904.32	2.57	0.28%
35	2.3	20	2.14589	0.00129	0.05434	0.00015	0.00259	0.00003	-9.87229	8.41081	-0.000043	0.00002	3.48E-14	100.59%	39.492	901.57	3.28	0.36%
36	2.4	20	5.88921	0.00445	0.14893	0.00035	0.00696	0.00006	15.60068	8.59170	0.000025	0.00001	9.56E-14	99.87%	39.495	901.62	2.26	0.25%
37	2.5	20	2.33027	0.00192	0.05865	0.00013	0.00279	0.00004	31.83651	14.41597	-0.000018	0.00001	3.78E-14	100.23%	39.730	905.85	2.76	0.30%
38	2.6	20	2.20052	0.00239	0.05556	0.00010	0.00260	0.00004	18.14844	8.18341	0.000017	0.00001	3.57E-14	99.77%	39.517	902.02	2.14	0.24%
39	2.7	20	2.57149	0.00269	0.06460	0.00014	0.00304	0.00004	17.97392	12.93060	0.000023	0.00001	4.17E-14	99.73%	39.698	905.27	2.41	0.27%
40	2.8	20	3.13632	0.00149	0.07899	0.00020	0.00365	0.00003	-13.76332	8.34989	0.000007	0.00001	5.09E-14	99.93%	39.680	904.94	2.38	0.26%

Total Gas Age= 910.8±3.4 Ma (95% conf.)
MSWD = 9.1, probability = 0.000
incl. 100% of the 39Ar, steps 1-26

BEN-6: Biotite

au25.1n.bio.2

1	0.5	30	0.04816	0.00056	0.00167	0.00008	0.00012	0.00003	-6.29647	9.91848	0.000054	0.00001	7.82E-16	66.64%	19.180	493.82	70.91	14.36%
2	0.55	30	0.00681	0.00036	0.00042	0.00007	-0.00002	0.00004	11.31131	8.43882	0.000032	0.00001	1.11E-16	-40.31%	-6.568	-205.82	-338.2	164.33%
3	0.6	30	0.01231	0.00042	0.00163	0.00011	0.00012	0.00003	2.15621	10.95178	0.000045	0.00001	2.00E-16	-7.51E-02	-0.566	-16.84	-80.43	477.58%
4	0.63	30	0.01256	0.00045	0.00191	0.00011	0.00016	0.00003	-0.37202	8.42054	0.000032	0.00001	2.04E-16	24.88%	1.638	47.86	63.62	132.93%
5	0.66	30	0.01993	0.00035	0.00219	0.00008	0.00018	0.00003	-6.07025	7.96544	0.000011	0.00002	3.24E-16	84.08%	7.657	213.62	64.01	29.97%

APPENDIX: ARGON DATA

ID	P	t	^{40}Ar (*+ atm)	± 1σ	$^{39}Ar_K$	± 1σ	^{38}Ar (atm)	± 1σ	$^{37}Ar_{Ca}$	± 1σ	^{36}Ar	± 1σ	$^{40}Ar^*$	%Rad	R	Age	± 1σ	%-sd
#		(sec)	(V)		(V)		(V)		(V)		(V)		(mol)			(Ma)		
6	0.69	30	0.05024	0.00034	0.00238	0.00010	0.00010	0.00002	-16.92746	10.05242	0.000000	0.00001	8.16E-16	100.26%	21.091	536.37	31.16	5.81%
7	0.72	30	0.02778	0.00033	0.00151	0.00007	0.00006	0.00002	-11.96725	9.52379	-0.000012	0.00001	4.51E-16	112.31%	18.370	475.49	62.29	13.10%
8	0.75	30	0.06815	0.00022	0.00323	0.00006	0.00009	0.00002	-19.15988	9.43372	0.000030	0.00001	1.11E-15	87.13%	18.383	475.78	21.32	4.48%
9	0.78	30	0.11329	0.00048	0.00418	0.00008	0.00010	0.00002	-19.44119	9.92532	0.000043	0.00001	1.84E-15	88.86%	24.102	601.41	20.61	3.43%
10	0.81	30	0.23523	0.00039	0.00725	0.00014	0.00032	0.00002	-23.24463	5.36546	0.000052	0.00001	3.82E-15	93.43%	30.300	728.36	17.54	2.41%
11	0.84	30	0.13082	0.00032	0.00358	0.00009	0.00019	0.00001	-38.90812	8.21985	-0.000014	0.00001	2.12E-15	103.17%	36.492	846.86	31.93	3.77%
12	0.87	30	0.28883	0.00019	0.00735	0.00011	0.00034	0.00001	-39.53295	7.39434	0.000021	0.00001	4.69E-15	97.81%	38.437	882.51	15.27	1.73%
13	0.91	30	0.59001	0.00079	0.01510	0.00010	0.00072	0.00002	-7.79906	9.73226	0.000025	0.00001	9.58E-15	98.74%	38.574	885.02	7.20	0.81%
14	0.95	30	0.96609	0.00092	0.02397	0.00013	0.00116	0.00003	-9.90334	3.86689	0.000022	0.00001	1.57E-14	99.31%	40.028	911.18	5.59	0.61%
15	1	30	1.43122	0.00176	0.03556	0.00012	0.00172	0.00002	-5.62849	7.42296	-0.000014	0.00002	2.32E-14	100.30%	40.253	915.20	4.48	0.49%
16	1.05	30	0.69080	0.00075	0.01751	0.00013	0.00091	0.00002	1.83950	8.26411	-0.000009	0.00002	1.12E-14	100.38%	39.458	900.97	9.40	1.04%
17	1.1	30	1.30547	0.00144	0.03258	0.00013	0.00161	0.00002	2.82427	10.53849	0.000004	0.00002	2.12E-14	99.92%	40.033	911.28	5.50	0.60%
18	1.15	30	2.38745	0.00189	0.05940	0.00016	0.00290	0.00004	19.45012	9.81938	0.000024	0.00001	3.88E-14	99.70%	40.074	912.00	3.07	0.34%
19	1.2	30	2.64595	0.00228	0.06539	0.00018	0.00323	0.00004	-6.49750	5.42514	0.000034	0.00001	4.30E-14	99.62%	40.314	916.29	3.05	0.33%
20	1.25	30	3.33583	0.00214	0.08219	0.00018	0.00400	0.00004	4.52647	11.19582	0.000032	0.00001	5.42E-14	99.72%	40.470	919.07	2.42	0.26%
21	1.3	30	2.79654	0.00154	0.07036	0.00033	0.00326	0.00004	0.98257	8.91087	0.000013	0.00001	4.54E-14	99.86%	39.692	905.17	4.48	0.49%
22	1.35	30	3.97186	0.00226	0.09944	0.00039	0.00471	0.00004	2.05504	9.47268	0.000026	0.00001	6.45E-14	99.81%	39.865	908.28	3.67	0.40%
23	1.4	30	3.17366	0.00267	0.07923	0.00024	0.00376	0.00002	29.14297	6.61530	0.000011	0.00001	5.15E-14	99.90%	40.017	910.98	3.09	0.34%
24	1.5	30	4.33491	0.00228	0.10949	0.00048	0.00514	0.00006	19.46090	11.83051	0.000020	0.00001	7.04E-14	99.86%	39.539	902.42	4.09	0.45%
25	1.6	30	4.63885	0.00294	0.11631	0.00026	0.00545	0.00003	6.71087	8.05889	0.000034	0.00001	7.53E-14	99.78%	39.797	907.05	2.23	0.25%

APPENDIX: ARGON DATA

ID	P	t	^{40}Ar (*+ atm)	± 1σ	$^{39}Ar_K$	± 1σ	^{38}Ar (atm)	± 1σ	$^{37}Ar_{Ca}$	± 1σ	^{36}Ar	± 1σ	$^{40}Ar^*$	%Rad	R	Age	± 1σ	%-sd
#		(sec)	(V)		(V)		(V)		(V)		(V)		(mol)			(Ma)		
26	1.7	30	7.70460	0.00384	0.19347	0.00051	0.00925	0.00007	17.59302	8.89608	0.000004	0.00001	1.25E-13	99.99%	39.819	907.44	2.48	0.27%
27	1.8	30	7.90878	0.00931	0.19954	0.00060	0.00943	0.00006	46.93288	9.74317	-0.000012	0.00001	1.28E-13	100.04%	39.635	904.15	2.94	0.33%
28	1.9	30	3.91629	0.00425	0.09851	0.00031	0.00463	0.00004	28.94381	6.90926	-0.000011	0.00001	6.36E-14	100.08%	39.755	906.29	3.14	0.35%
29	2	30	8.81210	0.00962	0.22326	0.00066	0.01112	0.00013	35.33377	11.07028	0.000002	0.00002	1.43E-13	99.99%	39.467	901.13	2.89	0.32%
30	2.1	30	8.72947	0.00933	0.22015	0.00071	0.01030	0.00008	33.64948	7.65276	-0.000010	0.00001	1.42E-13	100.04%	39.652	904.45	3.09	0.34%
31	2.2	30	12.68411	0.00747	0.32114	0.00063	0.01523	0.00009	175.11204	8.33843	0.000047	0.00002	2.06E-13	99.89%	39.454	900.90	1.92	0.21%
32	2.35	30	3.75443	0.00247	0.09405	0.00027	0.00455	0.00007	43.27268	7.61001	0.000052	0.00001	6.10E-14	99.59%	39.757	906.34	2.83	0.31%
33	2.5	30	11.09189	0.00697	0.28115	0.00085	0.01314	0.00011	146.47375	11.02858	0.000087	0.00001	1.80E-13	99.77%	39.360	899.21	2.79	0.31%
34	2.65	30	2.38653	0.00185	0.06033	0.00018	0.00286	0.00006	56.96946	9.15831	0.000017	0.00001	3.87E-14	99.79%	39.479	901.35	3.20	0.35%
35	2.8	30	2.09589	0.00180	0.05324	0.00019	0.00245	0.00002	26.77980	7.55709	0.000035	0.00001	3.40E-14	99.51%	39.174	895.86	3.69	0.41%

Plateau Age= 903.3±1.3 Ma (1σ)
MSWD = 1.2, probability = 0.28
incl. 66.3% of the 39Ar, steps 14-22

BEN-6: K-feldspar

au25.1h.ksp.2

1	0.6	30	13.48726	0.00706	0.02458	0.00020	0.00709	0.00006	0.06806	0.00287	0.001601	0.00002	2.19E-13	96.49%	530.801	4107.63	34.61	0.84%
2	0.7	30	15.38345	0.01498	0.26759	0.00087	0.01277	0.00012	0.09793	0.00411	0.001492	0.00002	2.50E-13	97.13%	55.891	1177.70	4.15	0.35%
3	0.75	30	2.47101	0.00234	0.10289	0.00020	0.00169	0.00003	0.01255	0.00236	0.000060	0.00001	4.01E-14	99.28%	23.857	598.10	1.41	0.24%
4	0.8	30	12.19762	0.01059	0.38153	0.00079	0.00672	0.00007	0.11610	0.00321	0.000507	0.00001	1.98E-13	98.77%	31.614	756.45	1.74	0.23%
5	0.85	30	7.70227	0.00854	0.27470	0.00038	0.00389	0.00003	0.04119	0.00222	0.000078	0.00001	1.25E-13	99.70%	27.972	683.82	1.28	0.19%

APPENDIX: ARGON DATA

ID	P	t	^{40}Ar (*+ atm)	± 1σ	$^{39}Ar_K$	± 1σ	^{38}Ar (atm)	± 1σ	$^{37}Ar_{Ca}$	± 1σ	^{36}Ar	± 1σ	$^{40}Ar^*$	%Rad	R	Age	± 1σ	%-sd
#		(sec)	(V)		(V)		(V)		(V)		(V)		(mol)			(Ma)		
6	0.9	30	6.19605	0.00610	0.21755	0.00047	0.00300	0.00003	0.04046	0.00356	0.000058	0.00001	1.01E-13	99.72%	28.423	692.99	1.67	0.24%
7	0.95	30	6.70237	0.00486	0.23830	0.00061	0.00334	0.00006	0.04144	0.00289	0.000053	0.00001	1.09E-13	99.77%	28.080	686.02	1.85	0.27%
8	1	30	8.77798	0.01166	0.30477	0.00048	0.00428	0.00005	0.04916	0.00330	0.000084	0.00002	1.43E-13	99.72%	28.740	699.38	1.48	0.21%
9	1.03	30	15.23159	0.01207	0.52324	0.00138	0.00810	0.00011	0.15412	0.00302	0.000304	0.00002	2.47E-13	99.41%	28.972	704.08	1.96	0.28%
10	1.06	30	7.98525	0.01341	0.28782	0.00078	0.00424	0.00005	0.03461	0.00158	0.000041	0.00002	1.30E-13	99.85%	27.715	678.59	2.21	0.33%
11	1.1	30	8.32959	0.00780	0.30262	0.00064	0.00449	0.00006	0.03126	0.00233	0.000150	0.00001	1.35E-13	99.47%	27.390	671.96	1.59	0.24%
12	1.14	30	8.54334	0.01347	0.30931	0.00058	0.00505	0.00007	0.02594	0.00387	0.000195	0.00001	1.39E-13	99.32%	27.444	673.05	1.68	0.25%
13	1.18	30	12.82397	0.01057	0.44534	0.00127	0.00800	0.00008	0.09840	0.00202	0.000351	0.00002	2.08E-13	99.19%	28.589	696.34	2.12	0.30%
14	1.22	30	23.66726	0.02659	0.81991	0.00091	0.01601	0.00020	0.14332	0.00318	0.000910	0.00002	3.84E-13	98.86%	28.558	695.71	1.12	0.16%
15	1.26	30	61.82062	0.07938	2.14681	0.00506	0.03888	0.00023	0.46228	0.00888	0.002162	0.00007	1.00E-12	98.97%	28.524	695.02	1.90	0.27%
16	1.28	30	73.54164	0.08463	2.50472	0.00901	0.03895	0.00032	0.43967	0.01336	0.00177	0.00007	1.19E-12	99.29%	29.173	708.10	2.70	0.38%
17	1.29	30	13.21863	0.01108	0.42975	0.00127	0.00683	0.00008	0.09315	0.00274	0.000316	0.00003	2.15E-13	99.29%	30.567	735.88	2.32	0.32%
18	1.3	30	20.55700	0.03785	0.67354	0.00174	0.01185	0.00015	0.12362	0.00344	0.000673	0.00002	3.34E-13	99.03%	30.247	729.54	2.35	0.32%
19	1.31	30	19.12469	0.03652	0.62712	0.00088	0.00997	0.00007	0.11766	0.00244	0.000563	0.00002	3.10E-13	99.13%	30.253	729.66	1.76	0.24%
20	1.32	30	14.88825	0.01475	0.48845	0.00142	0.00752	0.00015	0.08939	0.00207	0.000271	0.00003	2.42E-13	99.46%	30.338	731.34	2.30	0.31%
21	1.34	30	16.65001	0.00825	0.56117	0.00071	0.00821	0.00009	0.09658	0.00281	0.000231	0.00003	2.70E-13	99.59%	29.568	716.03	1.03	0.14%
22	1.36	30	11.15907	0.00803	0.36213	0.00084	0.00561	0.00006	0.09077	0.00210	0.000295	0.00002	1.81E-13	99.22%	30.604	736.61	1.82	0.25%
23	1.38	30	4.98628	0.00476	0.16565	0.00046	0.00243	0.00002	0.00791	0.00277	0.000042	0.00002	8.10E-14	99.75%	30.032	725.28	2.27	0.31%
24	1.4	20	9.21198	0.01235	0.31735	0.00082	0.00449	0.00005	0.01821	0.00333	0.000149	0.00001	1.50E-13	99.52%	28.896	702.54	2.07	0.29%
25	1.43	20	3.42976	0.00326	0.11499	0.00024	0.00160	0.00003	0.00323	0.00289	0.000078	0.00002	5.57E-14	99.33%	29.629	717.24	1.91	0.27%

APPENDIX: ARGON DATA

ID	P	t	^{40}Ar (*+ atm)	± 1σ	$^{39}Ar_K$	± 1σ	^{38}Ar (atm)	± 1σ	$^{37}Ar_{Ca}$	± 1σ	^{36}Ar	± 1σ	$^{40}Ar^*$	%Rad	R	Age	± 1σ	%-sd
#		(sec)	(V)		(V)		(V)		(V)		(V)		(mol)			(Ma)		
26	1.46	20	8.91345	0.01317	0.30573	0.00064	0.00426	0.00005	0.02042	0.00240	0.000113	0.00002	1.45E-13	99.63%	29.054	705.71	1.88	0.27%
27	1.5	20	3.32838	0.00431	0.10818	0.00047	0.00151	0.00003	0.00987	0.00262	0.000082	0.00002	5.40E-14	99.27%	30.554	735.62	3.54	0.48%
28	1.55	20	2.39331	0.00339	0.07833	0.00026	0.00102	0.00002	0.00290	0.00200	0.000009	0.00002	3.89E-14	99.89%	30.523	735.02	3.11	0.42%
29	1.6	20	1.78864	0.00130	0.05890	0.00017	0.00076	0.00003	0.00016	0.00376	0.000044	0.00002	2.90E-14	99.27%	30.144	727.50	2.87	0.39%
30	1.65	20	6.12652	0.00474	0.20456	0.00053	0.00283	0.00003	0.01720	0.00224	0.000109	0.00002	9.95E-14	99.48%	29.802	720.69	2.07	0.29%
31	1.7	20	3.35968	0.00240	0.11353	0.00029	0.00158	0.00002	0.01539	0.00233	0.000101	0.00001	5.45E-14	99.11%	29.344	711.54	2.08	0.29%
32	1.8	20	0.42727	0.00042	0.01393	0.00017	0.00018	0.00002	0.00764	0.00257	0.000017	0.00002	6.94E-15	98.84%	30.379	732.15	13.03	1.78%
33	1.9	20	0.30707	0.00067	0.01008	0.00011	0.00014	0.00002	0.00422	0.00250	0.000012	0.00002	4.99E-15	98.84%	30.170	728.01	14.95	2.05%
34	2	20	1.19753	0.00195	0.03851	0.00017	0.00055	0.00002	0.00674	0.00222	0.000062	0.00001	1.94E-14	98.47%	30.638	737.29	4.43	0.60%

Total Gas Age= 701±12 Ma (95% conf.)
MSWD = 306, probability = 0.000
incl. 100% of the 39Ar, steps 3-34

BEN-10: K-feldspar

au25.2b.ksp.10

1	0.5	30	0.43593	0.00098	0.00272	0.00011	0.00101	0.00004	0.00053	0.00249	0.00006	0.00001	7.08E-15	96.04%	154.150	2284.86	99.52	4.36%
2	0.6	30	1.29025	0.00147	0.02210	0.00011	0.00231	0.00004	0.00124	0.00349	0.000119	0.00002	2.09E-14	97.28%	56.799	1194.61	7.95	0.67%
3	0.7	30	4.62514	0.00370	0.12694	0.00025	0.00240	0.00004	0.00059	0.00424	0.000083	0.00001	7.51E-14	99.47%	36.244	847.01	1.86	0.22%
4	0.73	30	5.47628	0.00473	0.15337	0.00028	0.00208	0.00004	0.00354	0.00373	0.000026	0.00001	8.89E-14	99.86%	35.658	836.05	1.75	0.21%
5	0.75	30	7.81289	0.00799	0.22052	0.00060	0.00282	0.00004	0.00245	0.00382	0.000035	0.00001	1.27E-13	99.87%	35.384	830.90	2.43	0.29%
6	0.77	30	6.47150	0.00372	0.18252	0.00039	0.00234	0.00004	0.00413	0.00211	0.000019	0.00001	1.05E-13	99.91%	35.429	831.73	1.88	0.23%

APPENDIX: ARGON DATA

ID	P	t	^{40}Ar (*+ atm)	± 1σ	$^{39}Ar_K$	± 1σ	^{38}Ar (atm)	± 1σ	$^{37}Ar_{Ca}$	± 1σ	^{36}Ar	± 1σ	$^{40}Ar^*$	%Rad	R	Age	± 1σ	%-sd
#		(sec)	(V)		(V)		(V)		(V)		(V)		(mol)			(Ma)		
7	0.79	30	8.29479	0.01061	0.23446	0.00082	0.00307	0.00003	0.00473	0.00210	0.000026	0.00001	1.35E-13	99.91%	35.349	830.23	3.10	0.37%
8	0.81	30	7.51020	0.01202	0.21138	0.00045	0.00270	0.00004	0.00380	0.00225	0.000037	0.00001	1.22E-13	99.85%	35.479	832.68	2.24	0.27%
9	0.83	30	9.68970	0.01436	0.27355	0.00031	0.00349	0.00003	0.00557	0.00310	0.000040	0.00001	1.57E-13	99.88%	35.381	830.84	1.57	0.19%
10	0.85	30	9.29840	0.01582	0.26094	0.00047	0.00331	0.00004	0.00562	0.00233	0.000011	0.00001	1.51E-13	99.96%	35.624	835.41	2.09	0.25%
11	0.87	30	11.88943	0.00436	0.33404	0.00057	0.00444	0.00008	0.08186	0.00415	0.000092	0.00001	1.93E-13	99.77%	35.541	833.85	1.48	0.18%
12	0.91	30	18.49595	0.01442	0.52168	0.00100	0.00702	0.00010	0.06685	0.00269	0.000125	0.00001	3.00E-13	99.80%	35.399	831.18	1.73	0.21%
13	0.93	30	18.89105	0.01552	0.53113	0.00124	0.00702	0.00009	0.07708	0.00351	0.000124	0.00001	3.07E-13	99.81%	35.516	833.37	2.08	0.25%
14	0.97	30	14.06201	0.00669	0.39416	0.00101	0.00526	0.00006	0.06951	0.00320	0.000094	0.00001	2.28E-13	99.80%	35.626	835.45	2.18	0.26%
15	0.99	30	14.90371	0.01394	0.41784	0.00108	0.00561	0.00005	0.08589	0.00324	0.000108	0.00002	2.42E-13	99.79%	35.616	835.26	2.31	0.28%
16	1.01	30	17.93895	0.01335	0.50256	0.00086	0.00663	0.00009	0.07951	0.00323	0.000127	0.00001	2.91E-13	99.79%	35.640	835.70	1.58	0.19%
17	1.03	30	16.59659	0.01094	0.46747	0.00144	0.00616	0.00010	0.06716	0.00277	0.000117	0.00002	2.69E-13	99.79%	35.446	832.06	2.63	0.32%
18	1.05	30	13.29836	0.01345	0.37279	0.00091	0.00501	0.00007	0.07646	0.00232	0.000115	0.00002	2.16E-13	99.74%	35.606	835.07	2.22	0.27%
19	1.07	30	11.42230	0.00881	0.32026	0.00075	0.00437	0.00003	0.07327	0.00394	0.000076	0.00001	1.85E-13	99.80%	35.623	835.38	2.07	0.25%
20	1.09	30	11.55035	0.00822	0.32500	0.00103	0.00438	0.00005	0.07168	0.00373	0.000104	0.00001	1.88E-13	99.73%	35.472	832.55	2.72	0.33%
21	1.11	30	15.24293	0.00758	0.42681	0.00154	0.00574	0.00009	0.08195	0.00367	0.000085	0.00002	2.47E-13	99.83%	35.678	836.41	3.05	0.37%
22	1.13	30	17.12318	0.01377	0.47980	0.00102	0.00642	0.00005	0.08080	0.00319	0.000102	0.00001	2.78E-13	99.82%	35.646	835.81	1.91	0.23%
23	1.15	30	19.81291	0.01192	0.55572	0.00080	0.00745	0.00006	0.08505	0.00391	0.000123	0.00001	3.22E-13	99.82%	35.606	835.06	1.32	0.16%
24	1.17	30	20.74824	0.00879	0.58547	0.00141	0.00793	0.00010	0.07235	0.00286	0.000155	0.00001	3.37E-13	99.78%	35.375	830.72	2.04	0.25%
25	1.19	30	15.48744	0.01710	0.43441	0.00076	0.00593	0.00005	0.06869	0.00298	0.000138	0.00001	2.51E-13	99.74%	35.577	834.52	1.75	0.21%
26	1.21	30	18.81866	0.02040	0.52763	0.00093	0.00721	0.00006	0.09021	0.00360	0.000147	0.00001	3.06E-13	99.77%	35.604	835.03	1.74	0.21%

APPENDIX: ARGON DATA

ID	P	t	^{40}Ar (*+ atm)	± 1σ	$^{39}Ar_K$	± 1σ	^{38}Ar (atm)	± 1σ	$^{37}Ar_{Ca}$	± 1σ	^{36}Ar	± 1σ	$^{40}Ar^*$	%Rad	R	Age	± 1σ	%-sd
#		(sec)	(V)		(V)		(V)		(V)		(V)		(mol)			(Ma)		
27	1.23	30	21.84374	0.02907	0.61410	0.00109	0.00830	0.00008	0.07415	0.00275	0.000153	0.00001	3.55E-13	99.79%	35.511	833.28	1.86	0.22%
28	1.26	30	21.40440	0.02138	0.59396	0.00122	0.00801	0.00009	0.08487	0.00283	0.000166	0.00001	3.47E-13	99.77%	35.971	841.91	1.93	0.23%
29	1.29	30	24.01819	0.01317	0.66675	0.00162	0.00903	0.00005	0.08552	0.00216	0.000174	0.00002	3.90E-13	99.79%	35.961	841.72	2.11	0.25%
30	1.31	30	13.83338	0.02021	0.38679	0.00112	0.00521	0.00007	0.10072	0.00452	0.000110	0.00001	2.25E-13	99.76%	35.711	837.05	2.73	0.33%
31	1.34	30	22.22237	0.02107	0.61837	0.00158	0.00850	0.00009	0.08007	0.00134	0.000157	0.00002	3.61E-13	99.79%	35.878	840.17	2.29	0.27%
32	1.38	30	14.21991	0.01408	0.39592	0.00104	0.00537	0.00006	0.08235	0.00324	0.000123	0.00001	2.31E-13	99.74%	35.849	839.62	2.37	0.28%
33	1.42	30	21.13177	0.01832	0.58797	0.00114	0.00794	0.00008	0.08814	0.00291	0.000148	0.00001	3.43E-13	99.79%	35.884	840.28	1.80	0.21%
34	1.46	30	18.81510	0.01089	0.52386	0.00155	0.00707	0.00008	0.08199	0.00278	0.000137	0.00001	3.05E-13	99.78%	35.858	839.78	2.54	0.30%
35	1.5	30	21.03382	0.02081	0.58063	0.00062	0.00791	0.00006	0.09401	0.00369	0.000179	0.00002	3.41E-13	99.75%	36.154	845.32	1.25	0.15%
36	1.53	30	22.79032	0.01971	0.62600	0.00117	0.00852	0.00007	0.07670	0.00487	0.000181	0.00002	3.70E-13	99.76%	36.335	848.71	1.76	0.21%
37	1.57	30	6.06463	0.00755	0.16785	0.00047	0.00219	0.00003	0.00939	0.00367	0.000041	0.00001	9.85E-14	99.80%	36.066	843.68	2.61	0.31%
38	1.63	30	4.58701	0.00638	0.12609	0.00032	0.00165	0.00004	0.00383	0.00337	0.000030	0.00001	7.45E-14	99.80%	36.311	848.25	2.50	0.29%
39	1.7	30	4.46578	0.00530	0.12174	0.00035	0.00158	0.00003	-0.00138	0.00349	0.000019	0.00001	7.25E-14	99.88%	36.636	854.31	2.72	0.32%
40	1.8	20	1.29944	0.00230	0.03567	0.00014	0.00047	0.00003	-0.00007	0.00382	0.000012	0.00001	2.11E-14	99.72%	36.325	848.51	4.06	0.48%
41	1.9	20	1.18302	0.00141	0.03116	0.00021	0.00040	0.00003	0.00310	0.00388	0.000008	0.00001	1.92E-14	99.81%	37.902	877.66	6.27	0.71%
42	2	20	4.95155	0.00323	0.13021	0.00043	0.00172	0.00003	-0.00468	0.00164	0.000021	0.00001	8.04E-14	99.87%	37.975	878.99	2.97	0.34%
43	2.1	20	1.35473	0.00133	0.02988	0.00021	0.00042	0.00003	0.00573	0.00309	0.000016	0.00001	2.20E-14	99.65%	45.211	1006.94	7.24	0.72%

Plateau Age= 833.83±0.92 Ma (1σ)
MSWD = 0.96, probability = 0.52
incl. 62.4% of the 39Ar, steps 1-24

APPENDIX: ARGON DATA

ID	P	t	^{40}Ar (*+ atm)	± 1σ	$^{39}Ar_K$	± 1σ	^{38}Ar (atm)	± 1σ	$^{37}Ar_{Ca}$	± 1σ	^{36}Ar	± 1σ	$^{40}Ar^*$	%Rad	R	Age	± 1σ	%-sd
#		(sec)	(V)		(V)		(V)		(V)		(V)		(mol)			(Ma)		
BEN-5: K-feldspar																		
au25.1d.ksp.14																		
1	0.3	40	-0.00065	0.00028	-0.00010	0.00011	0.00001	0.00005	-0.00005	0.00029	0.000021	0.00002	-1.05E-17	1064.75%	65.992	1327.62	17.5E2	132.13%
2	0.4	40	3.11455	0.00332	0.00007	0.00010	0.00007	0.00005	-0.00011	0.00026	0.000063	0.00002	5.06E-14	99.40%	45284.435	11936.26	17.4E3	146.05%
3	0.5	40	0.87196	0.00085	0.00135	0.00010	0.00086	0.00005	-0.00017	0.00019	0.000128	0.00002	1.42E-14	95.67%	619.218	4358.96	331.25	7.60%
4	0.6	40	2.07922	0.00157	0.01130	0.00020	0.00080	0.00004	-0.00007	0.00020	0.000063	0.00002	3.38E-14	99.10%	182.404	2503.45	45.80	1.83%
5	0.63	40	1.92484	0.00154	0.00717	0.00012	0.00013	0.00004	0.00004	0.00020	0.000021	0.00002	3.12E-14	99.67%	267.708	3046.07	53.97	1.77%
6	0.66	40	1.60392	0.00176	0.02784	0.00023	0.00042	0.00004	0.00022	0.00022	-0.000011	0.00002	2.60E-14	100.20%	57.622	1204.30	10.76	0.89%
7	0.69	40	1.97520	0.00152	0.04877	0.00018	0.00066	0.00006	0.00034	0.00022	0.000017	0.00002	3.21E-14	99.74%	40.399	920.47	4.71	0.51%
8	0.72	40	1.49264	0.00140	0.03903	0.00011	0.00055	0.00003	-0.00014	0.00021	-0.000023	0.00003	2.42E-14	100.45%	38.245	881.61	5.07	0.58%
9	0.75	50	5.28006	0.00264	0.13612	0.00033	0.00196	0.00005	-0.00020	0.00015	0.000019	0.00002	8.57E-14	99.89%	38.749	890.78	2.44	0.27%
10	0.78	50	5.30692	0.00366	0.13896	0.00029	0.00199	0.00004	0.00002	0.00031	-0.000010	0.00002	8.62E-14	100.05%	38.190	880.62	2.16	0.25%
11	0.81	50	7.63406	0.00786	0.19438	0.00072	0.00282	0.00005	0.00025	0.00029	0.000015	0.00002	1.24E-13	99.94%	39.251	899.87	3.52	0.39%
12	0.835	50	10.11960	0.01173	0.26435	0.00085	0.00356	0.00008	0.00036	0.00021	0.000002	0.00002	1.64E-13	99.99%	38.279	882.24	3.06	0.35%
13	0.86	50	9.62371	0.01323	0.25275	0.00074	0.00343	0.00005	0.00019	0.00023	0.000016	0.00002	1.56E-13	99.95%	38.058	878.20	2.88	0.33%
14	0.88	50	9.01301	0.00620	0.23684	0.00073	0.00322	0.00004	0.00086	0.00020	-0.000011	0.00003	1.46E-13	100.03%	38.055	878.15	2.90	0.33%
15	0.9	50	6.99172	0.00766	0.18296	0.00059	0.00249	0.00005	0.00072	0.00024	0.000003	0.00003	1.14E-13	99.99%	38.210	880.97	3.23	0.37%
16	0.91	50	8.20110	0.00753	0.21448	0.00092	0.00281	0.00005	-0.00007	0.00022	-0.000002	0.00003	1.33E-13	100.01%	38.237	881.48	4.00	0.45%
17	0.92	50	7.75219	0.01043	0.20246	0.00034	0.00270	0.00006	0.00024	0.00031	0.000084	0.00002	1.26E-13	99.68%	38.167	880.20	2.02	0.23%
18	0.93	50	6.11578	0.00608	0.16019	0.00042	0.00221	0.00004	0.00048	0.00027	0.000066	0.00002	9.93E-14	99.68%	38.057	878.19	2.62	0.30%

APPENDIX: ARGON DATA

ID	P	t	^{40}Ar (*+ atm)	± 1σ	$^{39}Ar_K$	± 1σ	^{38}Ar (atm)	± 1σ	$^{37}Ar_{Ca}$	± 1σ	^{36}Ar	± 1σ	$^{40}Ar^*$	%Rad	R	Age	± 1σ	%-sd
#		(sec)	(V)		(V)		(V)		(V)		(V)		(mol)			(Ma)		
19	0.94	50	5.91523	0.00521	0.15466	0.00040	0.00225	0.00007	-0.00007	0.00025	0.000006	0.00002	9.60E-14	99.97%	38.234	881.41	2.54	0.29%
20	0.95	50	6.76046	0.00645	0.17548	0.00073	0.00245	0.00009	-0.00065	0.00034	0.000017	0.00002	1.10E-13	99.92%	38.496	886.19	3.88	0.44%
21	0.96	50	6.88451	0.00712	0.18014	0.00064	0.00259	0.00006	0.00052	0.00028	0.000038	0.00002	1.12E-13	99.84%	38.157	880.01	3.31	0.38%
22	0.98	50	6.61101	0.00679	0.17497	0.00058	0.00244	0.00006	0.00072	0.00022	-0.000055	0.00003	1.07E-13	100.25%	37.785	873.21	3.28	0.38%
23	1	50	9.20722	0.00780	0.24283	0.00071	0.00346	0.00006	0.00039	0.00023	-0.000069	0.00004	1.49E-13	100.22%	37.917	875.62	2.85	0.33%
24	1.03	50	21.32494	0.01078	0.56008	0.00063	0.00773	0.00014	-0.00029	0.00064	0.000079	0.00003	3.46E-13	99.89%	38.033	877.75	1.13	0.13%
25	0	0	18.03615	0.00859	0.47939	0.00083	0.00687	0.00011	0.00268	0.00032	0.000219	0.00003	2.93E-13	99.64%	37.488	867.77	1.62	0.19%
26	1.02	50	20.34603	0.01323	0.54124	0.00102	0.00727	0.00008	0.00356	0.00028	-0.000037	0.00007	3.30E-13	100.05%	37.593	869.68	1.95	0.22%
27	1.03	50	20.35858	0.00920	0.54020	0.00145	0.00728	0.00010	0.00410	0.00032	0.000199	0.00003	3.31E-13	99.71%	37.579	869.44	2.40	0.28%
28	1.04	50	18.25295	0.01791	0.48513	0.00093	0.00646	0.00009	0.00224	0.00014	0.000067	0.00003	2.96E-13	99.89%	37.585	869.54	1.90	0.22%
29	1.05	50	17.40266	0.01008	0.45965	0.00132	0.00590	0.00012	0.00343	0.00042	0.000050	0.00003	2.83E-13	99.92%	37.829	874.02	2.61	0.30%
30	1.06	50	14.90316	0.01364	0.39112	0.00052	0.00532	0.00007	0.00163	0.00052	-0.000094	0.00006	2.42E-13	100.19%	38.105	879.05	1.74	0.20%
31	1.08	50	14.95204	0.00822	0.39453	0.00056	0.00543	0.00005	0.00308	0.00026	0.000087	0.00003	2.43E-13	99.83%	37.834	874.11	1.43	0.16%
32	1.1	50	18.57917	0.00924	0.47857	0.00115	0.00656	0.00008	0.00324	0.00037	0.000080	0.00003	3.02E-13	99.87%	38.774	891.23	2.23	0.25%
33	1.12	50	11.38865	0.01210	0.30468	0.00080	0.00435	0.00006	0.00405	0.00029	0.000071	0.00003	1.85E-13	99.82%	37.312	864.53	2.53	0.29%
34	1.14	50	7.95592	0.00764	0.21244	0.00061	0.00283	0.00005	0.00062	0.00022	0.000002	0.00002	1.29E-13	99.99%	37.448	867.02	2.74	0.32%
35	1.16	50	6.63963	0.00696	0.17855	0.00041	0.00241	0.00005	0.00065	0.00026	0.000032	0.00002	1.08E-13	99.86%	37.134	861.25	2.34	0.27%
36	1.18	40	3.72032	0.00272	0.09919	0.00016	0.00133	0.00005	-0.00016	0.00021	-0.000027	0.00002	6.04E-14	100.22%	37.508	868.13	1.99	0.23%
37	1.2	40	3.30110	0.00356	0.08799	0.00021	0.00109	0.00005	-0.00014	0.00025	-0.000009	0.00002	5.36E-14	100.08%	37.516	868.28	2.71	0.31%
38	1.23	40	4.69355	0.00396	0.12104	0.00029	0.00145	0.00005	0.00007	0.00028	-0.000020	0.00002	7.62E-14	100.12%	38.776	891.27	2.51	0.28%

APPENDIX: ARGON DATA

ID	P	t	^{40}Ar (*+ atm)	± 1σ	$^{39}Ar_K$	± 1σ	^{38}Ar (atm)	± 1σ	$^{37}Ar_{Ca}$	± 1σ	^{36}Ar	± 1σ	$^{40}Ar^*$	%Rad	R	Age	± 1σ	%-sd
#		(sec)	(V)		(V)		(V)		(V)		(V)		(mol)			(Ma)		
39	1.26	40	7.21560	0.00770	0.18710	0.00042	0.00249	0.00006	0.00024	0.00022	-0.000080	0.00003	1.17E-13	100.33%	38.566	887.46	2.51	0.28%
40	1.3	40	14.98270	0.00918	0.39437	0.00098	0.00537	0.00008	0.00370	0.00032	0.000144	0.00003	2.43E-13	99.72%	37.885	875.03	2.29	0.26%
41	1.35	20	6.43392	0.00383	0.16962	0.00036	0.00234	0.00006	0.00044	0.00031	0.000116	0.00004	1.04E-13	99.47%	37.731	872.21	2.40	0.28%
42	1.4	20	1.18708	0.00133	0.03179	0.00027	0.00045	0.00004	0.00044	0.00037	-0.000011	0.00005	1.93E-14	100.27%	37.347	865.16	12.34	1.43%
43	1.45	20	3.65141	0.00259	0.09730	0.00021	0.00137	0.00006	0.00002	0.00026	0.000109	0.00004	5.93E-14	99.12%	37.197	862.41	3.16	0.37%
44	1.5	20	13.10315	0.00824	0.34731	0.00070	0.00496	0.00007	0.00281	0.00020	0.000126	0.00004	2.13E-13	99.72%	37.621	870.21	2.00	0.23%
45	1.55	20	7.96098	0.00829	0.21077	0.00051	0.00294	0.00005	0.00060	0.00025	0.000112	0.00003	1.29E-13	99.58%	37.614	870.08	2.54	0.29%
46	1.6	20	22.93258	0.01264	0.60893	0.00163	0.00819	0.00009	0.00314	0.00033	0.000201	0.00004	3.72E-13	99.74%	37.564	869.15	2.42	0.28%
47	1.58	20	8.28987	0.00591	0.22257	0.00069	0.00292	0.00006	0.00079	0.00025	0.000042	0.00002	1.35E-13	99.85%	37.191	862.29	2.82	0.33%
48	1.62	20	9.59395	0.01157	0.25549	0.00064	0.00347	0.00005	0.00051	0.00025	-0.000055	0.00003	1.56E-13	100.17%	37.551	868.92	2.55	0.29%
49	1.66	20	1.63530	0.00180	0.04276	0.00037	0.00060	0.00003	0.00046	0.00031	-0.000008	0.00002	2.65E-14	100.14%	38.247	881.65	8.42	0.95%
50	1.7	20	5.75635	0.00487	0.15338	0.00038	0.00207	0.00003	0.00089	0.00030	0.000041	0.00002	9.35E-14	99.79%	37.453	867.11	2.46	0.28%
51	1.75	20	1.30527	0.00186	0.03530	0.00020	0.00029	0.00006	0.00051	0.00033	0.000051	0.00002	2.12E-14	98.84%	36.550	850.43	6.46	0.76%

Total Gas Age = 875.2±2.6 Ma
(95% conf.), including J-error of .000011%)
MSWD = 13, probability = 0.000
100% of the 39Ar, steps 1 through 45

BEN-5: K-feldspar

au25.1d.ksp.15

1	0.3	50	-0.00006	0.00034	0.00003	0.00013	0.00003	0.00005	0.00032	0.00031	0.000071	0.00004	-1.00E-18	34125.51%	-626.052	-	-	-
2	0.4	50	0.37498	0.00098	0.00123	0.00009	0.00065	0.00005	0.00041	0.00018	0.000159	0.00003	6.09E-15	87.43%	267.015	3042.26	275.62	9.06%

APPENDIX: ARGON DATA

ID	P	t	^{40}Ar (*+ atm)	± 1σ	$^{39}Ar_K$	± 1σ	^{38}Ar (atm)	± 1σ	$^{37}Ar_{Ca}$	± 1σ	^{36}Ar	± 1σ	$^{40}Ar^*$	%Rad	R	Age	± 1σ	%-sd
#		(sec)	(V)		(V)		(V)		(V)		(V)		(mol)			(Ma)		
3	0.5	50	1.76033	0.00142	0.05804	0.00019	0.00089	0.00005	-0.00017	0.00028	0.000159	0.00003	2.86E-14	97.33%	29.523	715.12	4.70	0.66%
4	0.6	50	22.82842	0.01363	0.63034	0.00055	0.00890	0.00006	0.00319	0.00021	0.000276	0.00004	3.71E-13	99.64%	36.087	841.83	0.99	0.12%
5	0.63	50	7.24149	0.00381	0.20020	0.00029	0.00272	0.00004	0.00107	0.00015	-0.000014	0.00002	1.18E-13	100.06%	36.172	843.41	1.46	0.17%
6	0.66	50	19.34498	0.01640	0.53141	0.00059	0.00748	0.00010	0.00533	0.00034	0.000454	0.00004	3.14E-13	99.31%	36.152	838.05	1.28	0.15%
7	0.69	50	15.26911	0.01103	0.40060	0.00060	0.00545	0.00005	0.00322	0.00029	0.000071	0.00003	2.48E-13	99.86%	38.064	878.32	1.53	0.17%
8	0.72	50	21.61493	0.03022	0.55931	0.00066	0.00788	0.00010	0.00271	0.00025	0.000106	0.00004	3.51E-13	99.86%	38.590	887.90	1.69	0.19%
9	0.71	30	11.38849	0.00958	0.30944	0.00064	0.00419	0.00012	0.00214	0.00036	0.000030	0.00003	1.85E-13	99.92%	36.776	854.62	2.02	0.24%
10	0.72	30	7.92425	0.00784	0.20835	0.00045	0.00275	0.00005	0.00068	0.00031	0.000037	0.00002	1.29E-13	99.86%	37.983	876.83	2.21	0.25%
11	0.73	30	2.76281	0.00190	0.07352	0.00032	0.00090	0.00006	0.00036	0.00025	0.000013	0.00002	4.49E-14	99.86%	37.529	868.52	4.39	0.51%
12	0.74	40	4.28918	0.00318	0.11546	0.00019	0.00145	0.00004	0.00021	0.00012	0.000049	0.00002	6.96E-14	99.66%	37.024	859.22	2.00	0.23%
13	0.75	50	4.82297	0.00269	0.12980	0.00030	0.00154	0.00006	0.00022	0.00023	0.000004	0.00002	7.83E-14	99.98%	37.149	861.51	2.43	0.28%
14	0.76	50	3.59766	0.00296	0.09765	0.00025	0.00115	0.00006	0.00016	0.00035	0.000042	0.00002	5.84E-14	99.66%	36.715	853.50	2.70	0.32%
15	0.78	50	4.13263	0.00383	0.11319	0.00030	0.00150	0.00004	0.00027	0.00023	0.000012	0.00002	6.71E-14	99.92%	36.481	849.16	2.75	0.32%
16	0.8	50	1.34641	0.00241	0.03747	0.00019	0.00046	0.00005	0.00024	0.00027	0.000000	0.00002	2.19E-14	100.00%	35.937	839.03	6.00	0.72%
17	0.85	50	2.55110	0.00167	0.06978	0.00014	0.00093	0.00005	0.00014	0.00033	0.000058	0.00002	4.14E-14	99.32%	36.310	845.97	2.94	0.35%
18	0.9	50	5.58034	0.00392	0.15366	0.00039	0.00203	0.00005	0.00031	0.00028	-0.000005	0.00002	9.06E-14	100.02%	36.318	846.12	2.45	0.29%
19	0.95	50	7.81670	0.00940	0.21690	0.00054	0.00285	0.00006	0.00035	0.00018	0.000011	0.00002	1.27E-13	99.96%	36.023	840.65	2.43	0.29%
20	1	50	12.09644	0.00945	0.33036	0.00079	0.00449	0.00009	0.00186	0.00028	0.000038	0.00004	1.96E-13	99.91%	36.583	851.06	2.33	0.27%
21	1.1	40	9.37874	0.00609	0.25698	0.00061	0.00341	0.00005	0.00077	0.00026	0.000018	0.00002	1.52E-13	99.94%	36.476	849.06	2.17	0.26%
22	1.15	40	14.29717	0.01059	0.39979	0.00099	0.00534	0.00008	0.00325	0.00037	-0.000013	0.00003	2.32E-13	100.03%	35.763	835.77	2.22	0.27%

APPENDIX: ARGON DATA

ID	P	t	^{40}Ar (*+ atm)	± 1σ	$^{39}Ar_K$	± 1σ	^{38}Ar (atm)	± 1σ	$^{37}Ar_{Ca}$	± 1σ	^{36}Ar	± 1σ	$^{40}Ar^*$	%Rad	R	Age	± 1σ	%-sd
#		(sec)	(V)		(V)		(V)		(V)		(V)		(mol)			(Ma)		
23	1.2	40	2.36791	0.00282	0.06660	0.00018	0.00089	0.00004	0.00010	0.00015	-0.000016	0.00002	3.84E-14	100.19%	35.555	831.88	3.27	0.39%
24	1.25	40	2.31732	0.00192	0.06604	0.00018	0.00081	0.00005	0.00047	0.00029	0.000003	0.00002	3.76E-14	99.96%	35.077	822.91	3.34	0.41%
25	1.3	20	1.53141	0.00113	0.04356	0.00021	0.00055	0.00004	0.00048	0.00023	-0.000022	0.00002	2.49E-14	100.42%	35.161	824.48	5.30	0.64%
26	1.35	20	0.77378	0.00102	0.02155	0.00019	0.00042	0.00005	0.00038	0.00024	-0.000015	0.00002	1.26E-14	100.57%	35.908	838.49	9.49	1.13%
27	1.4	20	0.23754	0.00061	0.00674	0.00014	0.00012	0.00004	0.00069	0.00021	-0.000013	0.00002	3.86E-15	101.66%	35.260	826.35	27.07	3.28%
28	1.5	20	0.36852	0.00066	0.01040	0.00012	0.00014	0.00005	0.00006	0.00021	-0.000105	0.00003	5.98E-15	108.44%	35.449	829.90	22.91	2.76%
29	1.6	20	0.20273	0.00065	0.00114	0.00013	0.00068	0.00007	-0.00018	0.00015	0.000239	0.00003	3.29E-15	65.16%	115.975	1927.60	391.02	20.29%
30	1.7	20	0.19896	0.00083	0.00537	0.00012	0.00016	0.00004	0.00022	0.00014	0.000022	0.00002	3.23E-15	96.80%	35.846	837.32	29.93	3.57%

Total Gas Age = 850.3±8.0 Ma
(95% conf.), including J-error of .000011%)
MSWD = 84, probability = 0.000
100% of the 39Ar, steps 1 through 28

BEN-5: K-feldspar

au25.1d.ksp.16

1	0.3	50	-0.00005	0.00021	0.00006	0.00010	-0.00001	0.00004	0.00013	0.00018	0.000004	0.00002	-7.41E-19	2618.82%	-20.358	-737.21	-43.5E2	590.16%
2	0.4	50	0.13442	0.00035	0.00059	0.00010	0.00063	0.00004	0.00090	0.00017	0.000256	0.00002	2.18E-15	43.63%	100.047	1757.14	801.10	45.59%
3	0.5	50	0.41221	0.00060	0.01043	0.00011	0.00095	0.00006	0.00003	0.00026	0.000164	0.00002	6.69E-15	88.23%	34.859	818.80	17.27	2.11%
4	0.55	50	0.47744	0.00079	0.01471	0.00019	0.00020	0.00004	0.00025	0.00026	0.000024	0.00002	7.75E-15	98.51%	31.971	763.42	14.76	1.93%
5	0.6	50	1.79114	0.00246	0.04622	0.00012	0.00091	0.00004	-0.00002	0.00020	0.000463	0.00002	2.91E-14	92.37%	35.794	836.35	4.19	0.50%
6	0.61	50	0.84974	0.00140	0.02226	0.00015	0.00033	0.00004	0.00110	0.00024	0.000064	0.00002	1.38E-14	97.77%	37.328	864.82	9.55	1.10%
7	0.62	50	1.16210	0.00147	0.03067	0.00011	0.00059	0.00004	0.00030	0.00013	0.000056	0.00002	1.89E-14	98.58%	37.354	865.30	5.44	0.63%

APPENDIX: ARGON DATA

ID	P	t	^{40}Ar (*+ atm)	± 1σ	$^{39}Ar_K$	± 1σ	^{38}Ar (atm)	± 1σ	$^{37}Ar_{Ca}$	± 1σ	^{36}Ar	± 1σ	$^{40}Ar^*$	%Rad	R	Age	± 1σ	%-sd
#		(sec)	(V)		(V)		(V)		(V)		(V)		(mol)			(Ma)		
8	0.63	50	1.79657	0.00203	0.04577	0.00011	0.00163	0.00005	0.00032	0.00020	0.000063	0.00002	2.92E-14	98.96%	38.850	892.61	4.04	0.45%
9	0.64	50	1.95731	0.00260	0.05187	0.00016	0.00077	0.00005	-0.00025	0.00025	-0.000003	0.00002	3.18E-14	100.05%	37.735	872.29	3.56	0.41%
10	0.66	50	2.82637	0.00117	0.07372	0.00028	0.00179	0.00005	0.00037	0.00023	0.000035	0.00002	4.59E-14	99.63%	38.196	880.73	3.69	0.42%
11	0.68	50	2.41499	0.00207	0.06371	0.00016	0.00094	0.00005	0.00033	0.00024	-0.000028	0.00002	3.92E-14	100.34%	37.910	875.49	3.13	0.36%
12	0.7	50	2.81022	0.00188	0.07394	0.00018	0.00101	0.00004	0.00027	0.00026	0.000049	0.00003	4.56E-14	99.49%	37.811	873.68	3.62	0.41%
13	0.72	50	4.14447	0.00361	0.10944	0.00027	0.00123	0.00008	-0.00064	0.00032	0.000054	0.00003	6.73E-14	99.62%	37.724	872.09	2.96	0.34%
14	0.74	50	4.31397	0.00268	0.11312	0.00019	0.00152	0.00005	-0.00086	0.00052	0.000019	0.00003	7.00E-14	99.87%	38.088	878.75	2.64	0.30%
15	0.76	50	3.97763	0.00435	0.10372	0.00026	0.00136	0.00005	0.00061	0.00020	0.000090	0.00003	6.46E-14	99.33%	38.094	878.87	3.14	0.36%
16	0.78	50	4.62631	0.00519	0.11984	0.00033	0.00162	0.00003	0.00044	0.00021	0.000075	0.00003	7.51E-14	99.52%	38.420	884.81	3.15	0.36%
17	0.8	50	4.58717	0.00198	0.11955	0.00049	0.00167	0.00005	0.00039	0.00017	-0.000037	0.00003	7.45E-14	100.24%	38.370	883.90	3.99	0.45%
18	0.82	50	4.38795	0.00392	0.11460	0.00029	0.00150	0.00006	0.00021	0.00022	0.000020	0.00002	7.12E-14	99.86%	38.238	881.48	2.61	0.30%
19	0.84	50	5.02205	0.00370	0.13085	0.00051	0.00184	0.00006	0.00004	0.00016	0.000011	0.00002	8.15E-14	99.93%	38.354	883.60	3.65	0.41%
20	0.86	50	6.87070	0.00495	0.18190	0.00045	0.00252	0.00004	0.00023	0.00029	0.000019	0.00002	1.12E-13	99.92%	37.741	872.41	2.35	0.27%
21	0.88	50	9.31334	0.01154	0.24769	0.00054	0.00358	0.00005	0.00070	0.00022	0.000042	0.00002	1.51E-13	99.87%	37.550	868.90	2.26	0.26%
22	0.89	40	4.31431	0.00268	0.11315	0.00020	0.00147	0.00005	-0.00103	0.00052	0.000075	0.00003	7.00E-14	99.49%	37.933	875.93	2.39	0.27%
23	0	0	16.17575	0.01722	0.45574	0.00056	0.00734	0.00011	0.00500	0.00027	0.000870	0.00006	2.63E-13	98.41%	34.931	820.15	1.67	0.20%
24	0.88	40	16.17575	0.01722	0.45574	0.00056	0.00734	0.00011	0.00500	0.00027	0.000870	0.00006	2.63E-13	98.41%	34.931	820.15	1.67	0.20%
25	0	0	20.62454	0.02454	0.55957	0.00068	0.00953	0.00009	0.00414	0.00025	0.000890	0.00006	3.35E-13	98.72%	36.389	847.45	1.63	0.19%
26	0.88	40	10.46912	0.00550	0.27563	0.00052	0.00403	0.00008	0.00254	0.00019	0.000127	0.00005	1.70E-13	99.64%	37.848	874.36	2.16	0.25%
27	0.88	40	5.75186	0.00342	0.15149	0.00033	0.00214	0.00003	0.00055	0.00035	0.000065	0.00004	9.34E-14	99.67%	37.843	874.27	2.60	0.30%

APPENDIX: ARGON DATA

ID	P	t	^{40}Ar (*+ atm)	± 1σ	$^{39}Ar_K$	± 1σ	^{38}Ar (atm)	± 1σ	$^{37}Ar_{Ca}$	± 1σ	^{36}Ar	± 1σ	$^{40}Ar^*$	%Rad	R	Age	± 1σ	%-sd
#		(sec)	(V)		(V)		(V)		(V)		(V)		(mol)			(Ma)		
28	0.89	40	12.92380	0.00416	0.33967	0.00086	0.00533	0.00009	0.00036	0.00033	0.000217	0.00004	2.10E-13	99.50%	37.860	874.58	2.37	0.27%
29	0.9	40	5.42822	0.00494	0.14199	0.00041	0.00179	0.00007	-0.00099	0.00041	0.000116	0.00003	8.81E-14	99.37%	37.986	876.88	3.03	0.35%
30	0.91	40	4.19003	0.00335	0.11018	0.00023	0.00154	0.00004	0.00069	0.00022	0.000118	0.00003	6.80E-14	99.17%	37.714	871.91	2.70	0.31%
31	0.92	40	5.35634	0.00511	0.13961	0.00039	0.00191	0.00005	0.00045	0.00030	0.000127	0.00004	8.70E-14	99.30%	38.097	878.92	3.30	0.38%
32	0.93	40	7.24610	0.00796	0.19177	0.00067	0.00274	0.00005	-0.00085	0.00058	0.000145	0.00003	1.18E-13	99.41%	37.561	869.10	3.39	0.39%
33	0.95	30	7.61392	0.00565	0.20220	0.00039	0.00299	0.00006	0.00041	0.00032	0.000068	0.00003	1.24E-13	99.74%	37.556	869.01	2.15	0.25%
34	0.97	30	7.49093	0.00534	0.19809	0.00057	0.00280	0.00005	0.00031	0.00026	0.000014	0.00004	1.22E-13	99.95%	37.795	873.40	2.97	0.34%
35	1	30	9.71565	0.01211	0.25542	0.00040	0.00355	0.00005	0.00051	0.00026	0.000043	0.00004	1.58E-13	99.87%	37.989	876.94	2.00	0.23%
36	1.03	30	4.70078	0.00501	0.12216	0.00029	0.00166	0.00005	-0.00013	0.00011	0.000031	0.00003	7.63E-14	99.80%	38.404	884.51	3.00	0.34%
37	1.06	20	3.46506	0.00305	0.08939	0.00016	0.00122	0.00004	0.00040	0.00030	0.000002	0.00002	5.63E-14	99.98%	38.757	890.92	2.33	0.26%
38	1.1	20	4.18741	0.00267	0.10813	0.00022	0.00137	0.00004	-0.00016	0.00029	0.000031	0.00003	6.80E-14	99.78%	38.641	888.83	2.62	0.29%
39	1.15	20	1.91423	0.00130	0.05018	0.00018	0.00060	0.00004	0.00034	0.00017	-0.000005	0.00003	3.11E-14	100.07%	38.151	879.91	4.98	0.57%
40	1.2	20	0.53192	0.00064	0.01373	0.00018	0.00011	0.00004	-0.00025	0.00028	-0.000012	0.00004	8.64E-15	100.67%	38.741	890.63	20.97	2.35%
41	1.25	20	0.15674	0.00055	0.00405	0.00014	0.00005	0.00005	0.00001	0.00030	0.000014	0.00003	2.54E-15	97.27%	37.640	870.56	61.61	7.08%
42	1.3	20	0.09459	0.00045	0.00221	0.00016	-0.00003	0.00006	-0.00030	0.00023	0.000079	0.00003	1.54E-15	75.29%	32.211	768.09	126.34	16.45%

Total Gas Age = 865.9±7.1 Ma
(95% conf.), including J-error of .000011%)
MSWD = 60, probability = 0.000
100% of the 39Ar, steps 1 through 40

APPENDIX: ARGON DATA

ID	P	t	^{40}Ar (*+ atm)	± 1σ	$^{39}Ar_K$	± 1σ	^{38}Ar (atm)	± 1σ	$^{37}Ar_{Ca}$	± 1σ	^{36}Ar	± 1σ	$^{40}Ar^*$	%Rad	R	Age	± 1σ	%-sd
#		(sec)	(V)		(V)		(V)		(V)		(V)		(mol)			(Ma)		
BEN-24: K-feldspar																		
au25.2n.ksp.11																		
1	0.5	40	0.01926	0.00021	0.00073	0.00010	-0.00001	0.00004	0.00059	0.00020	-0.000009	0.00002	3.13E-16	113.70%	26.513	655.73	216.32	32.99%
2	0.6	40	0.14231	0.00018	0.00484	0.00011	0.00009	0.00003	0.00011	0.00022	0.000005	0.00002	2.31E-15	98.95%	29.094	708.47	34.65	4.89%
3	0.7	40	0.35360	0.00057	0.01303	0.00011	0.00016	0.00005	-0.00020	0.00023	0.000006	0.00002	5.74E-15	99.50%	26.998	665.76	14.64	2.20%
4	0.75	40	0.75834	0.00084	0.02956	0.00009	0.00038	0.00003	-0.00026	0.00021	0.000001	0.00002	1.23E-14	99.95%	25.638	637.50	5.54	0.87%
5	0.78	40	1.38381	0.00061	0.05417	0.00020	0.00070	0.00004	0.00004	0.00021	-0.000004	0.00002	2.25E-14	100.09%	25.548	635.60	4.00	0.63%
6	0.81	40	1.98767	0.00176	0.07816	0.00022	0.00104	0.00004	0.00035	0.00030	-0.000005	0.00002	3.23E-14	100.08%	25.433	633.18	2.68	0.42%
7	0.84	40	4.43600	0.00230	0.17383	0.00040	0.00237	0.00005	0.00022	0.00023	0.000044	0.00002	7.20E-14	99.70%	25.445	633.44	1.72	0.27%
8	0.87	40	9.71306	0.00896	0.37236	0.00037	0.00514	0.00004	0.00098	0.00021	0.000000	0.00002	1.58E-13	100.00%	26.086	646.84	1.00	0.16%
9	0.9	40	20.85184	0.01679	0.77552	0.00088	0.01142	0.00008	0.00364	0.00030	0.000187	0.00003	3.39E-13	99.74%	26.817	662.02	0.96	0.14%
10	0.91	40	9.09725	0.01449	0.32908	0.00053	0.00465	0.00004	0.00071	0.00012	0.000019	0.00002	1.48E-13	99.94%	27.627	678.69	1.60	0.24%
11	0.92	40	46.23316	0.07407	1.65639	0.00358	0.02352	0.00027	0.01017	0.00062	0.000372	0.00006	7.51E-13	99.76%	27.846	683.17	1.86	0.27%
12	0.92	30	15.17886	0.00842	0.53107	0.00141	0.00757	0.00009	0.00307	0.00020	0.000097	0.00003	2.46E-13	99.81%	28.529	697.05	1.93	0.28%
13	0.925	30	9.99989	0.01388	0.34479	0.00034	0.00477	0.00006	0.00105	0.00040	0.000014	0.00002	1.62E-13	99.96%	28.991	706.39	1.29	0.18%
14	0.93	30	4.13250	0.00352	0.14250	0.00026	0.00197	0.00005	0.00088	0.00022	0.000008	0.00002	6.71E-14	99.94%	28.984	706.25	1.79	0.25%
15	0.95	30	7.30055	0.00754	0.24811	0.00083	0.00333	0.00004	0.00017	0.00017	-0.000018	0.00002	1.19E-13	100.07%	29.424	715.11	2.57	0.36%
16	0.97	40	0.43075	0.00082	0.01447	0.00019	0.00019	0.00005	-0.00022	0.00029	0.000013	0.00002	6.99E-15	99.12%	29.505	716.73	13.45	1.88%
17	1	40	0.41911	0.00058	0.01402	0.00012	0.00023	0.00004	-0.00030	0.00024	0.000031	0.00002	6.80E-15	97.80%	29.240	711.40	11.53	1.62%

APPENDIX: ARGON DATA

ID	P	t	^{40}Ar (*+ atm)	± 1σ	$^{39}Ar_K$	± 1σ	^{38}Ar (atm)	± 1σ	$^{37}Ar_{Ca}$	± 1σ	^{36}Ar	± 1σ	$^{40}Ar^*$	%Rad	R	Age	± 1σ	%-sd
#		(sec)	(V)		(V)		(V)		(V)		(V)		(mol)			(Ma)		
18	1.05	40	7.33205	0.00242	0.24714	0.00070	0.00337	0.00005	0.00089	0.00035	0.000054	0.00002	1.19E-13	99.78%	29.603	718.70	2.13	0.30%
19	1.1	40	3.40060	0.00280	0.11655	0.00045	0.00167	0.00005	0.00034	0.00023	0.000019	0.00002	5.52E-14	99.84%	29.130	709.20	3.03	0.43%
20	1.15	40	7.49565	0.00691	0.26979	0.00056	0.00359	0.00004	0.00064	0.00026	0.000092	0.00002	1.22E-13	99.64%	27.683	679.82	1.64	0.24%
21	1.15	40	7.49576	0.00691	0.26991	0.00055	0.00374	0.00005	0.00024	0.00026	0.000057	0.00002	1.22E-13	99.78%	27.709	680.37	1.62	0.24%
22	1.2	40	1.25386	0.00163	0.04433	0.00012	0.00074	0.00006	-0.00038	0.00030	-0.000031	0.00002	2.04E-14	100.72%	28.284	692.09	3.53	0.51%
23	1.3	30	0.94578	0.00075	0.03349	0.00014	0.00055	0.00005	-0.00072	0.00018	0.000001	0.00002	1.54E-14	99.96%	28.226	690.90	4.71	0.68%
24	1.4	30	0.93989	0.00106	0.03283	0.00014	0.00063	0.00005	-0.00017	0.00031	-0.000043	0.00003	1.53E-14	101.36%	28.632	699.14	6.90	0.99%
25	1.5	30	0.12090	0.00042	0.00430	0.00009	0.00021	0.00005	-0.00004	0.00024	-0.000040	0.00003	1.96E-15	109.75%	28.132	688.98	49.20	7.14%
26	1.6	30	0.11302	0.00053	0.00400	0.00011	0.00027	0.00005	-0.00038	0.00032	-0.000042	0.00002	1.83E-15	110.96%	28.222	690.82	35.08	5.08%

Total Gas Age = 675±11 Ma
(95% conf.), including J-error of .000011%)
MSWD = 161, probability = 0.000
100% of the 39Ar, steps 1 through 25

BEN-24: K-feldspar

au25.2n.ksp.12

1	0.3	40	0.00024	0.00020	-0.00004	0.00008	0.00009	0.00004	0.00001	0.00028	0.000100	0.00003	3.94E-18	-12042.96%	809.920	4810.58	10.8E3	226.0%
2	0.4	40	0.89308	0.00127	0.00174	0.00007	0.00048	0.00004	0.00028	0.00020	0.000136	0.00003	1.45E-14	95.49%	489.928	3983.80	177.90	4.47%
3	0.5	40	2.71674	0.00221	0.01672	0.00015	0.00175	0.00004	0.00048	0.00022	0.000317	0.00004	4.41E-14	96.56%	156.913	2307.94	22.89	0.99%
4	0.6	40	3.26067	0.00242	0.11960	0.00052	0.00267	0.00006	0.00052	0.00024	0.000354	0.00003	5.29E-14	96.79%	26.388	653.14	3.63	0.56%
5	0.75	40	9.58887	0.00668	0.47483	0.00106	0.00701	0.00009	0.00156	0.00023	0.000159	0.00004	1.56E-13	99.51%	20.096	517.50	1.36	0.26%
6	0.78	40	4.73663	0.00419	0.22145	0.00055	0.00278	0.00006	0.00024	0.00024	0.000072	0.00002	7.69E-14	99.55%	21.294	544.12	1.65	0.30%

APPENDIX: ARGON DATA

ID	P	t	^{40}Ar (*+ atm)	± 1σ	$^{39}Ar_K$	± 1σ	^{38}Ar (atm)	± 1σ	$^{37}Ar_{Ca}$	± 1σ	^{36}Ar	± 1σ	$^{40}Ar^*$	%Rad	R	Age	± 1σ	%-sd
#		(sec)	(V)		(V)		(V)		(V)		(V)		(mol)			(Ma)		
7	0.81	40	5.17145	0.00388	0.22466	0.00065	0.00289	0.00007	0.00050	0.00025	-0.000019	0.00003	8.40E-14	100.11%	23.019	581.79	2.07	0.36%
8	0.84	40	6.80579	0.00664	0.28326	0.00039	0.00364	0.00006	0.00050	0.00019	-0.000023	0.00003	1.10E-13	100.10%	24.027	603.42	1.33	0.22%
9	0.86	40	5.46919	0.00689	0.22071	0.00040	0.00282	0.00004	0.00020	0.00024	-0.000063	0.00004	8.88E-14	100.34%	24.780	619.44	1.87	0.30%
10	0.87	40	9.73232	0.01158	0.36597	0.00083	0.00488	0.00005	0.00068	0.00013	0.000060	0.00002	1.58E-13	99.82%	26.545	656.40	1.74	0.27%
11	0.88	40	6.88090	0.00682	0.25344	0.00082	0.00323	0.00003	0.00030	0.00016	0.000047	0.00002	1.12E-13	99.80%	27.095	667.76	2.34	0.35%
12	0.89	30	5.94888	0.00450	0.21201	0.00054	0.00281	0.00007	0.00090	0.00018	-0.000073	0.00004	9.66E-14	100.36%	28.059	687.51	2.21	0.32%
13	0.9	30	5.91899	0.00578	0.20462	0.00053	0.00278	0.00005	0.00098	0.00030	0.000038	0.00003	9.61E-14	99.81%	28.873	704.01	2.14	0.30%
14	0.91	30	3.38234	0.00224	0.11505	0.00037	0.00160	0.00005	0.00117	0.00024	0.000024	0.00002	5.49E-14	99.79%	29.338	713.38	2.70	0.38%
15	0.92	30	1.02101	0.00112	0.03488	0.00014	0.00048	0.00005	0.00058	0.00016	-0.000018	0.00002	1.66E-14	100.53%	29.276	712.14	5.19	0.73%
16	0.93	30	1.00060	0.00083	0.03371	0.00016	0.00046	0.00006	0.00044	0.00025	0.000007	0.00002	1.62E-14	99.80%	29.625	719.13	5.48	0.76%
17	0.94	30	1.88729	0.00174	0.06234	0.00020	0.00086	0.00006	0.00050	0.00032	-0.000025	0.00002	3.06E-14	100.40%	30.274	732.09	3.23	0.44%
18	0.95	30	3.52261	0.00251	0.11700	0.00039	0.00160	0.00004	-0.00030	0.00029	0.000060	0.00002	5.72E-14	99.50%	29.956	725.75	2.74	0.38%
19	0.97	30	9.51532	0.01050	0.31424	0.00122	0.00441	0.00007	-0.00055	0.00051	0.000075	0.00002	1.54E-13	99.77%	30.209	730.79	2.98	0.41%
20	1	30	9.51532	0.01050	0.31424	0.00122	0.00441	0.00007	-0.00055	0.00051	0.000075	0.00002	1.54E-13	99.77%	30.209	730.79	2.98	0.41%
21	0	0	13.70570	0.01087	0.43047	0.00065	0.00702	0.00007	0.00588	0.00018	0.001689	0.00004	2.23E-13	96.36%	30.682	740.16	1.46	0.20%
22	1	40	13.70614	0.01087	0.43039	0.00065	0.00700	0.00007	0.00643	0.00018	0.001701	0.00004	2.23E-13	96.33%	30.680	740.13	1.45	0.20%
23	0	0	13.70614	0.01087	0.43039	0.00065	0.00700	0.00007	0.00643	0.00018	0.001701	0.00004	2.23E-13	96.33%	30.680	740.13	1.45	0.20%
24	0	0	13.70614	0.01087	0.43039	0.00065	0.00700	0.00007	0.00643	0.00018	0.001701	0.00004	2.23E-13	96.33%	30.680	740.13	1.45	0.20%
25	0	0	21.05133	0.02877	0.59732	0.00093	0.00870	0.00006	0.00596	0.00025	0.000270	0.00005	3.42E-13	99.62%	35.110	825.74	1.81	0.22%
26	0.97	30	4.88631	0.00302	0.14054	0.00033	0.00197	0.00006	0.00030	0.00021	0.000031	0.00003	7.93E-14	99.81%	34.703	818.04	2.34	0.29%

APPENDIX: ARGON DATA

ID	P	t	^{40}Ar (*+ atm)	± 1σ	$^{39}Ar_K$	± 1σ	^{38}Ar (atm)	± 1σ	$^{37}Ar_{Ca}$	± 1σ	^{36}Ar	± 1σ	$^{40}Ar^*$	%Rad	R	Age	± 1σ	%-sd
#		(sec)	(V)		(V)		(V)		(V)		(V)		(mol)			(Ma)		
27	0.98	40	4.57370	0.00350	0.13225	0.00033	0.00181	0.00007	0.00005	0.00028	-0.000042	0.00003	7.43E-14	100.27%	34.583	815.75	2.77	0.34%
28	0.99	40	6.04483	0.00272	0.16982	0.00055	0.00236	0.00006	-0.00084	0.00036	0.000053	0.00002	9.81E-14	99.74%	35.502	833.12	2.85	0.34%
29	1	40	6.98104	0.00839	0.20334	0.00072	0.00280	0.00006	0.00023	0.00023	0.000069	0.00002	1.13E-13	99.71%	34.232	809.08	3.17	0.39%
30	1.01	40	8.53455	0.01163	0.24720	0.00071	0.00337	0.00007	0.00046	0.00026	0.000062	0.00002	1.39E-13	99.79%	34.452	813.27	2.67	0.33%
31	1.02	40	3.03492	0.00232	0.08913	0.00021	0.00113	0.00006	0.00069	0.00024	0.000014	0.00002	4.93E-14	99.87%	34.007	804.80	2.68	0.33%
32	1.05	30	1.21418	0.00174	0.03530	0.00029	0.00049	0.00004	-0.00026	0.00013	-0.000025	0.00002	1.97E-14	100.60%	34.394	812.16	7.66	0.94%
33	1.2	30	12.60036	0.00789	0.36869	0.00051	0.00518	0.00008	0.00257	0.00020	0.000150	0.00003	2.05E-13	99.65%	34.057	805.74	1.37	0.17%
34	1.35	20	17.43404	0.02007	0.51505	0.00072	0.00736	0.00009	0.00264	0.00025	0.000190	0.00003	2.83E-13	99.68%	33.740	799.70	1.52	0.19%
35	1.45	20	12.45751	0.00716	0.36839	0.00079	0.00530	0.00009	0.00348	0.00041	0.000102	0.00003	2.02E-13	99.76%	33.735	799.60	1.87	0.23%
36	1.55	20	12.79867	0.00968	0.38004	0.00113	0.00524	0.00006	0.00301	0.00017	0.000069	0.00002	2.08E-13	99.84%	33.624	797.48	2.50	0.31%
37	1.65	20	7.51213	0.00771	0.22130	0.00044	0.00311	0.00006	0.00105	0.00030	0.000048	0.00002	1.22E-13	99.81%	33.881	802.39	1.90	0.24%

Total Gas Age = 675±11 Ma
(95% conf.), including J-error of .000011%)
MSWD = 161, probability = 0.000
100% of the 39Ar, steps 1 through 25

BEN-24: K-feldspar

au25.2n.ksp.13

1	0.3	30	-0.00001	0.00030	-0.00005	0.00010	-0.00001	0.00005	0.00008	0.00011	0.000007	0.00002	-2.04E-19	16817.5%	43.935	985.03	2940.2	298.4%
2	0.4	20	0.47264	0.00047	-0.00003	0.00009	-0.00001	0.00004	0.00004	0.00023	0.000012	0.00002	7.67E-15	99.23%	-13633.05			
3	0.5	20	7.78806	0.00347	0.00326	0.00014	0.00154	0.00007	0.00091	0.00016	0.000147	0.00002	1.26E-13	99.44%	2376.614	6668.06	280.33	4.20%
4	0.6	20	5.66371	0.00392	0.06287	0.00047	0.00165	0.00004	0.00064	0.00014	0.000100	0.00002	9.20E-14	99.48%	89.613	1639.65	12.49	0.76%

APPENDIX: ARGON DATA

ID	P	t	^{40}Ar (*+ atm)	± 1σ	$^{39}Ar_K$	± 1σ	^{38}Ar (atm)	± 1σ	$^{37}Ar_{Ca}$	± 1σ	^{36}Ar	± 1σ	$^{40}Ar^*$	%Rad	R	Age	± 1σ	%-sd
#		(sec)	(V)		(V)		(V)		(V)		(V)		(mol)			(Ma)		
5	0.65	20	1.69511	0.00216	0.07943	0.00053	0.00112	0.00004	-0.00021	0.00032	0.000044	0.00002	2.75E-14	99.23%	21.179	541.58	4.08	0.75%
6	0.7	40	3.52308	0.00225	0.18711	0.00052	0.00253	0.00004	0.00023	0.00030	0.000057	0.00002	5.72E-14	99.52%	18.739	486.86	1.63	0.33%
7	0.73	40	3.57923	0.00325	0.17949	0.00043	0.00234	0.00005	0.00039	0.00021	0.000075	0.00002	5.81E-14	99.38%	19.818	511.26	1.55	0.30%
8	0.76	40	3.54706	0.00133	0.17181	0.00071	0.00223	0.00005	-0.00008	0.00018	0.000056	0.00002	5.76E-14	99.53%	20.548	527.59	2.40	0.45%
9	0.79	40	4.57803	0.00370	0.20866	0.00051	0.00272	0.00006	0.00035	0.00028	0.000066	0.00002	7.43E-14	99.57%	21.846	556.26	1.64	0.30%
10	0.82	40	3.64495	0.00425	0.16495	0.00054	0.00208	0.00003	0.00011	0.00024	0.000084	0.00002	5.92E-14	99.32%	21.946	558.44	2.12	0.38%
11	0.85	40	1.75660	0.00111	0.07816	0.00029	0.00098	0.00004	-0.00026	0.00017	0.000004	0.00002	2.85E-14	99.93%	22.460	569.67	2.77	0.49%
12	0.88	40	2.92508	0.00228	0.12755	0.00033	0.00146	0.00007	-0.00005	0.00024	0.000025	0.00002	4.75E-14	99.75%	22.875	578.67	2.04	0.35%
13	0.9	30	1.27225	0.00127	0.05529	0.00015	0.00066	0.00006	-0.00060	0.00024	0.000000	0.00002	2.07E-14	100.00%	23.011	581.61	3.29	0.57%
14	0.91	30	3.47129	0.00229	0.14303	0.00056	0.00183	0.00005	-0.00001	0.00017	-0.000021	0.00002	5.64E-14	100.18%	24.270	608.60	2.61	0.43%
15	0.92	30	3.52178	0.00240	0.14202	0.00036	0.00181	0.00005	-0.00012	0.00021	0.000006	0.00002	5.72E-14	99.95%	24.786	619.56	1.87	0.30%
16	0.93	30	2.40765	0.00231	0.09495	0.00039	0.00117	0.00005	0.00077	0.00026	-0.000054	0.00003	3.91E-14	100.67%	25.357	631.60	3.55	0.56%
17	0.94	30	1.87929	0.00213	0.07265	0.00023	0.00093	0.00004	0.00105	0.00018	0.000002	0.00002	3.05E-14	99.97%	25.860	642.13	2.85	0.44%
18	0.95	30	2.03271	0.00121	0.07605	0.00023	0.00101	0.00005	0.00088	0.00024	0.000029	0.00002	3.30E-14	99.57%	26.615	657.85	2.96	0.45%
19	0.96	30	1.64711	0.00148	0.06131	0.00013	0.00081	0.00003	0.00103	0.00021	-0.000114	0.00004	2.67E-14	102.04%	26.867	663.05	5.00	0.75%
20	0.97	30	1.24975	0.00122	0.04638	0.00017	0.00057	0.00003	0.00045	0.00018	-0.000037	0.00002	2.03E-14	100.89%	26.945	664.66	4.15	0.62%
21	0.98	30	1.43514	0.00183	0.05177	0.00023	0.00068	0.00004	-0.00083	0.00022	0.000038	0.00002	2.33E-14	99.21%	27.499	676.06	4.47	0.66%
22	0.99	30	2.66814	0.00178	0.09446	0.00027	0.00131	0.00004	-0.00055	0.00021	0.000048	0.00002	4.33E-14	99.47%	28.095	688.23	2.75	0.40%
23	1	30	2.43207	0.00388	0.08518	0.00031	0.00105	0.00003	-0.00121	0.00021	0.000006	0.00002	3.95E-14	99.93%	28.532	697.11	3.43	0.49%
24	1.01	30	2.42599	0.00192	0.08422	0.00026	0.00108	0.00003	-0.00095	0.00016	-0.000001	0.00003	3.94E-14	100.01%	28.805	702.63	3.40	0.48%

APPENDIX: ARGON DATA

ID	P	t	^{40}Ar (*+ atm)	± 1σ	$^{39}Ar_K$	± 1σ	^{38}Ar (atm)	± 1σ	$^{37}Ar_{Ca}$	± 1σ	^{36}Ar	± 1σ	$^{40}Ar^*$	%Rad	R	Age	± 1σ	%-sd
#		(sec)	(V)		(V)		(V)		(V)		(V)		(mol)			(Ma)		
25	1.02	30	2.24569	0.00158	0.07593	0.00013	0.00102	0.00004	-0.00102	0.00026	0.000067	0.00002	3.65E-14	99.12%	29.313	712.88	2.52	0.35%
26	1.05	30	2.54681	0.00178	0.08497	0.00029	0.00112	0.00003	-0.00038	0.00021	0.000118	0.00004	4.13E-14	98.63%	29.565	717.93	4.03	0.56%
27	1.1	30	11.89940	0.00803	0.38306	0.00063	0.00544	0.00008	0.00287	0.00016	0.000230	0.00004	1.93E-13	99.43%	30.887	744.23	1.56	0.21%
28	1.15	30	11.89940	0.00803	0.38306	0.00063	0.00544	0.00008	0.00287	0.00016	0.000230	0.00004	1.93E-13	99.43%	30.887	744.23	1.56	0.21%
29	0	0	23.85575	0.01157	0.70387	0.00113	0.01076	0.00011	0.00547	0.00042	0.000553	0.00004	3.87E-13	99.32%	33.661	798.18	1.41	0.18%
30	1.14	30	14.59759	0.00789	0.42582	0.00122	0.00614	0.00006	0.00354	0.00016	0.000116	0.00006	2.37E-13	99.77%	34.202	808.51	2.55	0.32%
31	1.15	30	13.85820	0.00847	0.39389	0.00091	0.00574	0.00007	0.00330	0.00035	0.000199	0.00005	2.25E-13	99.57%	35.034	824.30	2.15	0.26%
32	1.16	30	5.11415	0.00490	0.15229	0.00043	0.00219	0.00004	0.00042	0.00018	0.000162	0.00004	8.30E-14	99.06%	33.267	790.61	2.97	0.38%
33	1.18	20	2.53271	0.00167	0.08026	0.00015	0.00109	0.00005	-0.00057	0.00028	-0.000029	0.00002	4.11E-14	100.34%	31.557	757.40	2.23	0.29%
34	1.2	20	4.94320	0.00280	0.15349	0.00041	0.00212	0.00004	0.00005	0.00022	-0.000001	0.00002	8.03E-14	100.01%	32.206	770.07	2.27	0.29%
35	1.25	20	8.60589	0.00792	0.23619	0.00052	0.00322	0.00005	-0.00030	0.00026	0.000014	0.00002	1.40E-13	99.95%	36.419	850.26	2.10	0.25%
36	1.3	20	5.77157	0.00588	0.17670	0.00040	0.00236	0.00005	0.00025	0.00028	0.000003	0.00002	9.37E-14	99.98%	32.659	778.88	2.06	0.26%
37	1.4	20	3.04607	0.00334	0.09439	0.00039	0.00125	0.00004	-0.00007	0.00026	-0.000048	0.00002	4.95E-14	100.47%	32.270	771.33	3.65	0.47%
38	1.5	20	6.52417	0.00410	0.20104	0.00048	0.00278	0.00005	0.00016	0.00013	-0.000017	0.00003	1.06E-13	100.08%	32.452	774.85	2.24	0.29%
39	1.6	20	6.30056	0.00518	0.20479	0.00050	0.00277	0.00004	0.00022	0.00019	0.000040	0.00002	1.02E-13	99.81%	30.709	740.71	2.07	0.28%

Total Gas Age = 677±38 Ma
(95% conf.), including J-error of .000011%)
MSWD = 2389, probability = 0.000
100% of the 39Ar, steps 1 through 35

APPENDIX: ARGON DATA

ID	P	t	^{40}Ar (*+ atm)	± 1σ	$^{39}Ar_K$	± 1σ	^{38}Ar (atm)	± 1σ	$^{37}Ar_{Ca}$	± 1σ	^{36}Ar	± 1σ	$^{40}Ar^*$	%Rad	R	Age	± 1σ	%-sd
#		(sec)	(V)		(V)		(V)		(V)		(V)		(mol)			(Ma)		
BEN-17: K-feldspar																		
au25.3p.ksp.17																		
1	0.3	50	0.00008	0.00029	0.00008	0.00008	0.00002	0.00003	0.00000	0.00025	-0.000067	0.00003	1.34E-18	24.0E3%	0.968	28.74	7486.7	26.0E3%
2	0.4	50	0.09807	0.00046	0.00022	0.00009	0.00007	0.00002	0.00021	0.00023	0.000014	0.00002	1.59E-15	95.70%	422.152	3752.22	1666.2	44.41%
3	0.5	50	5.84918	0.00388	0.00624	0.00012	0.00306	0.00005	0.00058	0.00031	0.000344	0.00004	9.50E-14	98.26%	920.848	5032.86	96.59	1.92%
4	0.55	50	3.38093	0.00289	0.01576	0.00011	0.00153	0.00005	0.00027	0.00023	0.000191	0.00002	5.49E-14	98.33%	210.993	2713.58	20.69	0.76%
5	0.6	50	2.20391	0.00282	0.06889	0.00013	0.00167	0.00003	0.00062	0.00020	0.000131	0.00002	3.58E-14	98.24%	31.431	757.08	2.78	0.37%
6	0.63	50	0.61749	0.00121	0.03432	0.00018	0.00055	0.00004	0.00031	0.00023	0.000051	0.00002	1.00E-14	97.57%	17.556	461.14	5.05	1.09%
7	0.66	50	1.76559	0.00176	0.09982	0.00044	0.00143	0.00003	0.00042	0.00028	0.000077	0.00002	2.87E-14	98.71%	17.460	458.91	2.61	0.57%
8	0.69	50	1.78022	0.00158	0.08784	0.00028	0.00124	0.00003	0.00065	0.00031	0.000010	0.00002	2.89E-14	99.83%	20.233	522.13	2.29	0.44%
9	0.72	50	1.42445	0.00133	0.06083	0.00016	0.00084	0.00004	0.00003	0.00031	0.000029	0.00002	2.31E-14	99.40%	23.278	589.10	2.92	0.49%
10	0.75	50	1.67381	0.00111	0.06456	0.00022	0.00087	0.00005	0.00017	0.00019	0.000022	0.00002	2.72E-14	99.62%	25.826	643.31	3.05	0.47%
11	0.78	50	4.52021	0.00134	0.12782	0.00027	0.00184	0.00006	0.00008	0.00030	0.000041	0.00002	7.34E-14	99.73%	35.271	831.08	2.13	0.26%
12	0.79	50	2.10495	0.00181	0.06928	0.00028	0.00092	0.00004	0.00060	0.00019	0.000013	0.00002	3.42E-14	99.81%	30.328	735.24	3.58	0.49%
13	0.8	50	1.46027	0.00160	0.04864	0.00012	0.00058	0.00004	0.00011	0.00031	0.000005	0.00002	2.37E-14	99.90%	29.993	728.57	3.47	0.48%
14	0.82	50	1.95740	0.00116	0.06470	0.00028	0.00104	0.00007	0.00008	0.00016	0.000009	0.00002	3.18E-14	99.87%	30.213	732.96	3.79	0.52%
15	0.84	50	3.84216	0.00305	0.11949	0.00046	0.00158	0.00004	0.00046	0.00027	-0.000019	0.00003	6.24E-14	100.15%	32.156	771.28	3.60	0.47%
16	0.86	50	3.27259	0.00299	0.10473	0.00023	0.00139	0.00005	0.00031	0.00024	0.000006	0.00002	5.31E-14	99.94%	31.230	753.12	2.20	0.29%
17	0.9	50	6.59107	0.00516	0.20034	0.00071	0.00273	0.00006	0.00096	0.00024	0.000045	0.00002	1.07E-13	99.80%	32.835	784.48	2.96	0.38%
18	0.91	50	10.62935	0.01018	0.33993	0.00062	0.00452	0.00007	0.00313	0.00018	0.000100	0.00003	1.73E-13	99.72%	31.183	752.19	1.70	0.23%

APPENDIX: ARGON DATA

ID	P	t	^{40}Ar (*+ atm)	± 1σ	$^{39}Ar_K$	± 1σ	^{38}Ar (atm)	± 1σ	$^{37}Ar_{Ca}$	± 1σ	^{36}Ar	± 1σ	$^{40}Ar^*$	%Rad	R	Age	± 1σ	%-sd
#		(sec)	(V)		(V)		(V)		(V)		(V)		(mol)			(Ma)		
19	0.92	50	7.49188	0.00710	0.24521	0.00073	0.00312	0.00006	-0.00105	0.00052	0.000020	0.00002	1.22E-13	99.92%	30.528	739.23	2.37	0.32%
20	0.93	50	3.91975	0.00248	0.12824	0.00026	0.00145	0.00006	0.00025	0.00022	0.000060	0.00002	6.36E-14	99.55%	30.427	737.22	2.08	0.28%
21	0.94	50	4.96830	0.00330	0.16247	0.00038	0.00208	0.00005	0.00041	0.00029	-0.000036	0.00004	8.07E-14	100.22%	30.580	740.25	2.39	0.32%
22	0.95	50	7.55155	0.00978	0.24596	0.00056	0.00322	0.00005	0.00106	0.00020	0.000028	0.00002	1.23E-13	99.89%	30.669	742.02	2.06	0.28%
23	0.96	50	6.42828	0.00613	0.20951	0.00058	0.00279	0.00005	0.00109	0.00028	0.000000	0.00004	1.04E-13	100.00%	30.683	742.29	2.53	0.34%
24	0.97	50	6.68238	0.00748	0.21884	0.00093	0.00281	0.00005	0.00070	0.00035	-0.000025	0.00003	1.08E-13	100.11%	30.535	739.37	3.39	0.46%
25	0.98	50	4.06660	0.00311	0.13111	0.00026	0.00175	0.00005	-0.00084	0.00040	-0.000050	0.00003	6.60E-14	100.36%	31.016	748.90	2.29	0.31%
26	0.99	50	8.06256	0.00898	0.25967	0.00098	0.00332	0.00005	0.00091	0.00023	0.000050	0.00002	1.31E-13	99.82%	30.993	748.44	3.00	0.40%
27	1	50	7.06769	0.00878	0.22843	0.00067	0.00293	0.00007	0.00089	0.00026	0.000046	0.00002	1.15E-13	99.81%	30.881	746.22	2.45	0.33%
28	1.02	50	6.87251	0.00588	0.22119	0.00069	0.00291	0.00004	0.00049	0.00026	0.000000	0.00002	1.12E-13	100.00%	31.071	749.98	2.50	0.33%
29	1.04	50	7.83102	0.01113	0.25155	0.00076	0.00326	0.00005	0.00032	0.00034	0.000018	0.00002	1.27E-13	99.93%	31.110	750.76	2.58	0.34%
30	1.06	50	6.39356	0.00590	0.20518	0.00081	0.00266	0.00005	0.00027	0.00027	-0.000090	0.00004	1.04E-13	100.41%	31.161	751.76	3.31	0.44%
31	1.08	50	9.39903	0.01255	0.29884	0.00057	0.00394	0.00008	0.00035	0.00026	0.000006	0.00003	1.53E-13	99.98%	31.446	757.37	1.87	0.25%
32	1.1	50	9.79694	0.01253	0.30967	0.00041	0.00407	0.00005	-0.00011	0.00034	-0.000004	0.00003	1.59E-13	100.01%	31.637	761.12	1.51	0.20%
33	1.12	50	11.92431	0.00931	0.37550	0.00089	0.00506	0.00011	0.00147	0.00023	0.000059	0.00003	1.94E-13	99.85%	31.710	762.55	2.00	0.26%
34	1.14	50	12.61140	0.00875	0.39565	0.00112	0.00542	0.00007	0.00341	0.00027	0.000045	0.00003	2.05E-13	99.89%	31.842	765.15	2.29	0.30%
35	1.16	40	11.32866	0.00847	0.35433	0.00061	0.00474	0.00008	0.00142	0.00022	-0.000023	0.00003	1.84E-13	100.06%	31.972	767.69	1.57	0.20%
36	1.18	40	22.40077	0.01490	0.69397	0.00130	0.00937	0.00006	0.00337	0.00032	0.000068	0.00003	3.64E-13	99.91%	32.251	773.13	1.58	0.20%
37	1.2	30	21.40559	0.01960	0.65934	0.00136	0.00872	0.00011	0.00299	0.00023	0.000067	0.00003	3.48E-13	99.91%	32.436	776.74	1.78	0.23%
38	1.25	30	24.09426	0.02218	0.73803	0.00098	0.00979	0.00009	0.00329	0.00032	0.000114	0.00003	3.91E-13	99.86%	32.602	779.96	1.31	0.17%

APPENDIX: ARGON DATA

ID	P	t	^{40}Ar (*+ atm)	± 1σ	$^{39}Ar_K$	± 1σ	^{38}Ar (atm)	± 1σ	$^{37}Ar_{Ca}$	± 1σ	^{36}Ar	± 1σ	$^{40}Ar^*$	%Rad	R	Age	± 1σ	%-sd
#		(sec)	(V)		(V)		(V)		(V)		(V)		(mol)			(Ma)		
39	0	0	16.63945	0.01261	0.52018	0.00048	0.00778	0.00013	0.00492	0.00041	0.000000	0.00003	2.70E-13	100.00%	31.988	768.00	1.01	0.13%
40	1.24	30	16.77275	0.00912	0.49793	0.00086	0.00711	0.00007	0.00331	0.00018	0.000134	0.00003	2.72E-13	99.76%	33.606	799.37	1.50	0.19%
41	1.25	20	10.63078	0.00668	0.31641	0.00089	0.00447	0.00005	0.00354	0.00030	-0.000056	0.00005	1.73E-13	100.16%	33.600	799.24	2.52	0.32%
42	1.26	20	13.80849	0.01190	0.40240	0.00055	0.00581	0.00006	0.00115	0.00032	0.000041	0.00003	2.24E-13	99.91%	34.285	812.37	1.40	0.17%
43	1.27	0	19.91033	0.02885	0.54769	0.00133	0.00780	0.00010	0.00390	0.00027	-0.000009	0.00005	3.23E-13	100.01%	36.354	851.41	2.50	0.29%
44	1.26	20	15.86962	0.00641	0.44520	0.00057	0.00627	0.00006	0.00407	0.00030	0.000021	0.00003	2.58E-13	99.96%	35.633	835.57	1.21	0.14%
45	1.26	0	17.57876	0.02862	0.47897	0.00118	0.00680	0.00007	0.00136	0.00049	0.000077	0.00003	2.85E-13	99.87%	36.654	854.63	2.55	0.30%
46	1.26	20	13.01002	0.00793	0.35486	0.00051	0.00498	0.00012	0.00293	0.00021	0.000088	0.00003	2.11E-13	99.80%	36.590	853.45	1.42	0.17%
47	1.26	20	12.09843	0.01166	0.33184	0.00078	0.00471	0.00005	0.00252	0.00024	0.000055	0.00003	1.96E-13	99.87%	36.411	852.47	2.25	0.26%
48	1.27	20	9.22071	0.01158	0.24582	0.00081	0.00329	0.00005	-0.00008	0.00020	-0.000041	0.00002	1.50E-13	100.13%	37.510	872.86	3.13	0.36%
49	1.28	20	5.80827	0.00771	0.16300	0.00051	0.00226	0.00003	0.00025	0.00041	-0.000018	0.00002	9.43E-14	100.09%	35.634	837.92	2.94	0.35%
50	1.29	20	6.75338	0.00558	0.18782	0.00047	0.00260	0.00004	0.00047	0.00024	0.000003	0.00002	1.10E-13	99.99%	35.952	843.89	2.29	0.27%
51	0	0	15.71555	0.03284	0.43294	0.00087	0.00606	0.00007	0.00191	0.00021	0.000197	0.00003	2.55E-13	99.63%	36.165	847.88	2.52	0.30%
52	1.29	20	19.72525	0.01265	0.55143	0.00130	0.00766	0.00008	0.00414	0.00011	0.000160	0.00003	3.20E-13	99.76%	35.686	838.90	2.09	0.25%
53	1.3	20	5.70018	0.00675	0.16532	0.00045	0.00220	0.00004	0.00027	0.00025	-0.000021	0.00002	9.25E-14	100.11%	34.481	816.09	2.52	0.31%
54	1.31	20	24.32006	0.00920	0.69237	0.00134	0.00980	0.00011	0.00085	0.00043	0.000118	0.00003	3.95E-13	99.86%	35.076	827.39	1.66	0.20%
55	1.32	20	4.11381	0.00356	0.11966	0.00021	0.00157	0.00004	0.00005	0.00015	0.000023	0.00002	6.68E-14	99.83%	34.322	813.07	1.99	0.24%
56	1.33	20	4.23194	0.00186	0.12361	0.00028	0.00167	0.00006	0.00023	0.00026	0.000006	0.00002	6.87E-14	99.96%	34.223	811.17	2.16	0.27%
57	1.35	20	3.49643	0.00321	0.10210	0.00015	0.00137	0.00004	-0.00114	0.00050	0.000050	0.00002	5.68E-14	99.58%	34.099	808.81	1.96	0.24%
58	1.4	20	5.90634	0.00411	0.17122	0.00032	0.00229	0.00004	-0.00117	0.00045	0.000029	0.00002	9.59E-14	99.85%	34.444	815.40	1.85	0.23%

APPENDIX: ARGON DATA

ID	P	t	^{40}Ar (*+ atm)	± 1σ	$^{39}Ar_K$	± 1σ	^{38}Ar (atm)	± 1σ	$^{37}Ar_{Ca}$	± 1σ	^{36}Ar	± 1σ	$^{40}Ar^*$	%Rad	R	Age	± 1σ	%-sd
#		(sec)	(V)		(V)		(V)		(V)		(V)		(mol)			(Ma)		
59	1.45	20	5.30469	0.00556	0.14996	0.00035	0.00201	0.00005	0.00022	0.00017	0.000009	0.00002	8.61E-14	99.95%	35.358	832.72	2.27	0.27%
60	1.5	20	9.86148	0.01098	0.28437	0.00104	0.00379	0.00006	0.00022	0.00030	0.000012	0.00002	1.60E-13	99.97%	34.666	819.62	3.16	0.39%
61	1.55	20	16.79231	0.01440	0.47933	0.00062	0.00713	0.00012	0.00401	0.00045	0.000513	0.00003	2.73E-13	99.10%	34.718	820.60	1.35	0.16%

Total Gas Age = 781±17 Ma
(95% conf.), including J-error of .00001%)
MSWD = 1041, probability = 0.000
100% of the 39Ar, steps 1 through 57

APPENDIX: ARGON DATA

ID	Temp	Time	^{40}Ar	± 1σ	^{39}Ar	± 1σ	^{38}Ar	± 1σ	^{37}Ar	± 1σ	^{36}Ar	± 1σ	^{40}Ar*	%Rad	R	Age	± 1σ	%-sd
#	(°C)	(sec)	(V)		(V)		(V)		(V)		(V)		(mol)			(Ma)		
BEN-5: K-feldspar																		
*au25.1d.ksp.**diode***																		
1	350	3000	0.16082	0.00034	0.00625	0.00007	0.00015	0.00002	-3.92529	2.41801	0.000033	0.00001	2.61E-15	93.96%	24.177	604.91	16.70	2.76%
2	350	3000	0.03407	0.00038	0.00113	0.00007	0.00006	0.00002	2.64440	2.92609	-0.000014	0.00001	5.53E-16	112.57%	30.031	725.24	77.10	10.63%
3	413	3000	0.24690	0.00063	0.00777	0.00008	0.00015	0.00002	1.70216	1.75483	0.000003	0.00001	4.01E-15	99.64%	31.671	757.57	13.88	1.83%
4	413	3000	0.12445	0.00035	0.00355	0.00006	0.00006	0.00002	1.30012	2.01916	-0.000035	0.00001	2.02E-15	108.28%	35.061	822.60	25.08	3.05%
5	463	3000	0.65108	0.00081	0.01739	0.00005	0.00023	0.00002	1.40259	2.77150	0.000027	0.00001	1.06E-14	98.76%	36.982	858.44	4.95	0.58%
6	463	3000	0.31696	0.00075	0.00939	0.00008	0.00010	0.00002	2.78666	3.05485	-0.000024	0.00002	5.15E-15	102.19%	33.748	797.69	16.15	2.02%
7	516	3000	2.00412	0.00210	0.06145	0.00018	0.00092	0.00003	5.34538	3.57132	0.000096	0.00001	3.25E-14	98.59%	32.154	766.99	2.69	0.35%
8	516	3000	1.07434	0.00076	0.03418	0.00024	0.00053	0.00003	4.46244	3.57616	0.000089	0.00001	1.74E-14	97.56%	30.661	737.74	5.69	0.77%
9	570	3000	4.45661	0.00335	0.14044	0.00053	0.00190	0.00003	10.36453	2.48664	0.000045	0.00002	7.24E-14	99.70%	31.639	756.95	3.06	0.40%
10	570	3000	2.54741	0.00216	0.07914	0.00018	0.00107	0.00002	7.97370	3.92137	0.000086	0.00001	4.14E-14	99.01%	31.871	761.47	2.05	0.27%
11	615	2000	5.66853	0.00431	0.17410	0.00039	0.00228	0.00003	1.41684	3.49312	0.000083	0.00001	9.20E-14	99.57%	32.419	772.12	1.88	0.24%
12	658	1200	11.45319	0.00358	0.34273	0.00087	0.00462	0.00006	52.45759	2.90979	0.000135	0.00002	1.86E-13	99.65%	33.301	789.13	2.04	0.26%
13	622	2000	1.87179	0.00144	0.05457	0.00024	0.00070	0.00001	-0.00437	2.53704	0.000076	0.00001	3.04E-14	98.80%	33.890	800.40	3.88	0.48%
14	674	2000	7.61683	0.00510	0.21967	0.00044	0.00287	0.00004	-9.84810	4.15834	0.000065	0.00001	1.24E-13	99.75%	34.587	813.65	1.76	0.22%
15	674	2000	5.35052	0.00407	0.15175	0.00042	0.00211	0.00003	6.88545	2.46841	0.000077	0.00001	8.69E-14	99.58%	35.110	823.53	2.43	0.29%
16	726	2000	14.29055	0.00639	0.40262	0.00077	0.00536	0.00008	42.65287	3.66701	0.000121	0.00002	2.32E-13	99.75%	35.405	829.07	1.67	0.20%
17	726	2000	9.15204	0.00684	0.25994	0.00064	0.00347	0.00004	9.40038	4.00684	0.000085	0.00001	1.49E-13	99.72%	35.111	823.54	2.15	0.26%
18	777	1000	15.99853	0.00961	0.45471	0.00127	0.00630	0.00023	220.59937	20.44907	0.000485	0.00010	4.09E-14	99.10%	34.869	818.99	2.80	0.34%
19	777	1000	7.82202	0.00456	0.22346	0.00038	0.00291	0.00004	6.51248	2.74789	0.000051	0.00001	1.27E-13	99.81%	34.937	820.27	1.52	0.18%
20	830	1000	17.41559	0.00578	0.49825	0.00121	0.00668	0.00010	27.69647	4.95320	0.000118	0.00002	2.83E-13	99.80%	34.884	819.25	2.03	0.25%

APPENDIX: ARGON DATA

ID	Temp	Time	^{40}Ar	± 1σ	^{39}Ar	± 1σ	^{38}Ar	± 1σ	^{37}Ar	± 1σ	^{36}Ar	± 1σ	^{40}Ar*	%Rad	R	Age	± 1σ	%-sd
#	(°C)	(sec)	(V)		(V)		(V)		(V)		(V)		(mol)			(Ma)		
21	830	1000	10.23912	0.00569	0.29314	0.00036	0.00371	0.00008	2.84421	3.19233	0.000042	0.00001	1.66E-13	99.88%	34.887	819.31	1.14	0.14%
22	880	500	11.50615	0.00664	0.33114	0.00071	0.00445	0.00009	36.63392	1.63219	-0.000004	0.00003	1.87E-13	100.01%	34.748	816.69	1.89	0.23%
23	880	500	8.39128	0.00997	0.24105	0.00045	0.00311	0.00003	6.40418	3.94706	0.000007	0.00003	1.36E-13	99.97%	34.802	817.72	1.96	0.24%
24	930	500	14.58022	0.00815	0.41640	0.00071	0.00555	0.00008	43.70507	3.22803	0.000065	0.00001	2.37E-13	99.87%	34.969	820.87	1.49	0.18%
25	930	300	5.33264	0.00295	0.15197	0.00051	0.00204	0.00004	7.57715	2.50396	0.000012	0.00001	8.66E-14	99.94%	35.068	822.74	2.82	0.34%
26	980	300	9.69795	0.00503	0.27508	0.00064	0.00349	0.00009	10.87667	4.58592	0.000044	0.00001	1.57E-13	99.87%	35.208	825.37	1.99	0.24%
27	980	300	6.39904	0.00712	0.18038	0.00034	0.00233	0.00006	2.54465	3.30974	0.000018	0.00001	1.04E-13	99.92%	35.446	829.85	1.88	0.23%
28	1030	300	9.73163	0.01082	0.27367	0.00080	0.00360	0.00004	1.95140	2.77204	0.000033	0.00001	1.58E-13	99.90%	35.525	831.32	2.64	0.32%
29	1030	300	6.46707	0.00626	0.18173	0.00054	0.00236	0.00004	1.64317	3.53206	0.000005	0.00001	1.05E-13	99.98%	35.579	832.33	2.66	0.32%
30	1055	300	6.44592	0.00546	0.18073	0.00059	0.00238	0.00004	2.64336	3.71824	0.000018	0.00001	1.05E-13	99.92%	35.636	833.40	2.88	0.35%
31	1055	300	3.27398	0.00404	0.09230	0.00031	0.00122	0.00003	-0.67548	3.06617	0.000032	0.00001	5.32E-14	99.71%	35.370	828.41	3.07	0.37%

Total Gas Age = 781±17 Ma
(95% conf.), including J-error of .00001%)
MSWD = 1041, probability = 0.000
100% of the 39Ar, steps 1 through 57